THESIS ON NATURAL AND EXACT SCIENCES B108

Point-of-Care Analyser Based on Capillary Electrophoresis

ANDRUS SEIMAN

TUT PRESS

TALLINN UNIVERSIY OF TECHNOLOGY
Faculty of Science
Department of Chemistry

Dissertation was accepted for the defence of the degree of Doctor of Philosophy in Natural and Exact Sciences on April 13, 2011

Supervisor: Professor Mihkel Kaljurand, Department of Chemistry, Faculty of Science, Tallinn University of Technology, Estonia

Opponents: Professor František Foret, Institute of Analytical Chemistry, Czech Republic

Professor Peter C. Hauser, Department of Chemistry, University of Basel, Switzerland

Defence of the thesis: June 29, 2011

Declaration:
Hereby I declare that this doctoral thesis, my original investigation and achievement, submitted for the doctoral degree at Tallinn University of Technology has not been submitted for any academic degree.

Andrus Seiman

This work has been partially supported by graduate school „Functional materials and processes“ receiving funding from the European Social Fund under project 1.2.0401.09-0079 in Estonia.

ISSN 1406-4723
ISBN 978-9949-23-102-7 (publication)
ISBN 978-9949-23-103-4 (PDF)

LOODUS- JA TÄPPISTEADUSED B108

Kapillaarelektroforeesil põhinev kaasaskantav analüsaator

ANDRUS SEIMAN

TTÜ
KIRJASTUS

TABLE OF CONTENTS

LIST OF ORIGINAL PUBLICATIONS

This thesis is based on the following publications, which are referred to by Roman numerals within the text:

I. Seiman, A., Jaanus, M., Vaher, M., Kaljurand, M., A portable capillary electropherograph equipped with a cross-sampler and a contactless-conductivity detector for the detection of the degradation products of chemical warfare agents in soil extracts. *Electrophoresis* **2009**, *30*, 507-514.

II. Seiman, A., Makarõtševa, N., Vaher, M., Kaljurand, M., Detection of nerve agent degradation products in different soil fractions using capillary electrophoresis with contactless conductivity detection. *Chemistry and Ecology* **2010**, *26*, 145-155.

III. Kuban, P., Seiman, A., Makarõtševa, N., Vaher, M., Kaljurand, M. In situ determination of sarin, soman and VX nerve agents in various matrices by portable capillary electropherograph with contactless conductivity detection, *Journal of Chromatography A* **2011**, *1218*, 2618-2625.

IV. Seiman, A., Vaher, M., Kaljurand, M., Monitoring of the electroosmotic flow of ionic liquid solution in non-aqueous media using thermal marks. *Journal of Chromatography A* **2008**, *1189*, 266-273.

V. Seiman, A., Vaher, M., Kaljurand, M, Thermal marks as signal processing aid for portable capillary electropherograph, *Electrophoresis* **2011**, *DOI:10.1002/elps.20100057*

VI. Makarõtševa, N., Seiman, A., Vaher, M., Kaljurand, M. Analysis of the degradation products of chemical warfare agents using a portable capillary electrophoresis instrument with various sample injection devices. *Procedia Chemistry* **2010**, *2(S1)*, 20-25.

VII. Seiman, A.; Vaher, M.; Kaljurand, M.; Kapillaarelektroforeesi ristsisendseade kapillaarelektroforeesi analüsaatorisse proovi sisestamiseks (Capillary electrophoresis cross-injection device for sample introduction into a capillary electrophoresis instrument). EE 2008000037, May 27, **2008**

AUTHOR'S CONTRIBUTION

The contribution made by the author to the publications included is following:

I. The author was responsible for CE analysis, data analysis, and interpretation of the results. The author prepared the manuscript.

II. The author performed the coupling of capacitively-coupled contactless conductivity detection (C^4D) to a commercial CE instrument, carried out part of sample preparation, and CE analysis, processed and interpreted the data, and prepared the manuscript.

III. The author was responsible for running part of experiments with genuine nerve agents, developed algorithms for signal processing and peak integration and contributed to the interpretation of CE results.

IV. The author developed and tested algorithms. The author prepared the manuscript.

V. The author was responsible for electrophoretic experiments, data interpretation and preparation of the manuscript.

VI. The author tested the cross-sampler. The author also assisted in writing the manuscript and preparation of figures.

VII. The author prepared the patent. The author carried out all the tests and obtained the results used in the patent.

ABBREVIATIONS

AEDHP	aminoethyl dihydrogenphosphate
BET	Brunauer, Emmett, Teller isotherm
BGE	background electrolyte
BPA	1-butylphosphonic acid
C^4D	capacitively-coupled contactless conductivity detection
CBRNE materials	chemical, biological, radiological, nuclear, and explosive
CE	capillary electrophoresis
COW	correlation optimized warping
CWA	chemical warfare agents
DAD	diode array detection
DAQ	data acquisition
DTW	dynamic time warping
EMPA	ethyl methylphosphonic acid
EPA	ethylphosphonic acid
EOF	electroosmotic flow
FPD	flame photometry
GC	gas chromatography
His	L-histidine
HPLC	high-performance liquid chromatography
IMPA	isopropylmethyl-phosphonic acid
IMS	ion mobility spectrometry
LC	liquid chromatography
LIF	laser induced fluorecence
LOD	limit of detection
LOQ	limit of quantification
MES	2-(N-morpholino)ethanesulfonic acid
MS	mass spectrometry
N/A	not available
PMMA	polymethyl methacrylate
PMPA	pinacolyl methylphsophonic acid
PPA	propylphosphonic acid
PPE	personal protecting equipment
RSD	relative standard deviation
SAW	surface acoustic wave
S/N	signal-to-noise ratio
SPR	surface plasmon resonance
TIC	toxic industrial chemicals
UV	ultraviolet

1 INTRODUCTION

Miniaturization has become an important issue in various fields of science and technology, including electronics, medicine, chemistry, and other areas. This approach together with field analysis as well as the use of portable devices and point-of-care instruments are all important trends in modern analytical chemistry that have been supported by the progress in electronics, engineering, materials science, etc.

Portable objects in general terms could be defined as easily movable, convenient-to-carry, and capable of being transferred or adapted devices in altered situations [1]. For scientific instrumentation more specific features like the use outside the laboratory in the absence of mains power with some degree of miniaturization for relatively easy transportation and deployment have been highlighted. The list of key parameters for high-performance field analytical instruments could include the following [2,3]:

(i) weight and size;

(ii) number of personnel required for installation or operation;

(iii) possibility for modular design for ease of carriage;

(iv) potential vehicle mounting;

(v) impact, deployment, and response time;

(vi) satisfactory analytical performance (i.e. sufficient accuracy, selectivity, and sensitivity);

(vii) minimal sample preparation;

(viii) low consumption of solvents or gases.

Field portable instrument design opens a possibility for chemists to perform analysis wherever a sample is taken. Avoiding sample storage and transportation from the field to the lab reduces significantly the time and cost of analysis. In various environmental and point-of-care clinical analyses, or for the detection of chemical, biological, radiological, nuclear and explosive (CBRNE) materials or toxic industrial compounds (TIC), the time from collecting the sample to obtaining information should be as short as possible for immediate and fast decisions.

The so called “detect-to-protect” paradigm has become a widely accepted strategy for dealing with hazardous TIC or CBRNE materials. Analytical chemistry plays a key role in the success of such an approach. There are three main factors that reduce the efficiency of the detect-to-protect strategy [4]. Firstly, false positive or false negative results are a direct outcome of a low selectivity of an analytical technique. Secondly, the low speed of detection

affects directly the efficiency of a remedial action. And, thirdly, there is always an inevitable delay between the report of attack and an appropriate protective action. As the first two of these reasons have their origin in the nature of an analytical process, the overall effectiveness of the detect-to-protect strategy could be improved with better analytical techniques.

High separation efficiency, relatively short analysis time, low consumption of sample, chemicals, and power along with low technical requirements make capillary electrophoresis (CE) an attractive analytical technique for portable instruments. From the technical side only a separation capillary, high voltage (HV) power supply, and a detector are needed. Hence, the development of a portable CE instrument is a major objective of this thesis.

Despite its many advantages CE, however, is known to be notoriously irreproducible for various reasons. This unfortunate fact is discouraging for many possible applications of this technique. The reasonable reproducibility of the results to be obtained with the aid of commercial instruments can be achieved by applying rigorous column temperature control and robotic auto samplers. Though, such bulky supplements are not conceivable for portable instruments. This dissertation aims to demonstrate that improved sampling techniques, minor technical developments, and the use of advanced software would significantly enhance the reproducibility of analysis by the portable CE instrument.

2 LITERATURE OVERVIEW

2.1 Nerve agents

Organophosphorous nerve agents are one of the most toxic substances ever synthesized. Although having found limited use so far, the determination of these substances or their degradation products is still an important field of research, especially in the last ten years which have seen terroristic activity to be on the rise. Besides, there are at least three documented cases of use of nerve agents in the last 25 years, such as in the Kurdish village of Birjinni (1988) [5], Matsumoto city incident (1994) [6], and Tokyo subway attack (1995) [7]. Therefore, there is a continuous need for rapid and reliable methods for the detection of nerve agents and their degradation products. The nerve agents are categorized according to structure into two groups: G- and V-type ones. Both types of the agents have several similar structural features such as the existence of a double bond between the terminal oxygen and phosphorous, and one or two lipophilic groups and one leaving group bond to the phosphorous. These features make the nerve agents unique and distinct from the large group of organophosphates, such as herbicides, pesticides, insecticides, *etc*., that can be widely found in soil due to their use in agriculture.

In aqueous environments the organophosphorous nerve agents more or less easily hydrolyze to produce non-toxic and more stable compounds. The most important degradation products of nerve agents are alkyl alkylphosphonic acids

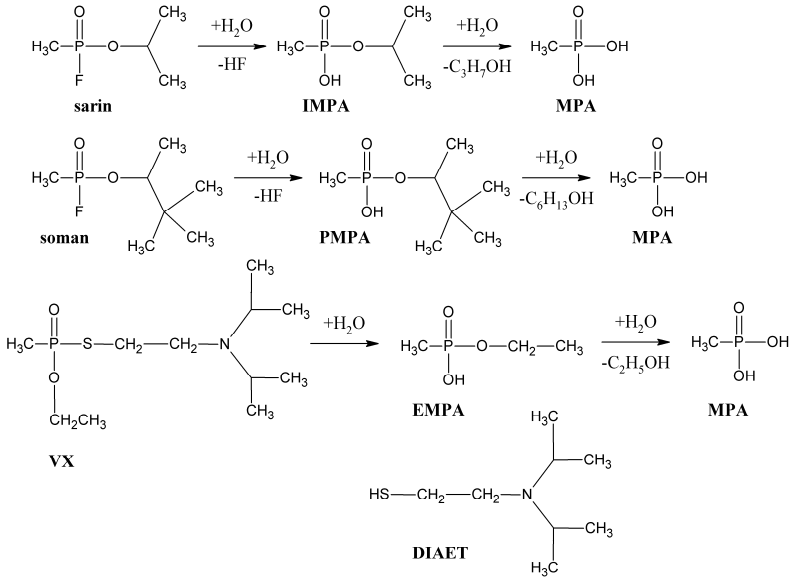

Figure 1. Main hydrolysis pathways of sarin, soman and VX.

which are suitable for the verification of the presence or use of organophosphorous nerve agents even if the nerve agents themselves have already been degraded. The hydrolysis of nerve agents is a two-step process that is described in Figure 1. In the first step – sarin and soman hydrolyze to form isopropyl methylphosphonate (IMPA or pinacolyl methylphosphonate (PMPA) respectively. VX follows different patterns of hydrolyzation depending on the pH of the solution. In case pH > 6.5, ethyl methylphosphonate (EMPA) and diisopropylaminoethanethiol (DIAET) are formed [8]. In the second stage, all three alkylphosphonates further degrade to methylphosphonate (MPA) and alcohol. However, this step is much slower than the first one.

The most popular method for the detection of nerve agents seems to be ion mobility spectrometry (IMS). It is an effective method capable of monitoring gaseous phase samples providing rapid detection of nerve agents [9]. Besides IMS, there are other interesting techniques for the detection of nerve agents like surface plasmon resonance (SPR), surface acoustic wave (SAW), and flame photometry (FPD) [10]. The pros and cons of various approaches for the detection of nerve agents have been discussed in a recent review [11]. As the agent is often deposited on a surface close to the attack site and is subject to hydrolysis due to atmospheric or soil humidity, the effectiveness of gas phase detectors is questionable under these circumstances.

Analysis of the breakdown products of nerve agents in liquid samples could be made by means of various separation methods such as gas (GC) [12] and high-performance liquid chromatographies (HPLC) [13] and capillary electrophoresis (CE) [14]. Nowadays the chromatographic methods developed for this purpose are mostly coupled to mass spectrometry [15,16]. GC is a suitable tool for analysing easily volatile nerve agents. However, because of their high polarity, low water solubility and low volatility, degradation products of nerve agents cannot be directly analyzed using GC. Therefore a derivatization procedure for the conversion of degradation products into more volatile compounds is needed. A detailed review of possible separation techniques for the analysis of nerve agents is given in [17].

The fast, simple and relatively inexpensive capillary electrophoresis (CE) is often preferred as phosphonic acids need no derivatization. CE analysis requires only simple sample preparation, involving dilution and filtration, and easy equipment operations and maintenance. CE is less sensitive to sample matrix and, therefore, real samples such as aqueous soil extracts and river water can be subjected to CE analysis [14,18,19].

In case of CE, both direct [14] and indirect UV-detection [20,21] may be used to detect the degradation products of organophosphorous nerve agents, though the latter is preferred, because it is more sensitive as alkyl phosphorous acids do not contain any chromophoric groups. In [22] it was shown that reversing the electroosmotic flow (EOF) combined with an electrokinetic sample injection can

provide more than a 100-fold improved LOD compared with the hydrodynamic injection. The breakdown products of organophosphorous nerve agents can easily be detected with C^4D [23, 24, 25] as they are strong acids and therefore dissociate completely in aqueous environments. Although the selectivity and sensitivity of the conductivity and indirect UV detections are rather similar, as reported in [20,23], the former has one advantage over the latter, and this is its potential use in portable devices.

2.2 Portable capillary electrophoresis instruments

The detection of chemical, biological, radiological, nuclear, and explosive (CBRNE) material that may be used to do harm poses analytical challenges which are exceptional in both quantitative and qualitative terms [26]. Portable devices could resolve stringent requirements for a fast and efficient CBRN detection to identify and quantify unknown entities. The transport and handling of the portable equipment must be addressed at an early stage in the system design to ensure maximum usability. Weight and size, number of personnel required for the operation of the equipment, vehicle mounting and response time, *etc*. are all key aspects to be considered in the system design stage [2].

Miniaturization is often a key way of developing a technology to make an instrument truly portable. This works well in a number of applications. It is not always possible, however, to miniaturize devices without compromising one or more factors. Capillary electrophoresis (CE) has many advantages over chromatographic separation techniques in terms of potential miniaturization. To name just a few, the CE device consists only of a high-voltage supply, a capillary, small background electrolyte (BGE) vessels and a detection system. What is most important is that CE requires no use of complex mechanical high-pressure pumps as liquid chromatography does. Recent applications of CE in portable instruments have been reviewed by Ryvolova *et al*. [27].

2.2.1 Capacitively-coupled contactless-conductivity detection

For portable CE instruments the most challenging task is to find an appropriate detection system as the most widely used UV-absorption detection is not suitable to be employed in portable devices owing to the high power consumption of light sources of the latter. Energy consuming UV-lamps could be replaced by light emitting diodes (LED), nevertheless, complex optics must still be used. The most popular alternatives to the UV-detection may be found amongst electrochemical detection techniques. Amperometric [28,29,30,31], potentiometric [28,32,33,34], and conductometric [35,36,37] detection systems may all be used in portable capillary or microchip electrophoresis devices. In recent years, the capacitively-coupled contactless-conductivity detection (C^4D) has become the most widely used electrochemical detection technique [38,39,40,41]. Its detection cell is of a very simple construction compared with

those of amperometric and potentiometric detection, though amperometric detection demonstrates a better limit of detection (LOD).

C^4D is a universal and sensitive tool that was first introduced independently by Zemann and colleagues [39] and da Silva and do Lago [38] in 1998. C^4D detectors are basically constructed of two axially-placed tubular electrodes which encompass a separation capillary. This means that the signal of C^4D is gathered longitudinally along the capillary instead of the transversal mode of conventional absorbance detection schemes. One of the two electrodes is excited with an AC signal and the other electrode is used to register the same signal after it has passed the cell.

In recent years C^4D has been implemented in a miniaturized electrophoresis microchip and portable CE systems. For instance, the portable CE system with the C^4D detection developed by Kubáň and colleagues can run the detector and the data acquisition system from the batteries for nine hours [42]. The high-voltage power supply with both polarities has an output of 15kV. The excitation sine wave is in the frequency range of from 100 to 1000 kHz and in the voltage range of from 2 to 20 V_{pp}. The samples are introduced in an electrokinetic or hydrodynamic mode by a manual turning or moving of the sample tray. A particular device runs on four 12V batteries. The detection system uses two batteries out of four. The high-voltage power supply and the data acquisition system use one battery each.

Xu and colleagues [43] have published the description of their portable CE instrument that is about the same size as the instrument developed by Kubáň and colleagues [42], but lighter, and its batteries last for only a couple of hours. The detector is working at a constant excitation frequency of 125 kHz and the signal voltage of 240 V_{pp}. The design of the detection cell is completely different from that of two commercially available C^4D instruments [44,45], in which tubular electrodes are placed in a rectangular aluminium case. It consists of a capillary, a copper electrode and a shielding with insulator layers screwed together between a circular-shaped aluminium cover and the base plates. The separation of eleven low-molecular-weight organic acids and sixteen chlorinated acid herbicides took place in single analysis which lasted for thirty-five minutes.

Wang and Fu developed a miniaturized CE system with the contactless-conductivity detection and the flow-injection sample introduction [46]. A 5.5 cm fused silica capillary was fixed to the detection cell consisting of two 2 mm tubular electrodes in between the glass slide and the silicone elastomer layer. The performance of the device was studied by analysis of cations in the surface water.

2.2.2 Sample injection

Using portable CE instruments in a field for analysis of toxic waste materials, detection of CBRNE materials, *etc*., could easily have a hazardous impact on the health of the person operating the instrument. It is very likely that some sort of personal protecting equipment (PPE) must be used. The design of the sample injection in the portable CE instrument must be carefully considered for the operation of the instrument to be robust enough for the use with PPE and as fast as possible to keep the exposure to hazardous materials minimum. Auto-samplers commonly used for sample injection in commercially available bench-top CE instruments might not be suitable for field portable CE instruments as they cannot be considered robust enough.

The portable CE devices reported earlier by several different groups [42,46,47,48,49,50] apply the electrokinetic or hydrodynamic sample injection familiar from bench-top CE systems. This kind of sample injection involves a lot of repeated manipulations with buffer and sample vials. These manipulations are automated in bench-top CE instruments, but have to be carried out manually in portable devices. For portable devices a simple, robust and quick sample injection is always favourable, especially when field analyses of toxic pollutants, nerve agents, *etc*. are performed. Moreover, it is very difficult to operate with tiny vials with protective gloves of PPE.

Gorbatšova *et al*. have integrated a digital microfluidic system based on electrowetting-on-dielectric (EWOD) phenomenon into a portable CE instrument [51]. Sample injection is performed by actuating electrodes of the digital microfluidic device for transporting manually the dispersed sample and buffer droplets in succeeding order under the capillary. This sort of an integrated system opens an interesting field of opportunities. However, in case of field experiments, especially when PPE is used, a certain drawback of this system concerning robustness could be seen.

One candidate for a robust sampling device for a portable instrument could be a cross-sampler. The cross-sampler [52] and its modifications – the T [53] and double-T [54] injection – have been used in microchip electrophoresis ever since the first electrophoresis microchips were introduced. Electrophoresis microchips, in general, consist of at least two channels – one is for sample injection and the other for separation. In microchips, the electrophoretic separation process usually takes place in two discrete steps. First, the sample is loaded into the sample injection channel and the sample plug is formed. Second, the sample plug is loaded into the separation channel and the separation process begins. While separation is always driven by electrophoretic forces, the sample plug may be formed by different forces, electrophoretic and pressure being most common.

In practice, problems occur when crossing capillaries are connected, as the dimensions of capillaries make it mechanically extremely complicated. There are only a few publications on cross-sampler systems for conventional CE. Zare and Huang have patented a cross- or T-shaped device for CE [55]. One makes the device by boring two holes in the separation capillary at the selected location, then introducing elongate guide members into the holes and threading members into the sample injection capillaries until the separation capillary contacts the sample injection capillaries. The way the device is operated is not defined in the patent, making both the hydrodynamic and electrokinetic injections possible. Tsukagoshi and colleagues [56] demonstrated a rather simple cross-sampler, as capillaries were fixed to the holes that were drilled into a Tygon tube. Their device was operated in multiple steps. First, the sample was electrokinetically driven from the sample reservoir to the sample waste reservoir so that it filled the cross-section of the sampler. Second, the sample in the cross-section was separated by the application of high voltage between the buffer and waste reservoirs.

Kulp et al. [57] used a cross-sampler automated by pressure for an on-line monitoring of enzymatic reaction kinetics. Later the same cross-sampler was redesigned for the use in field analyses. The pressurized control of the cross-sampler was replaced by a simple manual injection using plastic syringes. These modifications are part of this thesis [I,VI,VII] which used a portable CE instrument equipped with the C^4D detection and the cross-sampler device for the analysis of the degradation products of nerve agents.

2.3 Signal processing

Due to the specific nature of analysis of nerve agent degradation products, a very fast interpretation of the results is needed for executing an appropriate counteraction plan in the worst-case scenario. The circumstances are the same for the detection of TIC, CBRN and other materials. The speed of interpretation of CE analysis results would definitely benefit from properly chosen signal processing algorithms. Besides, fully automated signal processing algorithms would enable the use of the instrument by unqualified personnel, who is capable of running the analysis, but does not have enough experience to make crucial decisions.

Moreover, proper signal processing algorithms could solve some reproducibility problems associated with CE so often. Usually, problems with reproducibility are revealed by irreproducible peak areas and migration times. This affects both a quantitative and a qualitative analysis as concentrations of compounds are usually calculated using peak areas and it is very likely that analyte species are identified according to migration time or electrophoretic mobility. The low reproducibility of peak areas is mainly caused by an inaccurate sampling. Though, poor integration algorithms can also contribute to quantification errors

[58]. The reproducibility of the quantitative analysis can be controlled by the use of very precise injection procedures, though mostly it is more convenient just to use internal standards for correction purposes [59].

The need for signal processing is no news to separation scientists. Various signal processing algorithms have been developed from the early days of chromatography [60]. Commercial instruments have always been provided with algorithm packages for signal processing and peak integration. Apparently, the software provided by the manufacturer of CE instruments is not good for fixing the EOF drift or correcting the baseline.

Part of this thesis was focused on developing various signal processing algorithms with the aim to improve the reliability of the results and the simplicity of the interpretation of electropherograms [V]. Although the algorithms were developed with the intention to be used in a portable CE analyzer for the analysis of nerve agents, their principle is universal and therefore they could easily be applied to any kind of CE analysis. The algorithms developed cover every basic step of data acquisition from baseline correction needed for a precise peak area integration and detection of peaks to the integration process.

2.3.1 Baseline correction

Noise and baseline are two common problems in instrumental analysis as both can lead to the reduced precision. Noise, a high-frequency signal, which is mostly associated with the electronic components of the instrumental set-up, is usually removed by moving average filtering, exponential smoothing, Savitzky–Golay filtering, Fourier or wavelet transform. Baseline drift is a low-frequency noise resulting mainly from temperature variations during separation, or the presence of impurities in the composition of BGE. Baseline is a common problem not only in the separation science, but also in spectroscopy. The approximation of the baseline has been a general method to tackle baseline drift problem. While calculating peak areas or heights, most integration algorithms draw a straight line as a baseline from the start to the end of the peak. Calculations will lead to errors when the real baseline does not coincide with the straight line. Therefore, for reliable results the baseline needs to be corrected before the integration of peak areas can be done. So far reports have covered baseline correction via a multiple-pass moving average filtering [61], cubic smoothing splines with multivariate data analysis [62], an improved iterative polynomial fitting [63], and a wavelet analysis [64,65,66]. Wätzig [67] has developed an algorithm that determines all local maximums as potential baseline points. Of course, some of these maximums are actually located at peak maximums. These points are removed in the course of a secondary outlier elimination test.

The reliable peak identification and precise integration are as important as the baseline correction for an accurate quantification. A simple option for peak detection is selecting the part of the signal that exceeds a certain threshold. This sort of approach is very sensitive to the baseline fluctuation, but can be very effective and extremely fast in case the baseline is properly removed. The separation capability of CE is limited, and, therefore, the baseline separation of peaks is quite often not achieved. The threshold based peak detection apparently is not capable of telling how many components there are in a peak. Therefore, more advanced peak detection techniques are preferred. Algorithms that use the second or sometimes even the third derivative are capable of evaluating properly the actual number of peaks [68]. For determination of exact peak boundaries there is an algorithm that alternatively expands initial boundaries by one data point at the time to the left or the right [69]. As a result, the peak area is increased. The process stops when the increase is smaller than the threshold which is set by a standard deviation of the baseline noise. Together with the baseline correction algorithm using smoothing spline functions, the RSD reduction of roughly 50% was achieved.

2.3.2 Electropherogram alignment

For historical reasons a comparison of electrophoretic mobilities calculated according to migration times has been the most widely used approach for qualitative analysis. Only lately, with the development of fast scanning diode array detectors (DAD), it has become possible to use spectral data for identification purposes. Unluckily, with C^4D the peak identification based on electrophoretic mobilities is the only option.

While using electrophoretic mobilities for identification, it is essential to have a good reproducibility of migration times. The shift of migration times is a widely witnessed problem caused mostly by a non-reproducible EOF in between the runs or even during a run. For a good reproducibility quite a number of parameters must be precisely controlled, temperature control [70] and pre-treatment of the inner capillary surface [58,70] being the most common ones. Nevertheless, the adsorption of analytes on the inner surface of the separation capillary may result in heavily affected migration times that could lead to a faulty identification of unknown species.

Dynamic time warping (DTW) [71,72,73] and correlation optimized warping (COW) [72,73,74] are algorithms that have shown a great potential for the alignment correction of various signals in spectroscopic and chromatographic techniques. Therefore, these algorithms should be also suitable for improving the alignment of different electropherograms. However, DTW is sensitive to the difference in peak intensities. Assumed to preserve peak areas and shapes COW is considered better than DTW. In situations where there are significant changes in peak shapes like severe peak tailing the COW algorithm will face problems

[75]. Simply put, DTW and COW algorithms are built to match two signals so that their difference would be minimal. The nature of these algorithms is the main reason why they face problems when aligning electropherograms having a different number of peaks. For example, when trying to align an electropherogram with one peak to an electropherogram with peaks of several standards, it is very likely that a single peak will be aligned to a wrong peak.

Alternatively, one could use CE specific alignment techniques such as standardization by replacing time axis with electrophoretic mobility axis [76], or normalization of migration times with the aid of two identified peaks [77]. These CE specific aligning tools are based on correcting differences in EOF between the runs. However, there is no reason to expect that changes of the EOF flow rate will occur only in between the runs. It is more than likely that these changes could also happen during one run. Therefore, part of this thesis was devoted to improving the reproducibility of migration times by aligning electropherograms according to changes of EOF rate during a run. Of course, this is only possible if changes in EOF velocity could be monitored during the experiment.

2.3.3 Monitoring the electroosmotic flow

The electrokinetic phenomenon present in CE that carries cations, neutral molecules and anions from the sample inlet towards the detector in the same direction is known as EOF.

In CE, analytes are mostly identified by their peak migration times. Therefore in CE experiments the reproducibility of the migration time is of crucial importance. The latter is directly affected by the EOF which depends on the ζ-potential of the capillary wall, the electric field, and the temperature. The changes in pH, temperature, buffer composition, or the chemical composition of the capillary surface can lead to changes of the magnitude of the rate of the EOF. Therefore it is necessary to monitor the rate of the EOF to correct the changes in migration times caused by an irreproducible rate of the EOF.

The neutral marker method is a straightforward approach to measuring the rate of the EOF [78,79,80,81]. Neutral species are inserted in the sample plug and the EOF rate is calculated using the migration times of the species. The neutral marker method is limited to providing a single, average value of the EOF for the time marker migrating through the capillary. This means that the neutral marker method does not represent changes of the EOF after the marker has passed the detector. Besides, the method is not very suitable for measuring weak electroosmosis as it takes a very long time for the neutral marker to reach the detector. Righetti and co-workers have proposed an alternate time-saving method that is based on the injection of the neutral marker by means of electroosmosis [82]. After injection, a low pressure is applied to the capillary and the marker is recorded at the detector. The EOF rate is calculated from the quantified peak area. Weighting the effluent from the capillary is another

approach to measuring an average rate of the EOF. Due to the extremely low-volume EOF rates, the method is impractical, though has demonstrated good precision [83].

A technique that is used to measure the average rate of the EOF and is very similar to the neutral marker method is called the current monitoring. The solution filling the capillary is electrophoretically replaced by BGE of different concentrations. Consequently, the total conductivity in the capillary changes as the solution at the inlet replaces the solution in the capillary. The average rate of EOF is calculated using the time it takes from the beginning of experiment till the electric current becomes constant as the capillary has been filled with the solution from the inlet. The current monitoring has been used to measure the EOF rate in capillaries [79,84] and microfluidic devices [85,86].

The above-mentioned techniques are able to provide an average value of the EOF rate and, therefore, results could be used to fix the drift in the EOF velocity only between the runs. Many research groups have made an effort to develop systems for an on-line monitoring of the EOF. Zare and co-workers proposed a method for the real-time measurement of the EOF in CE [87]. The operating mechanism of the method proposed is based on the measurement of the dilution of the fluorescent dye solution introduced into the BGE downstream the detection zone. The fluorescent dye and the exuding buffer are mixed on-line, using a concentric capillary design for the post-column solution mixing. Another on-line method for monitoring the electroosmotic flow in CE separation is based on a periodic photobleaching and the laser-induced fluorescence (LIF) detection of the dilute neutral fluorophore mixed with a BG E [85,88,89]. Before experiment, the dilute neutral fluorophore is simply added to the running buffer. Therefore the post-column detection and solution addition are unnecessary.

Recently do Lago and co-workers proposed a new method for the measurement of the EOF by a contactless conductivity detection based on the use of the so-called thermal marks [90]. Thermal marks are small disturbances in the detector signal produced by a punctual heating of the separation capillary that move with almost the same velocity as the EOF and therefore could be used for monitoring it [90,IV]. These disturbances can be easily generated by heating the capillary with short pulses, using a tungsten filament or a surface mount device (SMD) resistor.

Heating causes changes in the electrophoretic mobility of BGE components. As these changes are not equal for different BGE components, a concentration dependent disturbance is formed. The nonhomogeneity zones created by thermal marks move through the capillary. Ideally they would have an effective mobility equal to that of the EOF. However, the problem of moving concentration boundaries is more complicated. The behaviour of the concentration boundaries created by thermal marks could be explained by the system zones theory [91]. As it is possible to observe the difference in migration between a neutral marker

and an actual EOF [80], therefore the difference in electrophoretic mobility between thermal marks and the EOF is also possible

However, it has been demonstrated that thermal marks are moving with the velocity of the EOF if the difference in concentration between the thermal mark and BGE is low [90].

Thermal marks could be monitored with the conductivity detection or indirect mode of UV or LIF. Thermal marks are usually produced somewhere in between the sample inlet and the detecting point. Therefore they have a relatively shorter migration time than most of the sample components do. Moreover, thermal marks could be produced during a run as there is no need for HV interruptions. This means that it is possible to produce several thermal marks and monitor EOF during one run.

In this thesis it is demonstrated how to use thermal marks to determine changes in EOF during the experiment and how this data can be used for the normalization of electropherograms.

3 OBJECTIVES OF THE STUDY

The main goal of the present thesis is to use a capillary C^4D-CE instrument for the analysis of the degradation products of nerve agents. The aims of the study may be split into three major tasks involving the development of the C^4D-CE instrumentation, the application of CE to the analysis of nerve agent degradation products, and the elaboration of the signal processing algorithm for developed applications. Instrumental goals of the research are as follows:

(i) developing of a simple and robust sample injection technique for the field portable CE instrument.

(ii) testing of the performance of the portable CE instrument equipped with a C^4D detector and developed cross-sampler

Phosphonic acids as degradation products of their parental nerve agents could possibly serve as fingerprint markers for the verification of the use of nerve agents. Therefore, further goals of this study are:

(iii) to find and optimize separation procedures for the analysis of phosphonic acids by means of a portable C^4D-Ce instrument;

(iv) to develop sampling procedures for field experiments with the intention to sample from different matrixes;

(v) to test the sampling and separation procedures with genuine nerve agents;

(vi) to study the adsorption behaviour of phosphonic acids in different fractions of loam and sand samples.

The interpretation of raw signals in CE can be challenging if there are unknown peaks, or the signal is corrupt due to baseline fluctuations and the drift of EOF mobility, *etc*. Signal processing may be required before the results can be interpreted. Moreover, situations in which the number of electropherograms is very high, or CE is used for monitoring purposes, or the personnel operating the instrument is not qualified enough would benefit from an automatic signal processing. So, a further goal of this study was to develop a package of signal processing algorithms for:

(vii) an automatic baseline correction based on testing local extremes;

(viii) an electropherogram alignment based on the information gathered with the aid of thermal marks, and the elaboration of a novel interface for generating thermal marks;

(ix) peaks identification using a fuzzy matching algorithm to compare peaks of the sample electropherogram to those of the reference electropherogram.

4 EXPERIMENTAL

4.1 Instrumental

4.1.1 Portable CE instrument

The portable CE instrument (Figure 2) with C^4D and the cross-sampler used in this study were made entirely in-house. The dimensions of the whole system were 330×180×130 mm and it weighted less than 4 kg. The CE system employed EMCO DX250 (Sutter Creek, CA, US) HV power supplies. The high-voltage output of the system was up to 25 kV. The operating time of the system running on batteries was at least 4 h. This should be enough as it is comparable to the battery supply of a standard laptop computer. The system used ten commonly available AA-type rechargeable batteries with an overall output of 15 V.

The detection cell (Figures 2A-3) used in the portable CE device was similar to the ones used in commercial devices. The cell itself had been built into a rectangular piece of alumina in which three holes had been milled for two tubular electrodes and an operational amplifier. Two tubular electrodes made of syringe needles with a length of 8 mm and a gap of 0.8 mm between them were located in separate chambers and the alumina between and around them is grounded and acted as a shielding. One of the electrodes was excited with a 60V peak-to-peak sine wave oscillating in a frequency range of from 50 to 300 kHz. The signal was picked up by the second electrode and further amplified. The exciting frequency and amplification amount were controlled by an external computer using software written in-house. In all experiments the default

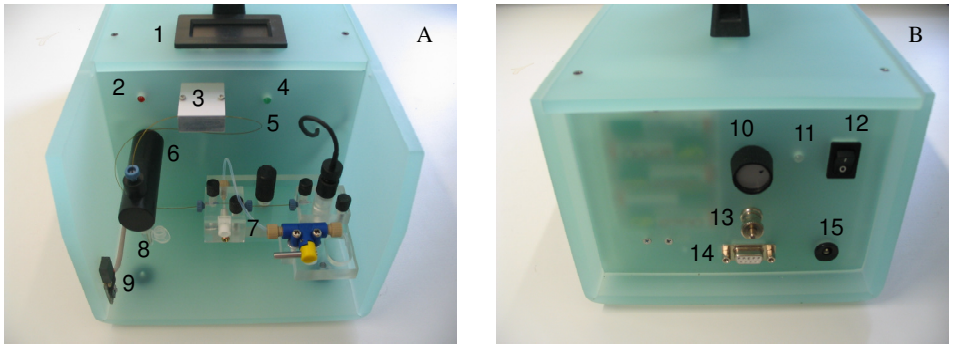

Figure 2. Front (A) and rear (B) view of the portable CE device. 1 – ammeter, 2 – high voltage indicator, 3 – detection cell, 4 – power on indicator, 5 – separation capillary, 6 – high voltage lead, 7 – cross-sampler, 8 – BGE vessel, 9 – safety switch, 10 – HV knob, 11 – battery charging indicator, 12 – power on switch, 13 – connection for grounding, 14 – RS-232 port, 15 – connection for a 18V adapter

frequency was 200 kHz. The influence of the oscillating frequency on the S/N ratio and the height of the peak were not studied. Data acquisition was carried out with the in-house 16-bit analog-to-digital converter (ADC) integrated inside the portable CE system detector electronics. An RS-232 port was used to communicate with the computer. With new laptops containing no RS-232 ports, a regular serial-to-USB adapter must be used.

4.1.2 Cross-sampler

The cross-sampler (Figures 2A-7 and Figure 3) used in the CE instrument was built according to ideas familiar from microchip electrophoresis. It was made of two pieces of a capillary, a Teflon tubing and necessary fittings which all had been connected to a rectangular PMMA block. The dimensions of the sampler (Figure 3A) were 22×22×8 mm. There were drilled sample injection and separation channels in the device. At different endings of the separation channel two capillaries with horizontally smooth endings were inserted. The capillaries were fixed so that their endings meet at the crossing channel. The device used fused silica capillaries with a length of 6 and 48 cm. A longer capillary served as a separation capillary (Figure 3B). The effective length between the crossing point and the detection cell was 42 cm. The fused silica capillaries (i.d. 75 µm × o.d. 365 µm) were obtained from Polymicro Technologies (Tucson, AZ, US).

A special socket (Figure 3C) to be used with threaded or conventional syringes was inserted into one side of the sample injection channel crossing the separation channel. The Teflon tube with an outer diameter of 1/16” was inserted

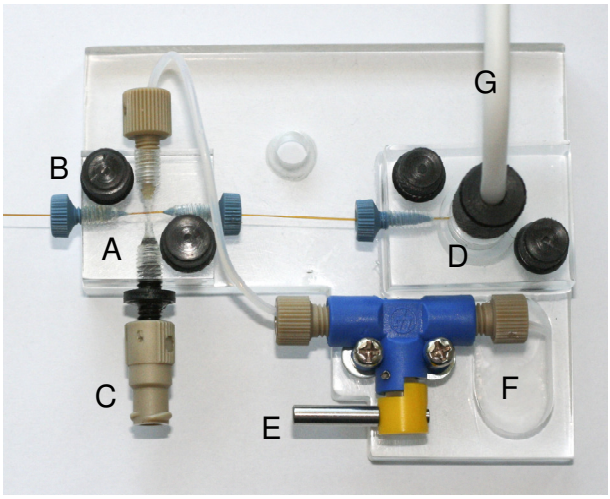

Figure 3. The cross-sampler used in the portable CE instrument. A – cross-sampler, B – separation capillary, C – socket for syringe, D – BGE vessel, E – shut-off valve, F – waste reservoir, G – high voltage lead.

into the other side of the sample injection channel and connected to the waste reservoir (Figure 3F). The sample was injected using syringes. During the injection the sample solution was pushed into the injection channel and part of the sample solution was inserted into the separation capillary while most of the liquid exited through the waste channel. The size of the injection was defined by the configuration of the system as the splitting ratio of the liquid flow between the separation capillary and the waste channel was defined by the hydrodynamic resistances of both channels. As the cross section of the capillaries was surrounded with the sample solution during analysis, it was possible that there was continuous diffusion of the sample into the separation channel during the analysis run which would have affected the baseline level. The size of the gap between two capillaries is crucial in terms of reducing the diffusion of the sample solution into the separation capillary during the run. Moreover, two capillaries must be perfectly in-line, otherwise the laminar flow of the liquids may be interrupted and the sample solution flow into the separation capillary will be increased by the turbulences formed. Ideally the gap between the capillaries is no bigger than the inner diameter of the capillary. In this case, the gap width was estimated with a microscope to be about 30 μm. The capillaries and tubes were fixed with 10/32" threaded *Upchurch Scientific Nanoport* (Oak Harbor, WA, US) fittings.

In the middle of the waste channel there was a shut-off valve (Figure 3E, *Upchurch Scientific* part no. P-782). During the sample injection the valve is opened and the excess sample exits through the waste channel. When the valve is closed, it is possible to rinse the capillaries as the liquid injected into the device cannot exit through the waste channel and is pushed into the capillaries instead. With this construction it was possible to reconfigure the device from the sampling mode to the rinsing mode just by changing the position of the waste channel valve.

4.1.3 Modifications in the CE instrument

The portable CE instrument used for the analysis of genuine nerve agents was an improved version of the instrument described above. The cross-sampler was replaced with the sample stream splitter [III,VI,92]. The liquid flow into the system during the injection is split between the separation capillary and the waste vial. The sample stream splitter serves as an inlet BGE vial. Therefore, the sample liquid must be replaced with BGE before the start of the analysis. This will require one extra operation compared to the use of the cross-sampler. However, the sample stream splitter is considered more robust as the capillaries do not have to be perfectly in-line. Due to the fact that BGE must first be replaced by the sample solution and later back to BGE, the consumption of the sample solution and BGE is very high (per run 0.5 and 1 ml, respectively).

For the adsorption analysis of nerve agent degradation products [II] all experiments were carried out using a commercially available Agilent Technologies CE instrument (Waldbronn, Germany) equipped with a diode array detector. For detection a C^4D detector was used instead of the UV detector. The C^4D detector is exactly the same as that used in the portable CE instrument. The combination of the in-house made C^4D detector and the conventional bench-top Agilent instrument enabled application of the detection schemes developed for C^4D to a large number of samples as the Agilent instrument provides possibilities for programming long sequences of separate analyses. The total length of the separation capillary was 55 cm. The length of the capillary to the C^4D cell was 45 cm and to the DAD cell, 49 cm. The sample was injected hydrodynamically for 10 s (50 mBar). In all experiments, the cartridge with the separation capillary was thermostated at 25°C. Separation voltage was 20 kV.

The CE system used for preliminary experiments with thermal marks [IV] employed a prototype version of the C^4D detection combined with a commercially available 0–30 kV Spellmann CZE2000 (Haupauge, NY, USA) HV power supply and the data acquisition system applied a 12-bit analog-to-digital converter (ADC) by ADAM modules (Advantech Inc., Taipei, Taiwan). The excitation voltage of C^4D was 60 V peak-to-peak and the oscillating frequency 180 kHz.

4.1.4 Generation of thermal marks

Thermal marks were generated using a heating coil constructed of a stainless steel wire (o.d. 100 µm) wrapped five times around the separation capillary (Figure 4B,C) [V]. A general DC power supply was used for heating purposes. The heating coil was located 8 cm from the detection point. The computer controlled relays of an ADAM 4060 module (Advantech Inc., Taipei, Taiwan)

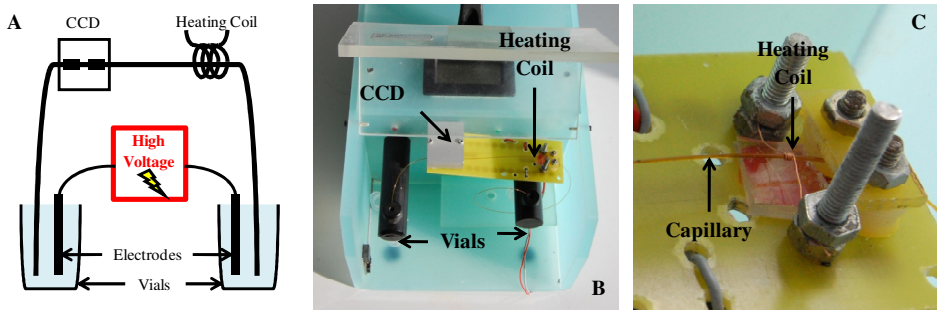

Figure 4. The portable CE instrument with a generator of thermal marks and C^4D detector. A – schematic of CE instrument, B – C^4D detector, heating coil for generation of thermal marks, C – closer look of the heating coil.

were used for switching the heating on and off. The relays were controlled with the custom software written in a Matlab environment (The Math Works, Inc., Natick, MA, USA). The precise parameters for generating thermal marks were 20 V and 0.5 s. The parameters were chosen so that the thermal marks produced would have maximum possible amplitude. Apparently, there is a limit of thermal energy that can be transferred from the heating coil to the capillary without damaging the solution inside the capillary. Even a slightly higher heating voltage or a heating period longer than 1 s will mess up the experiment. Attempts to produce more intensive thermal marks ended with ruined experiments witnessed by the drop in the electric current and the detector signal.

The initial experiments with thermal marks [IV] were carried out using the tungsten filaments of common light bulbs to generate thermal marks as proposed by do Lago's group [90]. The glass bulb was carefully removed and the tungsten filament was placed in contact with a fused silica capillary. The 100 W light bulbs were powered with an external power supply, the applied voltage being in the range of from 10 to 40 V. The lowest voltage capable of producing still visible thermal marks was chosen separately for each experiment.

4.2 Sample preparation and extraction

4.2.1 Genuine nerve agents

The extraction procedures carried out with genuine nerve agents were similar to those used in the adsorption analysis of nerve agent degradation products. The validation of extraction procedures was done at a testing site near Tapa, Estonia by using NA degradation products and the help of the staff of the Pioneer Battalion of the Estonian Army. Experiments with genuine nerve agents were carried out at a testing site near Vyškov, Czech Republic. The sample preparation and extraction procedures of nerve agents were performed by the staff of the testing site under the licence of the Ministry of Defence and Armed Forces of the Czech Republic.

Five different matrices (Teflon, ceramic tile, concrete, grass and soil) with an equal surface area of 25 cm^2 were contaminated with 100 mg of a pure nerve agent (sarin, soman, VX). During exposure the samples were kept outdoors (temperature 9°C). The samples were prepared in two batches by using the exposure time of 30 minutes and 3 hours, respectively. After the elapsed exposure time the samples were collected using the procedures described below.

After the application of the nerve agent on Teflon, a ceramic tile or concrete matrices, the surface of the matrix was carefully wiped with a DI water pre-moistened Ghost wipe tissue (Environmental Express, Mt. Pleasant, South Carolina, USA) by using tweezers. The tissue was placed into a plastic sample vial containing 10 ml of DI water. The nerve agent hydrolysis products as well as the unhydrolyzed nerve agents were extracted by vigorous shaking for 1

minute. The extract was filtered through a 0.45 µm filter (Filtropur S, Sarstedt, Numbrecht, Germany). Internal standards (400 µM AEDHPA, 100 µM salicylic acid) were added to the filtered sample, which was then directly injected into the CE system.

Soil and grass matrices consisted of 20 g of soil and 1 g of finely cut grass, respectively. After the application of the nerve agent, the samples were placed into a plastic sample vial containing 10 ml of DI water and extracted by vigorous shaking for 1 min, followed by filtration through a 0.45 µm filter, the addition of internal standards and the direct injection of the latter into the CE system.

4.2.2 Soil samples in adsorption analysis

Environmental soil samples were collected from two different locations in Estonia. The sand sample was taken in a park in the city of Tallinn (+59° 23' 42.13", +24° 40' 37.02") and that of loam, in a forest in Kõpu rural municipality, Viljandi County (+58° 19' 34.72", +25° 17' 45.19"). The samples were collected from the surface layer of soil at a maximum depth of 5 cm. The sand and loam samples had not been exposed to nerve agents or their degradation products before. The sampling sites were chosen far away from agricultural areas to avoid the possible contamination of samples with the other types of organophosphates used in agriculture, such as herbicides or insecticides.

A gravimetric analysis was used to determine the organic content of soil samples. Firstly, the crucibles used for the analysis were applied to 550ºC for 4 h in a muffle furnace to gain constant weight. Secondly, after cooling down for 30 min the crucibles were weighed and about 1 g of a particular soil sample was weighed into the crucibles. The soil samples were treated for 4 h at a temperature of 550 ºC. After a 30-minute cooling the crucibles with temperature treated samples were weighed again. The organic content of soil samples was calculated using the difference between the two masses. 4 h was long enough for all samples to lose their organic part.

The adsorption of phosphonic acids in soil may be considered as a sum of physicosorption and chemisorption. A simple explanation for this could be as follows. Phosphonic acids are adsorbed onto inorganic soil particles by undergoing physicosorption, while their adsorption onto the organic part of a soil sample takes place under the mechanism of chemisorption. This simplified theory may be applied to explaining the adsorptive behaviour of phosphonic acids in different types of soil. Therefore the organic content of soil samples was determined.

Data on the organic content of soil samples is presented in Table 1. The organic content of loam samples (5.64 to 7.03%) was ten times as high as that of sand samples (0.50 to 1.24%). The organic content of the finest fraction of the sand sample was about 2.5 times as high as that of the other two fractions. This means

that the organic matter of the sample contained small fractions of clay, silt and very fine sand. However, in case of loamy soil, the respective figures were slightly different. So, the organic content of its medium fraction was the highest and that of the finest fraction, the lowest.

Table 1. Organic content of different soil fractions.

Size of a fraction, µm	Organic content,%	
	Sand	Loam
below 100	1.24	5.64
100 to 200	0.55	7.03
200 to 400	0.50	6.05

Loam and sand samples were dried at room temperature until the mass of both samples was constant. The procedure took three to four days. After that the samples were fractionized by particle size by using three sieves with different hole sizes. The sand and loam samples were sieved into three fractions: <100, 100 to 200, and 200 to 400 µm. The samples with a particle size larger than 400 µm were disposed of. Basically, the fractions represented very fine, fine and medium-grained sand. Clay and silt were not thoroughly treated as Estonian soils are mainly sand based. Silt and clay were the components of the finest fraction of samples.

For sample preparation, 0.5 g of the fractionized soil material was weighed into 2 ml plastic vials. Then the samples were spiked with a 2 mM stock solution of five phosphonic acids. The added amounts of phosphonic acids were 12.5, 25, 37.5, 50, 75 or 100 µL, respectively. After a 50-minute exposure to phosphonic acids, MilliQ water was added to the soil samples to obtain a total volume of 1 mL. This means that the concentration of phosphonic acids in the samples was 25, 50, 75, 100, 150 or 200 µM, respectively. Then the samples were shaken for 10 min and also centrifuged for 10 min. 500 µL of an unfiltered supernatant was placed into 0.5 mL plastic vials and AEDHP was added as an internal standard. The concentration of the internal standard was 500 µM. The unfiltered samples were subjected to CE analysis.

4.3 Chemicals

For separation experiments a mixture of some harmless degradation products of organophosphorus nerve agents was chosen as the portable CE instrument used in this experiment was developed for the analysis of nerve agents. Three phosphonic acids – methylphosphonic acid (MPA), ethyl methylphosphonic acid (EMPA), and 1-butylphosphonic acid (1-BPA) were purchased from Alfa Aesar, Lancaster Synthesis (Windham, NH, USA). The two other components of the sample mixture – propylphosphonic acid (PPA), and pinacolyl methylphosphonic acid (PMPA) were purchased from Sigma-Aldrich

(Steinheim, Germany). Isopropylmethyl-phosphonic acid (IMPA) was purchased as a 1000 mg/L methanolic solution (Cerilliant Corp., Round Rock, TX, USA). Standard stock solutions were prepared by dissolving an exact amount of each phosphonic acid in DI water to a concentration of 10 mM.

Sarin (purity >99%), soman (purity >96.7%) and VX (purity >90.3%) were supplied by the staff of the testing site near Vyškov, Czech Republic under the licence of the Ministry of Defence and Armed Forces of the Czech Republic.

L-Histidine (His) and 2-(N-morpholino) ethanesulfonic acid hydrate (MES), were purchased from Merck (Darmstadt, Germany). For the separation, a 7.5 mM equimolar mixture of MES and His was used. This mixture is a very common BGE for C^4D-CE experiments due to its low conductivity and adequate ionic strength. The BGE for capillary electrophoresis analysis was prepared by dissolving an exact amount of His and MES in MilliQ purity water.

2-aminoethyldihydrogenphosphonate (AEDHPA) and salicylic acid of p.a. quality were purchased from Sigma-Aldrich.

4.4 Procedures of CE analysis

A new capillary was flushed with a 1 M NaOH for 10 min, thereafter with water for 10 min and with BGE for 10 min. Before starting the experiments the capillary was flushed with a 0.1 M NaOH for 3 min, with water for 10 min, and with BGE for 10 min every day. Between each run the capillary was rinsed with water for 2 min and with BGE for 3 min. The BGE was a 15 mM Mes/His buffer.

4.5 GC-MS and LC-MS

Agilent 6890N GC (Agilent Technologies, Waldbronn, Germany) chromatograph with Agilent 5975B MS detector was used for comparative data analysis. The column was a 30 m x 0.25 mm x 0.25 μm HP-5MS, with He as the flow gas at a constant velocity of 0.9 mL/min. Agilent 1200 Series LC chromatograph with a 6410 Triple Quadrupole MS detector was used for HPLC analysis. Agilent Zorbax Eclipse XDB, 150 x 4,6 mm, 5 μm particle size, with aqueous eluent containing trifluoroacetic acid (TFA) was used at a flow rate of 0.4 mL/min.

5 RESULTS AND DISCUSSION

5.1 Performance of the portable CE instrument

5.1.1 Separation optimization

The choice of the right BGE for conductivity detection is challenging as BGE must have a very low conductivity to achieve maximum sensitivity and, at the same time, have a sufficient ionic strength. Finding a suitable BGE is a major drawback of the conductivity detection as the list of possible BGE is short. For the experiments reported here, MES/His, one of the most commonly used BGE for conductivity detection, was chosen. The separation of nerve agent degradation products using this BGE takes place in a counter electroosmotic mode as deprotonated phosphonic acids migrate against the EOF. Therefore, the slowest migrating analyte, PMPA, appears first in the electropherogram while the fastest, MPA, appears last. The nonnecessity to add into BGE the EOF modifiers, such as CTAB, is one of the main advantages of the counter-electroosmotic separation mode. Additionally, in the counter electroosmotic separation mode there is no interference from small anions present in aqueous sample and extracts from environmental matrices as their velocities exceed the EOF and therefore they do not reach the detector.

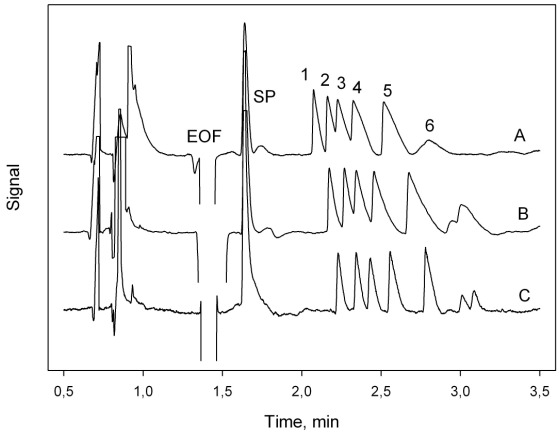

Figure 5. The effect of the BGE concentration on the separation of five phosphonic acids. The BGE solution is MES/His at a concentration of: A – 2.5 mM, B – 10 mM, C – 15 mM. Separation voltage: 20 kV; sample solution: 100 µM phosphonic acids dissolved in sand extraction water. 1 – PMPA, 2 – 1-BPA, 3 – PPA, 4 – EPA, 5 – MPA, 6 – peaks extracted from soil matrix, SP – system peak, EOF – electroosmotic flow.

Different BGE concentrations were tested to find an optimal one, as higher sensitivity is obtained by using BGE-s with a lower conductivity, and better separation is obtained with a higher ionic strength. The influence of three different concentrations of BGE is presented in Figure 5. A minimum BGE concentration of 7.5 mM is required to achieve sufficient separation although the S/N ratio for lower-concentration BGE-s is higher as the difference in conductivity between phosphonic acids and BGE is more noticeable. The electropherograms also reveal a system peak appearing at the detection point right after the EOF. The size, shape and even direction of system peaks are not stable and can change from experiment to experiment, though the migration time of system peaks is reproducible. There are a few peaks before the EOF that probably belong to metal cations like sodium, potassium, *etc*., although none of them were added to the solutions.

5.1.2 Basic performance of the cross sampler

A cross-sampler is convenient for the injection of sample into the separation capillary as changing and lifting BGE and sample vessels of bench-top CE instruments are replaced by a simple injection with plastic syringes. A drawback of the cross-sampler is that high amounts of the sample solution are consumed which exceed considerably those used in conventional hydrodynamic and electrokinetic sample injections. Moreover, most of the sample solution is discarded into the waste reservoir, as every time the sample is injected it has to replace the old solution from the last injection filling the cross-injection device. Experiments demonstrated the sample volumes of 0.05 to 0.10 ml per experiment to be optimal.

In an ideal case the amount of the sample injected into the separation capillary should be determined only by the configuration of capillaries and the injection device and not by the injection itself, *i.e*. the size of the injection is not affected by the force used to push the syringe or by the length of injection. In practice, it is extremely difficult to control hand movements and make reproducible injections from experiment to experiment. If one pushes a syringe too hard, it is possible to introduce huge amounts of the sample. It is therefore obvious that for the quantification of analytes some sort of an internal standard should be used. Since in our case the sample matrix is water, the neutral peak of the electroosmotic flow could be used as an internal standard as the area of the water peak directly represents the size of the injected sample plug. The size of the water peak is enormous compared to the small peaks of analytes. This leads to the situation where the detector amplification should be reduced to insure that the full water peak would stay in a narrow measurement range of a 16-bit ADC. The reduction of the detector amplification means that like the water peak, the analyte peaks are also reduced and this results in lower sensitivity that is not acceptable.

As it is difficult to control the cross-injection device manually to make reproducible sample injections, it is essential to take some measures to improve reproducibility. The use of internal standards is one obvious option to improve the injection precision [59]. Without any internal standard, at some concentrations of phosphonic acids the relative standard deviation (RSD) of peak areas varies up to 50 %. The use of an internal standard, *i.e*. the division of the peak area of the analyte by the peak area of the internal standard, will immediately improve reproducibility.

The performance of the portable CE system equipped with the cross-sampler and C^4D was studied by constructing calibration curves for 5 phosphonic acids. The RSD achieved using internal standards is 3.3 to 8.8%. The reproducibility of migration times is excellent as the RSD is below 5%. The LOD of phosphonic acids in soil extracts is calculated by interpolation of calibration curves. The LOD for different phosphonic acids is in the range of from 2.5 to 9.7 µM.

5.1.3 Battery-powered analyses

Electric energy is extremely important for portable devices as its lack may interrupt the performance of field analyses when batteries run empty. The simplest capillary electrophoresis devices consist of three energy-consuming parts. These are a detector, a data acquisition (DAQ) system and a high-voltage power supply. The consumption of energy by the DAQ system is rather low as it usually consists of low-power microelectronics. The consumption of energy by the C^4D detector is determined by the generator used for the excitation of one of the two electrodes. The electrode can be excited with a lower voltage, though higher sensitivity is observed using higher voltages. This leads to the conclusion that the HV power supply is probably the major consumer of power in the system. This has been proven by a simple test in which the data acquisition system and the C^4D detector were capable of working for eight hours, while the whole system, including the high-voltage power supply, started facing problems with high voltage switched on after four hours of constant working. The DAQ system and the detector continued their work, however, without any problems. Three or four hours are enough given the capacity of an average laptop computer battery. As the experiments were carried out in lab conditions, the influence of the temperature on the viscosity of solutions and, hence, on the analysis time was not investigated. In field analyses, temperature plays a crucial role. The higher viscosities caused by lower temperature will increase analysis time. This means that an analysis may last a long time or is impossible to perform even though the batteries are fully charged.

As batteries contribute heavily to the weight of the device, it should be possible to replace them to find a compromise between the weight of the instrument and the capacity of batteries.

5.2 Analysis of genuine nerve agents

5.2.1 Analysis of various matrices

For the analysis of genuine nerve agents in various matrices two internal standards (AEDHP and salicylic acid) were added to the extract. Besides the common peak area correction, internal standard peaks were used for aligning sample electropherograms to the peaks of the standard solution. Linking two (or more) peaks of internal standards allows the correction of the shifts in migration times due to the variations in the EOF [77].

Figure 6 demonstrates the separation of the extracts of sarin, soman and VX obtained from wipe-sampling a concrete matrix and that of a standard solution of degradation products, and also a blank solution of the same matrix. The figure shows an excellent match between the transformed migration times of the standards and the nerve agent hydrolysis products from aqueous extracts. It is to be noted that the electropherograms were recorded on three consecutive days, demonstrating an excellent reproducibility of the portable CE system and the efficiency of the software data processing.

Peaks of the hydrolysis products of different nerve agents appear in case of each sample. Particular peaks could easily be identified by comparing them to the peaks in the electropherogram of a standard solution. The peaks of the hydrolysis products of sarin, soman, and VX indeed correspond to IMPA, PMPA, and EMPA respectively.

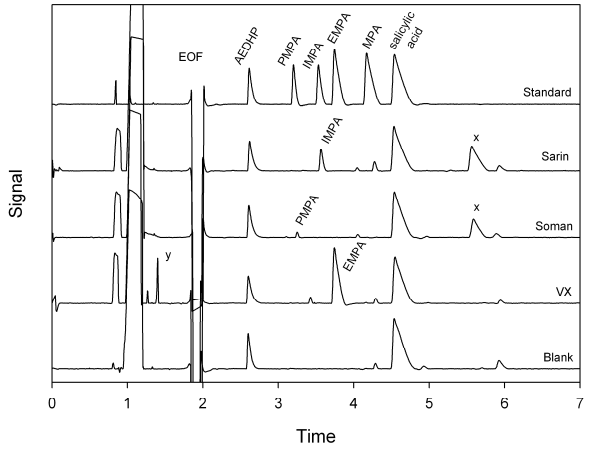

Figure 6. Separation of hydrolysis products of nerve agents sarin, soman and VX in a concrete matrix. CE conditions: separation voltage: -16 kV, BGE: 7.5 mM MES/HIS, pH 6.

A large unknown peak (Figure 6, marked with an *x*) occurred for all matrices contaminated with sarin and soman. This peak is not fluoride as was confirmed by spiking the samples with a fluoride standard. Additionally, this peak is not visible on the third set of electropherograms, which represent a nerve agent VX. On the contrary, a specific large cationic peak (Figure 6, marked with a *y*) appears at approximately 1.5 min for all matrices contaminated with VX.

Five different matrices were analyzed as described above in section 4.2. Concrete and ceramic tile were chosen to represent a typical solid surface of urban and public areas, while grass and soil were chosen as representatives of typical samples found in rural areas. Teflon was chosen as a reference material on which the absorption of NA was expected to be negligible.

The recovery rates for sarin, soman, and VX obtained using a portable CE were calculated and are presented in percentages in Table 2. The recoveries for the samples obtained from the other matrices ranged between 4.6 – 34.5 % for Teflon, between 2.7 – 16.7% for tile, between 3.2 – 9.4 % for grass and between 2.3 – 8.7 % for soil. As a rule of thumb, recovery rate is higher for the second batch of samples when the exposure time was 3 hours. Obviously, longer exposure times increase the rate of degradation and therefore improve recovery. In most cases, the recoveries for the soil and vegetation samples were lower than for the solid surface samples, such as tile or Teflon.

Table 2. Recovery data for sarin, soman and VX on various matrices.

Matrix	**Sarin**		**Soman**		**VX**	
	30 min	**3 h**	**30 min**	**3 h**	**30 min**	**3 h**
Soil	2.3%	7.6%	2.3%	5.9%	8.7%	5.1%
Grass	5.2%	9.4%	4.5%	3.7%	5.8%	3.2%
Teflon	7.9%	34.5%	4.6%	16.8%	6.4%	5.9%
Tile	4.4%	2.7%	6.6%	16.7%	5.4%	3.7%
Concrete	0.05%	0.04%	0.03%	0.11%	0.32%	0.41%

Of all five matrices, the lowest recovery (ranging between 0.03 and 0.4 %) was obtained in case of concrete. This is no surprise as the porosity of the concrete is much higher than that of the other solid matrices. The recovery rate of the samples obtained from the concrete matrix by using the wiping technique is up to two orders of magnitude lower than the recoveries from other matrices. To assure that the low recovery rate of the concrete matrix is due to the porous nature of the matrix, control experiments were performed employing different sampling methods. When the previously wiped samples were put in a container and covered with 10 ml of water and then sonicated for 10 min before analysis, no significant improvement of recoveries was witnessed. Therefore, wiping is considered an appropriate sampling technique even for porous materials like concrete.

5.2.2 Comparison of CE data to those of GC-MS and LC-MS

The results obtained by CE were compared to those from parallel experiments carried out using GC-MS and LC-MS with all five matrices. Sample preparation was slightly different as the samples were analyzed immediately after the extraction in a laboratory according to standard procedures for the determination of nerve agents and their degradation products with GC-MS and LC-MS.

The differences in the chemical nature of the solvents used in the extraction procedures do not allow a direct comparison of the results obtained with CE, GC-MS and LC-MS. However, the degradation process of nerve agents in various matrices should be independent of the analytical method. Therefore, it is possible to evaluate a CE method by comparing concentration differences between various batches measured with CE, GC-MS and LC-MS. The peak areas ratio $A_{0.5}^{Chr} / A_{3}^{Chr}$ measured by GC-MS or LC-MS was compared to the similar ratio $A_{3}^{CE} / A_{0.5}^{CE}$ measured by CE. The indexes *Chr* and *CE* indicate the analytical method used for obtaining the results corresponding to chromatographic methods and CE, respectively; while the indexes *0.5* and *3* mark the duration of the exposure time to the nerve agents. These ratios are reversed according to the exposure time, because with chromatographic techniques the ratio of the pure remaining nerve agent is measured while in CE that of the degradation product is measured. Therefore, if the ratio is greater than one, the nerve agent has decomposed over time. The data is presented in Table 3.

Table 3. Recovery data for sarin, soman and VX on various matrices*

Nerve agent	Matrix				
	Teflon	**Tile**	**Concrete**	**Soil**	**Grass**
			CE: $A_3^{CE}/A_{0.5}^{CE}$		
Sarin	4.6	0.6	**0.8**	3.2	1.8
Soman	**3.7**	2.5	3.4	3.0	0.8
VX	1.0	0.7	1.3	0.6	0.5
			GC-MS: $A_{0.5}^{Chr}/A_3^{Chr}$		
Sarin	4.6	0.3	0.1	3.0	1.6
Soman	1.8	2.8	3.1	3.7	3.2
VX	0.6	0.3	**3.2**	1.6	1.1
			HPLC-MS: $A_{0.5}^{Chr}/A_3^{Chr}$		
Sarin	2.3	**97.9**	2.5	2.0	1.6
Soman	1.6	1.6	4.0	3.8	1.9
VX	0.9	1.0	1.1	1.1	1.0

* obvious outliers are marked bold

According to the data, Teflon is the only material in whose case the nerve agents have decomposed over time. The performance of the rest of the matrices could be explained by the extent of adsorption. Nevertheless, it is still possible to

compare the data for different matrices and analytical methods. Excluding the obvious outliers (outside the 0.995 confidence band of the corresponding regression line), the square of correlation coefficients and the regression equation were calculated as follows:

$$\left(A_{0.5}^{GC-MS} / A_{3}^{GC-MS}\right) = \left(0.93 \pm 0.13\right)\left(A_{3}^{CE} / A_{0.5}^{CE}\right) + \left(0.2 \pm 0.3\right) \qquad (1)$$

The correlation exists only between CE and GC-MS data (R^2=*0.89*), while that between CE and LC-MS (R^2=*0.41*), and GC-MS and LC-MS (R^2=*0.30*) is nonexistent. These results might have been caused by an additional degradation of nerve agents during an aqueous elution in HPLC.

5.3 Adsorption of nerve agent degradation products in soil

In addition to the hydrolysis, sample extraction plays a crucial part in nerve agents analysis with CE. The samples are extracted straight from the contaminated soil or the ghost wipe used for sampling of hard surfaces. Due to the adsorption on the surface of the matrix, only a partial concentration is expected to be recovered in the extraction procedures. As the nerve agents are not freely available and their use even for research is severely restricted, the analysis of their adsorption behaviour was made using the degradation products.

Adsorption was studied in soil matrices. Two types of soil – sand and loam – were sieved into three fractions before spiking with various amounts of phosphonic acids. After the exposure time samples were extracted, analyzed and the adsorption curves were calculated. Altogether, four different adsorption models were tested to find an optimal model for phosphonic acids. The parameters and determination coefficients for all calculated isotherms (Langmuir, Freudlich, Redlich-Peterson, and BET) are given in Appendix I.

The adsorption capacity of sand is higher than that of loam according to the Langmuir isotherm parameter q_{max}. Figure 7 illustrates the adsorption of EPA in different soil samples. EPA was chosen as an example to illustrate the adsorptive behaviour of phosphonic acids tested in this thesis, with the exception of PMPA.

The adsorption of phosphonic acids in different fractions of sand and loamy soil samples was rather similar. The adsorption isotherms of 200 to 400 µm fractions of sand and loam are depicted in Figure 8. Of all four phosphonic acids, the adsorption of MPA is the highest. This could be explained by the smallest molecule size of all the tested phosphonic acids. The other three had a similar adsorption rate in both sand (Figure 8A) and loamy soil samples (Figure 8B).

The Langmuir, Freundlich and Redlich-Peterson isotherms describe the adsorption in one monolayer around the particle. An alternative model for the adsorptive behaviour of nerve agent degradation products in soil could be given using the BET-isotherm. The BET-isotherm assumes that the adsorption of phosphonic acids on the surface of soil particles takes place in several layers.

Statistically it is not possible to tell which model is more likely as there is no significant difference in determination coefficients (R^2) between the Langmuir and BET-isotherms, *i.e*. the quality of fitting both isotherms to experimental data is almost similar.

A comparison of two isotherms is given in Figure 9. Both isotherms follow the same path till the point where the second layer of the adsorbent starts to form in the BET-isotherm or the Langmuir isotherm starts to level as the monolayer around the soil particle is filling up. One of the three parameters describing the BET isotherm is q_{max}, which is the concentration corresponding to a complete monolayer adsorption. The definition of this parameter is exactly the same as in the case of the Langmuir isotherm equation. Apparently, the values of q_{max} of the Langmuir isotherm are 3 to 10 times higher than those of the BET isotherm.

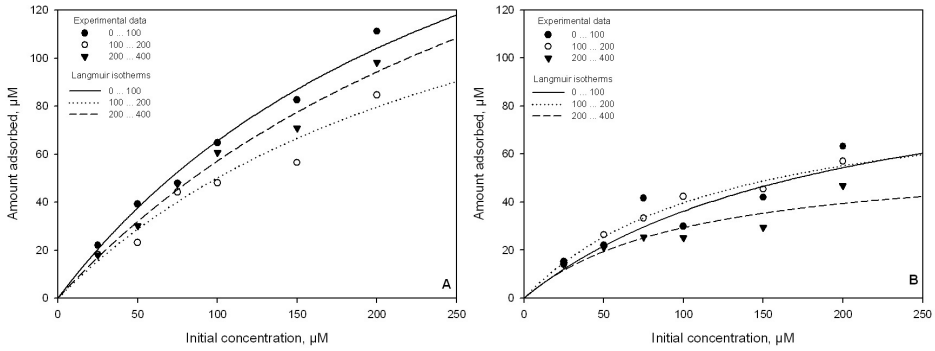

Figure 7. Adsorption data and fitted Langmuir isotherms of EPA in different soil fractions. A – sand samples, B – loamy soil samples.

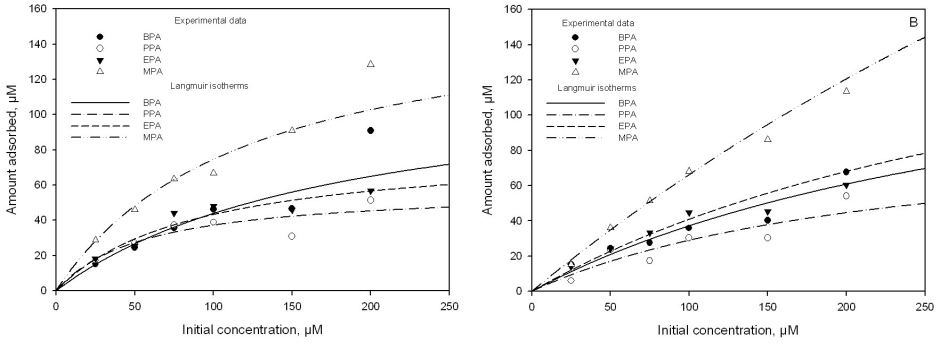

Figure 8. Adsorption data and fitted Langmuir isotherm of different phosphonic acids in soil fractions. A – phosphonic acids in sand, fraction 200 to 400 µm, B – phosphonic acids in loamy soil, fraction 200 to 400 µm.

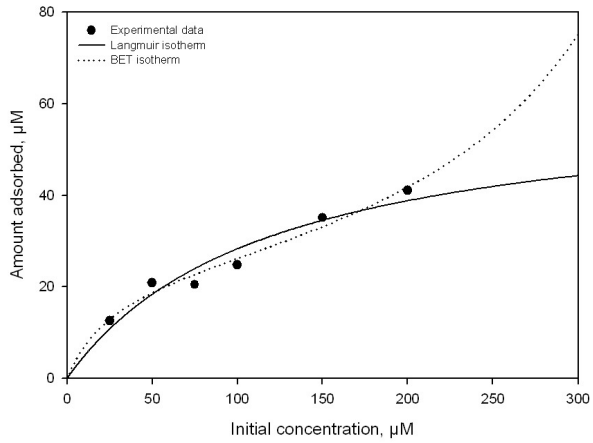

Figure 9. Comparison of fitting Langmuir and BET isotherms to the same experimental data. Experimental conditions: MPA in soil fraction sized 200 to 400 µm.

For all the phosphonic acids tested the adsorption mechanism is the same as their molecular structures are very similar. Therefore, it is unlikely that the adsorption concentration corresponding to the complete monolayer of one particular phosphonic acid could vary in such a wide range. Hence, the adsorption mechanism of nerve agent degradation products must be either Langmuir's or BET's. The concentration range investigated is apparently too narrow to tell us which of the two mechanisms is correct as the measured points are in the range in which only the first monolayer is filling up.

5.4 Signal processing algorithms for the portable CE instrument

5.4.1 Baseline correction

Besides a very common problem like a constant drift, problematic baselines may consist of all kinds of other baseline disturbances described by various amplitudes, directions, or velocities. Proper baseline correction algorithms should be able to deal equally efficiently with various baseline disturbances. The velocity and direction of the baseline drift may vary during the CE experiment. Therefore, the baseline algorithm developed looks only into a small part of the baseline at a time. The main principles of an algorithm are based on those of the baseline correction algorithm that tries to copy human judgment [67]. A particular algorithm considers all local maximums as potential points of the baseline. With several outliers tests algorithms get rid of points that are actually located on top of the peaks instead of the baseline.

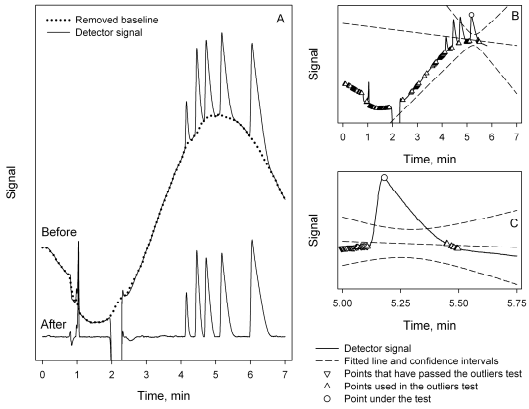

Figure 10. Figure 1. Baseline correction algorithm. A) An electropherogram before and after the baseline correction, along with the removed baseline. B) and C) The outliers test in the baseline correction algorithm. ○ – tested point, △ - points used in the outliers test, ▽ – points that have passed the outliers test, and are considered to be points located in the baseline, dashed lines belong to the straight line fitted through the points used in the outliers test that fell within the confidence intervals.

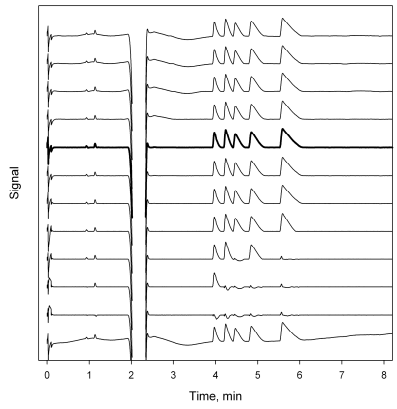

Figure 11. Performance of the baseline correction algorithm. The performance of the baseline correction algorithm depends on the number of points used in the outliers test before and after a particular test point. The baseline drift is modeled according to the experimental data. A bold line depicts the baseline correction using an optimal number of points; 17 points before and after the test point i.e. 35 points in total were found to be the most effective in the tests.

Several small but significant improvements have been added to the developed baseline correction algorithm. Most importantly the outliers test considers only one point at a time and compares it to the neighbouring points only. Due to this small improvement the developed baseline correction algorithm is not sensitive to changes in baseline drift speed or direction. The principles of the baseline correction algorithm in question are depicted in Figure 10A.

The step-by-step description of the performance of a particular baseline correction algorithm could be the following. First, the algorithm locates all local minimums and maximums. These points are obviously located on top of positive or negative peaks, but not only. Due to the detector noise most of these minimums and maximums are located on the baseline.

Secondly, the algorithm uses a simple outliers test to figure out which of the located points are actually located on the baseline. The algorithm is developed to check one point at a time by comparing it to a certain number of other potential baseline points locating before and after a particular point. Basically, the

baseline correction algorithm fits a straight line and calculates confidence intervals according to the coordinates of the tested point and a certain number of points locating around the tested point. The probability level could be set by the operator to suit better to particular experimental data. A 95% probability level was used for the experiments described in the thesis. If the point under evaluation is located between the confidence intervals it is considered as a point located on the baseline. While locating outside the confidence intervals, the point is dropped and is not used for testing other potential baseline points.

The particular outliers test is described in Figures 10B and 10C. This very simple outliers test has proven in experiments to be a very fast and efficient way to determine a true baseline point from the points located on top of the peaks. Though the algorithm is not capable of testing few points in the beginning and end of the detector signal, this is not a major drawback as there are no peaks in the beginning of the experiment and in the end it is possible to record enough data after the migration of the last peak.

Finally, after dropping all unsuitable points, the baseline is found by interpolation of the coordinates of the located baseline points to the whole time axis of the signal. Various interpolation algorithms could be chosen to suit better to the particular data. In the experiments reported here a cubic spline interpolation was used.

A good baseline correction algorithm must satisfy certain requirements. Simply put, algorithms must remove all the drift without affecting the size and shape of peaks and do it in as short a period of time as possible. The developed baseline algorithm requires two input parameters – the probability level and the number of points used in the outliers test. The optimization of input parameters was done experimentally. For this purpose, several electropherograms were constructed with various artificial baseline disturbances. The functions used for the generation of the baseline drift were linear, square, sinus, and sinus with increased frequency. Besides these functions, a signal with no drift at all and a signal with a drift modelled according to real experimental data were used.

An algorithm was applied to the generated electropherograms while the input parameters were changed. The performance of the algorithm was evaluated by comparing two values. First, the difference between the original baseline drift and the baseline drift found by the algorithm describes the efficiency of removing the baseline drift. Secondly, the peak areas after the baseline correction were compared to the original peak areas. Difference between peak areas before and after application of baseline correction algorithm should be minimal if the shape of the peaks has been unaffected by the algorithm. The variation of the number of the points used in the outliers test reveals that if the parameter value is too low, the algorithm will consider peaks as part of the baseline and will remove them eventually causing the loose of analytical information. On the other hand, when the value is too high, the algorithm is not

capable of removing the baseline drift. For the experimental data used in the present contribution, optimal is to use 17 points before and after a particular evaluated point, *i.e*. 35 points altogether in the outliers test (Figure 11), taking account also the point evaluated in the test.

5.4.2 Alignment of electropherograms

Besides baseline drift, a very common problem that CE analysis has to face is the irreproducibility of migration times. Migration times may be affected by various factors like temperature control, pre-treatment of the inner capillary surface, variable stacking depending on the ionic strength of the sample matrix, *etc*. Some of the well-known approaches for dealing with signal alignment (COW, DTW) are not really suitable for processing CE results, as they just shift points to minimize the difference between two signals and do not consider the facts that are specific to CE like the peaks that migrate longer are more affected by the drift of the EOF velocity. The other approaches developed especially for CE usually treat signals as the velocity of the EOF is constant during one experiment, and try to fix the difference in migration times between two signals by some specific mean. Mostly, the velocity of the EOF can be considered as a constant during one run, but in some occasions the EOF velocity may shift during a run, *e.g*. due to the adsorption of some analytes to the inner surface of the capillary wall.

If changes in EOF during the run could be measured, it would be possible to calculate a new time axis by using the corrected EOF value. This is an attractive possibility as it would be a great measure for correcting irreproducible migration times in between the runs. Only a small number of techniques providing the possibility to measure the EOF on-line are available, thermal marks being one of the few. Before aligning signals according to thermal marks [V], the nature of the latter was studied as part of a study addressing the EOF of ionic liquid solutions in non-aqueous media [IV]. Briefly, thermal marks were used to determine the EOF in various non-aqueous BGE-s made of seven different organic solvents and by adding various amounts of an ionic liquid ($[BMIm]^+[CF3COO]^-$). A detailed overview of the experiment and the results can be found in the copy of the publication in the appendix [IV].

What is important in the context of the portable CE and signal processing in general is the fact that the high number of experiments performed with various BGE-s demonstrates that thermal marks could be used for monitoring the EOF as the results obtained are the same as those from the neutral marker method. Of the 50 tested buffers based on seven different solvents, the linearity between the results obtained by the neutral marker and thermal marks was excellent (R^2>0.99) (Figure 12).

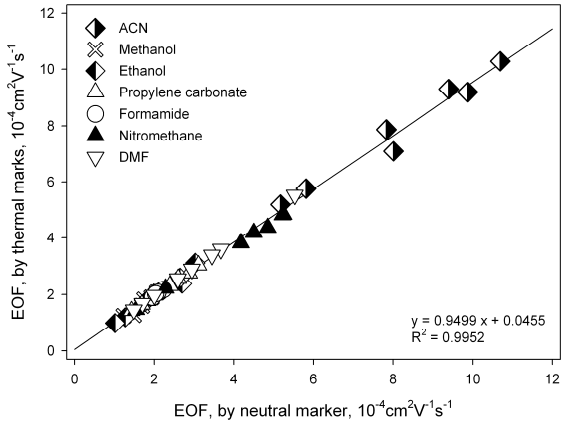

Figure 12. Comparison of the neutral marker and thermal marks methods for measuring the velocity of the EOF. Experiments were repeated in various non-aqueous BGE systems at different concentrations (0 to 10 mM) of an ion-liquid additive ($[BMIm]^+[CF3COO]^-$). Every point represents an average EOF value of different BGE system. Data is taken from [III] Figure 3.

In this thesis, a method for aligning several electropherograms is presented that takes into account also the drift of the EOF velocity during one run. The velocity of the EOF was monitored with the aid of thermal marks generated by the heating coil. As the distance between the heating coil and the detection point is very small compared to the distance between the sample inlet and the detection point, therefore it is possible to produce and monitor several thermal marks during one run as their migration time is much shorter than those of sample analytes. Therefore it is possible to collect enough points to construct the approximation of changes in the velocity of the EOF value during one run. In the experiments performed for this thesis, the spline function was used to fit a curve to the collected data. The spline function was preferred to the linear interpolation as the smoother result is expected to correspond slightly better to the real life situation. After the drift of the EOF velocity has been calculated (a dash dot line, Figure 13), it is easy to use an electrophoretic mobility equation to calculate a new time axis for the electropherogram that corresponds to the situation when the EOF velocity is constant (a dotted line, Figure 13).

To calculate a new time axis, first the electrophoretic mobilities corresponding to every single point in the electropherogram are found using the estimation of EOF mobilities. While keeping the electrophoretic mobilities of every point constant it is straightforward to calculate new time axis values by using a new constant value of the EOF mobility. In the present example (Figure 13), an average value of the EOF mobility was used as a new constant value of the latter. If the registered detector signal (a solid line, Figure 13) is compared to the new corrected detector signal (a dashed line, Figure 13), it can be noticed that

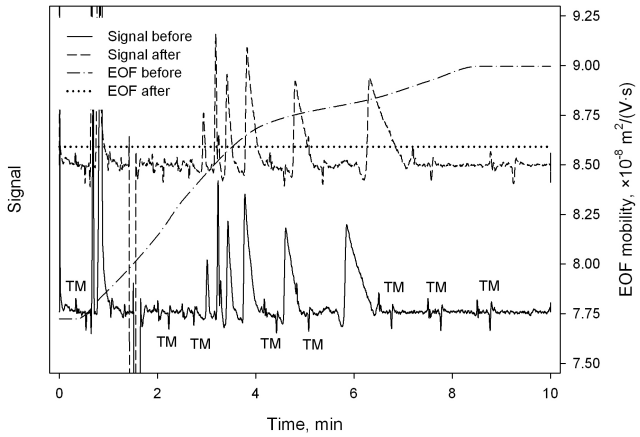

Figure 13. An electropherogram before and after the drift of the EOF mobility has been compensated for according to the data obtained with the aid of thermal marks. TM – location of thermal marks. The dash dotted line is an estimation of EOF mobility changes during the experiment calculated according to the migration times of thermal marks. The EOF mobility after the corrections is constant (a dotted line). The solid and dashed lines correspond to the detector line before and after the corrections of the EOF mobility. Corrections have been performed according to the electrophoretic mobility equation. The correction has been performed by calculating a new time axis while the electrophoretic mobility corresponding to a particular point is kept constant.

the first peaks are shifted forward as the corrected EOF value is higher than the EOF value of the original signal monitored with the aid of thermal marks. On the contrary, the last peaks are shifted backwards as the corrected EOF values are lower compared to the original's.

After the EOF drift is corrected several electropherograms could be aligned simply by recalculating time axis according to the new EOF value by using the same electrophoretic mobility equation. Figure 14 demonstrates the efficiency of the signal alignment calculated according to the data obtained by monitoring the EOF with the aid of thermal marks. The extreme differences in migration times may easily cause major misinterpretations of electropherograms. Figures 14A and 14C demonstrate the efficiency of the electropherogram alignment monitored with the aid of thermal marks. These two figures depict the same pair of electropherograms before and after the signal alignment. The migration times before the alignment are shifted, though it is still possible to tell it is the same sample by the number and size of the peaks.

In a situation when there is no independent technique for obtaining additional information, migration times are the only information that could be used for the identification of unknown species. The CWA analysis with C^4D-CE relies on the detection of degradation products that are specific for every nerve agent. For the

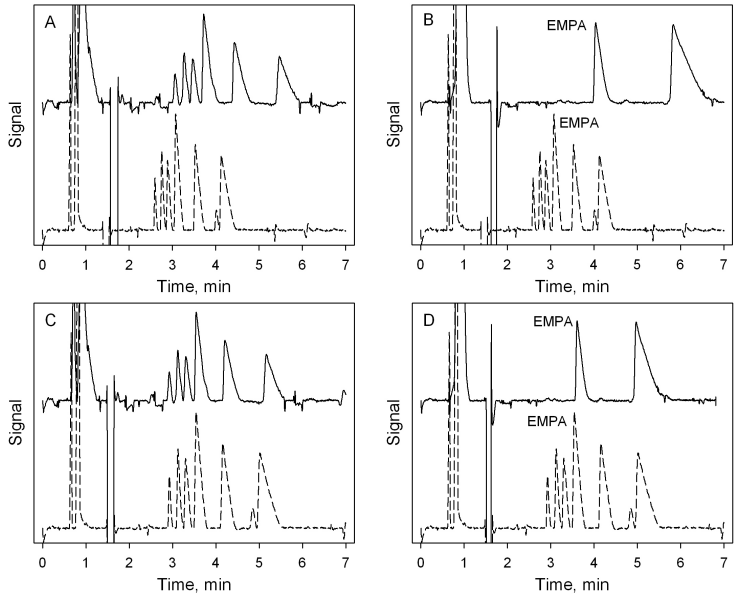

Figure 14. Two examples of the signal alignment obtained with the aid of thermal marks. A and B – uncorrected electropherograms, C and D – same pairs of electropherograms after the alignment according to thermal marks. The solid line – the sample electropherogram, the dashed line – the reference electropherogram. Peaks from left to right: PMPA, BPA, PPA, EMPA, MPA and salicylic acid. In example B, it is to be noticed how the migration times of EMPA differ before and after alignment. This could potentially lead to errors in identification. After the signal alignment has been done, example D, peaks of EMPA in both electropherograms have similar migration times and should be identified with no problem.

nerve agent VX the specific degradation product is EMPA. When comparing the untreated signal of EMPA (Figure 14B) with a standard mixture of various nerve agent degradation products, it would be impossible to identify EMPA without any additional information. In extreme cases the precise identification cannot be done without a proper signal alignment. After the alignment (Figure 14D) it is no problem to tell that the peak corresponds to EMPA.

Thermal marks can be produced with the aid of all kinds of heating sources as long as the part of the capillary that is heated is very small. In this thesis, thermal marks have been produced using a simple heating coil made of a stainless steel wire wrapped a couple of times around the separation capillary. The other tools for the generation of thermal marks reported before are a surface mounted device (SMD) resistor [90], a tungsten filament of a light bulb [90, IV], a simple wire [V] or a laser [93]. No matter what is used for generation of thermal marks, the precise control of certain parameters is necessary. The precise time of the

generation of thermal marks is essential for calculating the estimation of the EOF mobility that is used for a precise electropherogram alignment. The length of the heating impulse and the temperature of the source must be precisely controlled to have a reproducible shape and size of thermal marks.

Due to the fact that no complex instrumentation is needed for the generation of thermal marks, the possibility to generate thermal marks could easily be implemented into future CE instruments. Thermal marks could easily be applied to CE experiments to monitor changes in the velocity of the EOF, so that changes in EOF mobility could later be reproduced. The information on EOF mobility changes during the experiment opens a possibility to correct them, so that the mobility of the EOF would be constant. Moreover, the electropherograms with constant EOF mobilities could easily be aligned. The greatest challenge of this approach is producing thermal marks so that they will not co-migrate with analyte peaks. With an unknown sample nothing could be expected from the first run. Starting from the second experiment the migration times of sample peaks could be predicted and it is possible to produce thermal marks so that they will not co-migrate with sample peaks.

5.4.3 Peak matching

A comparison of unknown peaks of the sample electropherogram and the peaks of standard substances of the reference electropherogram is still the most widely used method for peak identification. Although the interpretation of two electropherograms is simple for experienced researchers and is usually performed visually, it could also be automated with the aid of a proper computer algorithm. For example, situations where the number of electropherograms is very high, or CE is used for monitoring purposes, or the personnel operating the instrument is not qualified enough would benefit from peak matching algorithms.

All the algorithms described in this paper were developed to be used with the portable CE instrument for the determination of specific compounds of interest like environmental pollutants, chemical warfare agents, *etc*. Peak identification is achieved by matching peaks in the sample and reference electropherograms. Peak identification is based on the exact principles of the fuzzy matching algorithm developed for the warping of chromatograms by Walczak and Wu [94].

According to the fuzzy sets theory, the belonging of a given element to a considered set is described by the continuous membership function varying from 0 to 1. Each peak of the reference electropherogram is considered as a centre of the Gaussian membership function. As there are five standards in the reference sample, there are five Gaussian functions as well (Figure 15C). There are three peaks in the sample electropherogram that intersect the Gaussian functions defined for the reference electropherogram. The values of the resulting

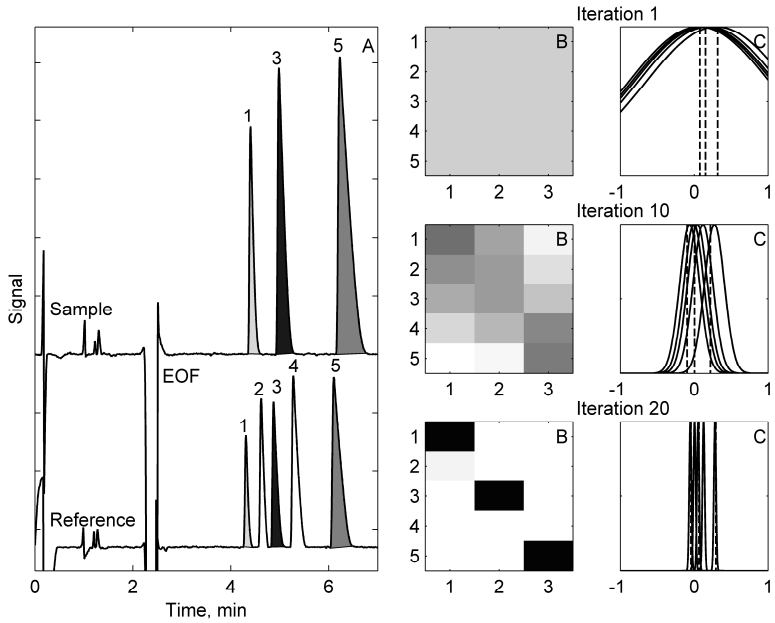

Figure 15. An automatic peak matching between the sample and the reference electropherograms according to migration times with the aid of the fuzzy matching algorithm. A – matched peaks in the sample and the reference electropherograms. Peaks 1 to 5 correspond to PMPA, BPA, PPA, EMPA and MPA, respectively. Separation conditions are: sample concentration 100 µM, BGE 15mM MES/His, separation voltage 18kV. B – matrix of similarity, rows correspond to 5 peaks of the reference electropherogram, 3 columns correspond to 3 peaks of the sample electropherogram. Darker colors correspond to higher similarity. C – the fuzzy matching of peaks, 5 Gaussian functions correspond to the peaks in the reference sample, 3 dashed lines correspond to the peaks in the sample solution.

intersections are defined as a measure of similarity and can be collected into a 5-by-3 matrix of similarity (Figure 15B).

As several peaks of the sample electropherogram may be highly similar to the same peak of the reference electropherogram, the normalization process is needed. The Sinkhorn standardization [95] is used to obtain a matrix with a sum of elements in each row and column equal to 1. After centring and scaling the results, the whole process is repeated. However, the width of Gaussian functions is reduced with each iteration. The process is repeated till the convergence is achieved or a certain number of iterations has been performed. The peaks of two electropherograms (Figure 15A) are considered to belong to the same substance if the measure of similarity is higher than a certain set value.

The successful peak identification relies on a proper alignment of electropherograms as the identification is based on the fuzzy matching of

migration times. For testing the reliability of the algorithms, a random bunch of electropherograms measured during a period of one month was selected. Various combinations of sample and reference electropherograms were created and analyzed. The results were satisfying, except for one specific electropherogram that could not be correctly aligned with an automatic algorithm and therefore the peak matching failed. This kind of an improper alignment could easily be recognized by the operator. After a manual alignment with this particular electropherogram, the fuzzy matching was able to identify the peaks correctly.

Out of 500 tests, only nine pairs of electropherograms were discovered where peaks of one or two nerve agent degradation products were not recognized. No problems with matching wrong peaks were discovered. The alignment was achieved without using thermal marks. The new time axis was calculated according to the migration time of the neutral marker, *i.e*. the EOF peak. This sort of an alignment was chosen as the set of data already existed and there was no need for additional experiments. Besides, the aim was to study the performance of the fuzzy matching algorithm and not the alignment itself.

Analysis of such a high number of electropherograms is possible as the algorithm does not spend more than three seconds for analyzing a pair of electropherograms. It should be noticed that during the analysis of one pair the baseline correction and peak detection algorithms are run twice both for the sample and the reference electropherograms. The fuzzy matching algorithm was also tested without the alignment on the same data set, but the tests were stopped after 50 experiments as already 60% of the calculated results had mismatching peaks due to the irreproducible migration times. This means that the precise peak matching is not possible without a proper electropherogram alignment. These results are contrary to the report by Walczak and Wu [94], who used fuzzy matching for locating pairs of peaks belonging to the same substance on two electropherograms with the intention to align these signals according to the pairs found.

6 CONCLUSIONS

The main goal of this thesis was to develop a portable CE instrument for field analysis of nerve agents and their degradation products. Extra attention was paid to developing simple sample extraction procedures, easy operation of the instrument, and an automatic signal-processing and data interpretation.

The results of this study could be summarized as follows:

- The portable capillary electrophoresis device equipped with a C^4D detection and a cross-sampler is a small and comfortable analytical system that may be carried easily into the field. The cross sampler and the sample stream splitter makes sample introduction simple compared with manual hydrodynamic or electrokinetic injections, thus making the operation of the instrument by a person wearing a protective suit possible.
- Quantitative analysis is possible with the aid of an internal standard. Reproducibility could be improved by compensating inaccurate sample injections by the use of the ratio between the analyte and internal standard peak areas. The RSD of the corrected peak areas was below 8 %. The reproducibility of migration times is good as the RSD is less than 5%.
- Phosphonic acids as degradation products of their parental nerve agents could possibly serve as excellent fingerprint markers. Sarin, soman, and VX were positively identified in five matrices according to degradation products. The sampling and extraction procedures developed allow a rapid analysis of nerve agents from soil, vegetation samples and hard surface matrices. There was a good correlation between the results obtained with CE and the reference GC-MS method. The recoveries for the samples obtained from various matrices ranged between 2.3 to 34.5%. The concrete matrix produced lowest recovery (0.03 to 0.41%) due to its high porocity.
- CE has proven to be a suitable tool for separating phosphonic acids and could therefore easily be used for the analysis of their adsorption. Moreover, it enables analysis of the adsorption of several components on the same adsorbent simultaneously. This offers a great opportunity to study a competitive adsorption of similar molecules on the same adsorption sites.
- CE as a separation technique has always been promoted for its very efficient separation, low sample consumption and simple instrument design with no high-pressure pumps contrary to HPLC. In reality, CE has never been accepted for the routine analyses. This is most likely because of the low reproducibility that accompanies CE, as has been cited in so many papers. Signal processing could be a key solution to solve the reproducibility problems of CE. What cannot be solved before the experiment on

instrumental side could possibly be corrected after the experiment with a proper signal processing.

- Results of qualitative analysis can be improved with good electropherogram alignment algorithms that correct irreproducible migration times, while quantitative analysis benefits from the precise baseline correction and proper peak integration.
- Together with peak detection, integration, signal alignment, and peak identification algorithms; signal processing programs are capable of identifying and quantifying target compounds in the field, such as nerve agent degradation products, in as fast as a few seconds. With a proper electropherogram alignment, precision higher than 98.2% (out of 500 experiments) has been obtained.
- An automatic baseline correction algorithm was developed based on testing local extremes. The points that pass this test are then used to interpolate a new baseline that is subtracted from the original signal. Because the algorithm works only on small parts of the baseline at a time, this approach is very flexible and is capable of fixing baseline disturbances of various speeds, amplitudes and directions.
- The electropherogram alignment based on the information gathered with the aid of thermal marks is very efficient, because it takes into account not only the EOF differences between the runs considered by most current approaches, but also changes in EOF during a run.
- Signal processing as a field of research should earn more attention, because with the aid of appropriate computer algorithms it is possible to improve the reliability of CE experiments both in quantitative and qualitative analysis. With improved reproducibility, it might be possible to really take advantage of the very efficient separation and low sample consumption always associated with CE.

7 REFERENCES

1. McMahon, G. *Analytical instrumentation: a guide to laboratory, portable and miniaturized instruments;* Wiley: Chichester, UK, 2007.
2. Turl, D. E. P.; Wood, D. R. W. Detection for security. **2008,** *133,* 558-662.
3. Hou, X. D.; Jones, B. T. Field instrumentation in atomic spectroscopy. *Microchem, J.* **2000,** *66,* 115-145.
4. Janata, J. Role of analytical chemistry in defense strategies against chemical and biological attack. *Annu. Rev. Anal. Chem.* **2009,** *2,* 321-331.
5. Black, G. In *Genocide in Iraq: The Anfal Campaign Against the Kurds;* Human Rights Watch: New York, 1993; p 271.
6. Nakajima, T.; Sato, S.; Morita, H.; Yanagisawa, N. Sarin poisoning of a rescue team in the Matsumoto sarin incident in Japan. *Occup. Environ. Med.* **1997,** *54,* 697-701.
7. Murakami, H. *Underground: The Tokyo Gas Attack and the Japanese Psyche;* Vintage International: New York, 2000.
8. The Merck Index, 11 ed. Budavari, S., O'Niel, M. J., Smith, A., Heckelmanm, P. E., Eds.; Merck & Co.: Rahway, NJ, US, 1989; p 594.
9. Mäkinen, M. A.; Anttalainen, O. A.; Sillanpää, M. E. Ion mobility spectrometry and its applications in detection of chemical warfare agents. *Anal. Chem.* **2010,** *82,* 9594–9600.
10. 2007. Guide for the Selection of Chemical Detection Equipment for Emergency First Responders, 3rd Edition. https://www.rkb.us/contentdetail.cfm?content_id=97670 (accessed March 9, 2011).
11. Sferopoulos, R. *A Review of Chemical Warfare Agent (CWA) Detector Technologies and Commercial-Off-The-Shelf Items;* Human Protection and Performance Division, DSTO Defence Science and Technology Organisation: Fishermans Bend Australia, 2008.
12. Sega, G. A.; Tomkins, B. A.; Griest, W. H. Analysis of methylphosphonic acid, ethyl methylphosphonic acid and isopropyl methylphosphonic acid at low microgram per liter levels in groundwater. *J. Chromatogr. A* **1997,** *790,* 143-152.
13. Hooijschuur, E. W. J.; Kientzb, C. E.; Brinkman, U. A. T. Application of microcolumn liquid chromatography and capillary electrophoresis with flame photometric detection for the screening of degradation products of chemical warfare agents in water and soil. *J. Chromatogr. A* **2001,** *928,* 187-199.
14. Nassar, A.-E. F.; Lucas, S. V.; Myler, C. A.; Jones, W. R.; Campisano, M.; Hoffland, L. D. Quantitative Analysis of Chemical Warfare Agent

Degradation Products in Reaction Masses Using Capillary Electrophoresis. *Anal. Chem.* **1998,** *70,* 3598–3604.

15. Zhao, R.-S.; Yuan, J.-P.; Li, H.-F.; Jiang, T.; Lin, J.-M. Nonequilibrium hollow-fiber liquid-phase microextraction with in situ derivatization for the measurement of triclosan in aqueous samples by gas chromatography–mass spectrometry. *Anal. Bioanal. Chem.* **2007,** *387,* 2911-2915.
16. Black, R. M.; Read, R. W. Application of liquid chromatography-atmospheric pressure chemical ionisation mass spectrometry, and tandem mass spectrometry, to the analysis and identification of degradation products of chemical warfare agents. *J. Chromatogr. A* **1997,** *759,* 79-92.
17. Hooijschuur, E. W. J.; Kientz, C. E.; Brinkman, U. A. T. Analytical separation techniques for the determination of chemical warfare agents. *J. Chromatogr. A* **2002,** *982,* 177-200.
18. Cheicante, R. L.; Stuff, J. R.; Durst, H. D. Separation of sulfur containing chemical warfare related compounds in aqueous samples by micellar electrokinetic chromatography. *J. Chromatogr. A* **1995,** *711,* 347-352.
19. Mercier, J.-P.; Morin, P.; Dreux, M.; Tambute, A. Capillary electrophoresis analysis of chemical warfare agent breakdown products I. Counterelectroosmotic separation of alkylphosphonic acids and their monoester derivatives. *J. Chromatogr. A* **1996,** *741,* 279-285.
20. Nassar, A.-E. F.; Lucas, S. V.; Jones, W. R.; Hoffland, L. D. Separation of Chemical Warfare Agent Degradation Products by the Reversal of Electroosmotic Flow in Capillary Electrophoresis. *Anal. Chem.* **1998,** *70,* 1085-1091.
21. Pianetti, G. A.; Taverna, M.; Baillet, A.; Mahuzier, G.; Baylocq-Ferrier, D. Determination of alkylphosphonic acids by capillary zone electrophoresis using indirect UV detection. *J. Chromatogr. A* **1993,** *630,* 371-377.
22. Melanson, J. E.; Wong, B. L.-Y.; Boulet, C. A.; Lucy, C. A. High-sensitivity determination of the degradation products of chemical warfare agents by capillary electrophoresis–indirect UV absorbance detection. *J. Chromatogr. A* **2001,** *22*.
23. Rosso, T. E.; Bossle, P. C. Capillary ion electrophoresis screening of nerve agent degradation products in environmental samples using conductivity detection. *J. Chromatogr. A* **1998,** *824,* 125-134.
24. Xu, L.; Hauser, P. C.; Lee, H. K. Determination of nerve agent degradation products by capillary electrophoresis using field-amplified sample stacking injection with the electroosmotic flow pump and contactless conductivity detection. *J. Chromatogr. A* **2009,** *1216,* 5911-5916.
25. Xu, L.; Hauser, P. C.; Lee, H. K. Electro membrane isolation of nerve agent degradation products across a supported liquid membrane followed by capillary electrophoresis with contactless conductivity detection. *J.*

Chromatogr. A **2008,** *1214,* 17-22.

26. Bell, A.; Vadgama, P. Editorial – Detection for Security. *Analyst* **2008,** *133,* 557.
27. Ryvolova, M.; Preisler, J.; Brabazon, D.; M., M. Portable capillary-based (non-chip) capillary electrophoresis. *Trend. Anal. Chem.* **2010,** *29,* 339-353.
28. Huang, X.; Zare, R. N.; Sloss, S.; Ewing, A. G. End-column detection for capillary zone electrophoresis. *Anal. Chem.* **1991,** *63,* 189-192.
29. Kappes, T.; Schnierle, P.; Hauser, P. C. Field-portable capillary electrophoresis instrument with potentiometric and amperometric detection. *Anal. Chim. Acta* **1999,** *30,* 77-82.
30. Chen, D.-C.; Chang, S.-S.; Chen, C.-H. Parallel-opposed dual-electrode detector with recycling amperometric enhancement for capillary electrophoresis. *Anal. Chem.* **1999,** *71,* 3200-3205.
31. Kappes, T.; Hauser, P. C. Simplified amperometric detector for capillary electrophoresis. *Analyst* **1999,** *124,* 1035-1039.
32. De Backer, B. L.; Nagels, L. J. Potentiometric Detection for Capillary Electrophoresis: Determination of Organic Acids. *Anal. Chem* **1996,** *68,* 4441-4445.
33. Kappes, T.; Hauser, P. C. Portable capillary electrophoresis instrument with potentiometric detection. *Anal. Comm.* **1998,** *35,* 325-329.
34. Li, F. Y.; Wei, H.; Wang, T.; Wu, Y. Field analysis of environmental samples using a portable capillary electrophoresis instrument. *Proc. SPIE* **2001,** *4199,* 51–58.
35. Zemann, A. J. Capacitively coupled contactless conductivity detection in capillary electrophoresis. *Electrophoresis* **2003,** *24,* 2125–2137.
36. Kuban, P.; Hauser, P. C. A review of the recent achievements in capacitively coupled contactless conductivity detection. *Anal. Chim. Acta 2008* **2008,** *607,* 15-29.
37. Kuban, P.; Hauser, P. C. Fundamentals of electrochemical detection techniques for CE and MCE. *Electrophoresis* **2009,** *30,* 3305-3314.
38. da Silva, J. A. F.; do Lago, C. L. An Oscillometric Detector for Capillary Electrophoresis. *Anal. Chem.* **1998,** *70,* 4339-4343.
39. Zemann, A. J.; Schnell, E.; Volgger, D.; Bonn, G. K. Contactless Conductivity Detection for Capillary Electrophoresis. *Anal. Chem.* **1998,** *70,* 563-567.
40. Mayrhofer, K.; Zemann, A. J.; Schnell, E.; Bonn, G. K. Capillary Electrophoresis and Contactless Conductivity Detection of Ions in Narrow Inner Diameter Capillaries. *Anal. Chem.* **1999,** *71,* 3828–3833.
41. Kuban, P.; Hauser, P. C. Ten years of axial capacitively coupled contactless conductivity detection for CZE - a review. *Electrophoresis* **2009,** *30,* 176-

188.

42. Kuban, P.; Nguyen, H. T. A.; Macka, M.; Haddad, P. R.; Hauser, P. C. New Fully Portable Instrument for the Versatile Determination of Cations and Anions by Capillary Electrophoresis with Contactless Conductivity Detection. *Electroanalysis* **2007,** *19,* 2059-2065.
43. Xu, Y.; Wang, W.; Li, S. F. Y. Simultaneous determination of low-molecular-weight organic acids and chlorinated acid herbicides in environmental water by a portable CE system with contactless conductivity detection. *Electrophoresis* **2007,** *28,* 1530-1539.
44. TraceDec® Contactless Conductivity Detector. http://www.istech.at/product.htm (accessed March 15, 2011).
45. eDAQ C4D Introduction page. http://www.edaq.com/C4D_intro.php (accessed March 15, 2011).
46. Wang, L.; Fu, C. Miniaturized Capillary Electrophoresis System with Contactless Conductivity Detection and Flow Injection Sample Introduction. *Instrum. Sci. Technol.* **2004,** *32,* 303-309.
47. Hutchinson, J. P.; Evenhuis, C. J.; Johns, C. A.; Kazarian, A.; Breadmore, M. C.; Macka, M.; Hilder, E. F.; Guijt, R. M.; Dicinoski, G. W.; Haddad, P. R. Identification of inorganic improvised explosive devices by analysis of postblast residues using portable capillary electrophoresis instrumentation and indirect photometric detection with a light-emitting diode. *Anal. Chem.* **2007,** *79,* 7005-7013.
48. Xu, Y.; Qin, W.; Li, S. F. Y. Portable capillary electrophoresis system with potential gradient detection for separation of DNA fragments. *Electrophoresis* **2005,** *26,* 517-523.
49. Kappes, K.; Galliker, B.; Schwarz, M. A.; Hauser, P. C. Portable capillary electrophoresis instrument with amperometric, potentiometric and conductometric detection. *Trend. Anal. Chem.* **2001,** *20,* 133-139.
50. Lee, M.; Cho, K.; Yoon, D.; Yoo, D. J.; Kang, S. H. Portable capillary electrophoresis system for identification of cattle breeds based on DNA mobility. *Electrophoresis* **2010,** *31,* 2787-2795.
51. Gorbatšova, J.; Jaanus, M.; Kaljurand, M. Digital Microfluidic Sampler for a Portable Capillary Electropherograph. *Anal. Chem.* **2009,** *81,* 8590-8595.
52. Jacobson, S. C.; Hergenroder, R.; Koutny, L. B.; Warmack, R. J.; Ramsey, J. M. Effects of Injection Schemes and Column Geometry on the Performance of Microchip Electrophoresis Devices. *Anal. Chem.* **1994,** *66,* 1107-1113.
53. Harrison, D. J.; Manz, A.; Fan, Z. H.; Ludi, H.; Widmer, H. M. Capillary electrophoresis and sample injection systems integrated on a planar glass chip. *Anal. Chem.* **1992,** *64,* 1926-1932.
54. Effenhauser, C. S.; Manz, A.; Widmer, H. M. Glass chip for high-speed

capillary electrophoresis separations with submicrometer plate heights. *Anal. Chem.* **1993,** *65,* 2637-2642.

55. Zare, R. N.; Huang, X.; Pentoney, S. L. J. Capillary Device. 5298134, March 29, 1994.
56. Tsukagoshi, K.; Suzuki, T.; Nakajima, R. Small-Sized Capillary Electrophoresis with a Chemiluminescence Detector Equipped with Cross-Intersection for Sample Injection. *Anal. Sci.* **2002,** *18,* 1279-1280.
57. Kulp, M.; Vaher, M.; Kaljurand, M. Miniaturization of sampling for chemical reaction monitoring by capillary electrophoresis. *J. Chromatogr. A* **2005,** *1100,* 126-129.
58. Faller, T.; Engelhardt, H. How to achieve higher repeatabilityand reproducibility in capillary electrophoresis. *J. Chromatogr. A* **1999,** *853,* 83-94.
59. Dose, E. V.; Guiochon, G. A. Internal standardization technique for capillary zone electrophoresis. *Anal. Chem.* **1991,** *63,* 1154–1158.
60. Kullik, E.; Kaljurand, M.; Koel, M. *Применение ЭВМ в газовой хроматографии;* Издательство "Наука": Moscow, 1978.
61. Solis, A.; Rex, M.; Campiglia, A. D.; Sojo, P. Accelerated multiple-pass moving average: A novel algorithm for baseline estimation inCE and its application to baseline correctionon real-time bases. *Electrophoresis* **2007,** *28,* 1181-1188.
62. Bernabe-Zafon, V.; Torres-Lapasio, J. R.; Ortega-Gadea, S.; Simo-Alfonso, E. F.; Ramis-Ramos, G. . J. Capillary electrophoresis enhanced by automatic two-way backgroundcorrection using cubic smoothing splines and multivariate data analysisapplied to the characterisation of mixtures of surfactants. *J. Chromatogr. A* **2005,** *1065,* 301-313.
63. Gan, F.; Ruan, G.; Mo, J. Baseline correction by improved iterative polynomial fitting withautomatic threshold. *Chemometr. Intell. Lab.* **2006,** *82,* 59-65.
64. Shao, X. G.; Cai, W.; Pan, Z. X. Wavelet transform and its applications in high performance liquid chromatography (HPLC) analysis. *Chem. Intell. Lab.* **1999,** *45,* 249-256.
65. Perrin, C.; Walczak, B.; Massart, D. L. The Use of Wavelets for Signal Denoising in Capillary Electrophoresis. *Anal. Chem.* **2001,** *73,* 4903-4917.
66. Ma, X. G.; Zhang, Z.-X. Application of wavelet transform to background correction in inductively coupled plasma atomic emission spectrometry. *Anal. Chim. Acta* **2003,** *485,* 233-239.
67. Wätzig, H. Peak recognition technique by a computer program copying the human judgement. *Chromatographia* **1992,** *33,* 218-224.
68. Vivo-Truyols, G.; Torres-Lapasio, J. R.; van Nederkassel, A. M.; Vander

Heyden, Y.; Massart, D. L. Automatic program for peak detection and deconvolution of multi-overlapped chromatographic signals. Part I: Peak detection. *J. Chromatogr. A* **2005,** *1096,* 133-145.

69. Schirm, B.; Wätzig, H. Peak Recognition Imitating Human Judgement. *Chromatographia* **1998,** *48,* 331-346.
70. Altria, K. D.; Fabre, H. An evaluation of the use of capillary electrophoresis to monitor trace drug residues following the manufacture of pharmaceuticals. *Chromatographia* **1995,** *40,* 313–320.
71. Kassidas, A.; MacGregor, J. F.; Taylor, P. A. Synchronization of Batch Trajectories Using Dynamic Time Warping. *AIChE J.* **1998,** *44,* 864-875.
72. Pravdova, V.; Walczak, B.; Massart, D. L. A comparison of two algorithms for warping of analytical signals. *Anal. Chim. Acta* **2002,** *456,* 77-92.
73. Tomasi, G.; van den Bergand, F.; Andersson, C. Correlation optimized warping and dynamic time warping as preprocessing methods for chromatographic data. *J. Chemometrics* **2004,** *18,* 231-241.
74. Vest Nielsen, N.-P.; Carstensen, J. M.; Smedsgaard, J. Aligning of single and multiple wavelength chromatographic profiles for chemometric data analysis using correlation optimised warping. *J. Chromatogr. A* **1998,** *805,* 17-35.
75. Skov, T.; van den Berg, F.; Tomasi, G.; Bro, R. Automated alignment of chromatographic data. *J. Chemometrics* **2006,** *20,* 484–497.
76. Ikuta, N.; Yamada, Y.; Yoshiyama, T.; Hirokawa, T. New method for standardization of electropherograms obtained in capillary zone electrophoresis. *J. Chromatogr. A* **2000,** *894,* 11-17.
77. Reijenga, J. C.; Martens, J. H. P. A.; Giuliani, A.; Chiari, M. Pherogram normalization in capillary electrophoresis and micellar electrokinetic chromatography analyses in cases of sample matrix-induced migration time shifts. *J. Chromatogr. B* **2002,** *770,* 45-51.
78. Lukacs, K. D.; Jorgensen, J. W. Capillary zone electrophoresis: Effect of physical parameters on separation efficiency and quantitation. *J. High. Res. Chromatog.* **1985,** *8,* 407-411.
79. Huang, X.; Gordon, M. J.; Zare, R. N. Current-Monitoring Method for Measuring the Electroosmotic Flow Rate in Capillary Zone Electrophoresis. *Anal. Chem.* **1988,** *60,* 1837-1838.
80. Kenndler-Blachkolm, K.; Popelka, I.; Gaš, B.; Kenndler, E. Apparent baseline irregularities for neutral markers in capillary zone electrophoresis with electroosomotic flow. *J. Chromatogr. A* **1996,** *734,* 351-356.
81. Sazelova, P.; Kašička, V.; Koval, D.; Prusik, Z.; Fanali, S.; Aturki, Z. Control of EOF in CE by different ways of application of radial electric field. *Electrophoresis* **2007,** *28,* 756-766.

82. Ermakov, S. V.; Capelli, L.; Righetti, P. G. Method for measuring very weak, residual electroosmotic flow in coated capillaries. *J. Chromatogr. A* **1996,** *744,* 55-61.

83. van de Goor, A. A. A. M.; Wanders, B. J.; Everaerts, F. M. Modified methods for off- and on-line determination of electroosmosis in capillary electrophoretic separations. *J. Chromatogr.* **1989,** *470,* 95-104.

84. Arulanandam, S.; Li, D. Determining ξ Potential and Surface Conductance by Monitoringthe Current in Electro-osmotic Flow. *J. Colloid Interface Sci.* **2000,** *225,* 421-428.

85. Pittman, J. L.; Henry, C. S.; Gilman, S. D. Experimental Studies of Electroosmotic Flow Dynamics in Microfabricated Devices during Current Monitoring Experiments. *Anal. Chem.* **2003,** *75,* 361-370.

86. Gaudioso, J.; Craighead, G. H. Characterizing electroosmotic flow in microfluidic devices. *J. Chromatogr. A* **2002,** *971,* 249-253.

87. Lee, T. T.; Dadoo, R.; Zare, R. N. Real-Time Measurement of Electroosmotic Flow in Capillary Zone Electrophoresis. *Anal. Chem. 66,* 2694–2700.

88. Schrum, K. F.; Lancaster III, J. M.; Johnston, S. E.; Gilman, S. D. Monitoring Electroosmotic Flow by Periodic Photobleaching of a Dilute, Neutral Fluorophore. *Anal. Chem.* **2000,** *72,* 4317–4321.

89. Pittman, J. L.; Schrum, K. F.; Gilman, S. D. On-line monitoring of electroosmotic flow for capillaryelectrophoretic separation. *Analyst* **2001,** *126,* 1240-1247.

90. Saito, R. M.; Neves, C. A.; Lopes, F. S.; Blanes, L.; Brito-Neto, J. G. A.; do Lago, C. L. Monitoring the Electroosmotic Flow in Capillary Electrophoresis Using Contactless Conductivity Detection and Thermal Marks. *Anal. Chem.* **2007,** *79,* 215-223.

91. Gaš, B.; Kenndler, E. System zones in capillary zone electrophoresis. *Electrophoresis* **2004,** *25,* 3901-3912.

92. Kuban, P.; Seiman, A.; Kaljurand, M. Improving precision of manual hydrodynamic injection in capillary electrophoresis with contactless conductivity detection. *J. Chromatogr. A* **2011,** *1218,* 1273-1280.

93. St. Claire, J. C.; Hayes, M. A. Heat Index Flow Monitoring in Capillaries with Interferometric Backscatter Detection. *Anal. Chem.* **2000,** *72,* 4726-4730.

94. Walczak, B.; Wu, W. Fuzzy warping of chromatograms. *Chemom. Intell. Lab. Syst.* **2005,** *77,* 173-180.

95. Sinkhorn, R. A. A relationship between arbitrary positive matrices and doubly stochastic matrices. *Ann. Math. Stat.* **1964,** *35,* 876–879.

96. Kothawala, D. N.; Moore, T. R.; Hendershot, W. H. Adsorption of dissolved

organic carbon to mineral soils: a comparison of four isotherm approaches. *Geoderma* **2008,** *148,* 43-50.

97. Vasanth Kumar, K.; Sivanesan, S. Comparison of linear and non-linear method in estimating the sorption isotherm parameters for safranin onto activated carbon. *J. Hazard. Mater.* **2005,** *123,* 288–292.
98. Ebadi, A.; Mohammadzadeh, S. J. S.; Khudiev, A. What is the correct form of BET isotherm for modelling liquid phase adsorption? *Adsorption* **2009,** *15,* 65-73.

Table. Parameters of various adsorption isotherms for san and loam samples.

Sand		Below 100 µm				100 to 200 µm				200 to 400 µm			
		BPA	PPA	EPA	MPA	BPA	PPA	EPA	MPA	BPA	PPA	EPA	MPA
Lang-muir	q_{max}	238.3	205.5	252.8	495.2	323.6	62.2	193.4	282.6	581.4	241.7	268.9	339.9
	K_a	0.0036	0.0042	0.0035	0.0022	0.0017	0.0162	0.0035	0.0038	0.001	0.0026	0.0027	0.0033
	r^2	0.9681	0.937	0.9808	0.9837	0.8856	0.9191	0.9376	0.9735	0.9971	0.9867	0.9804	0.9967
Freund-lich	n_F	1.9377	2.1648	1.9888	2.0327	1.1653	3.983	1.5924	2.6812	0.8138	1.0074	1.3423	2.1561
	K_F	1.3332	1.4033	1.3302	1.2281	1.2679	2.071	1.3598	1.3877	1.0992	1.1915	1.235	1.2702
	r^2	0.9795	0.9494	0.9912	0.9902	0.8872	0.8938	0.9474	0.9842	0.997	0.9728	0.98	0.9914
Redlich-Peterson	K_R	0.3013	0.3362	0.2941	0.2398	0.2076	0.5458	0.3169	0.3306	0.1360	0.2126	0.2426	0.2657
	a_R	3.9656	4.4092	3.9590	4.2556	1.8591	8.1942	3.3096	5.5674	1.6945	2.0340	2.7244	4.3811
	b_R	1.3516	1.3996	1.3419	1.2711	1.2307	1.7260	1.3729	1.3917	1.1457	1.2369	1.2746	1.3043
	r^2	0.9790	0.9491	0.9912	0.9903	0.8921	0.8970	0.9474	0.9838	0.9970	0.9749	0.9805	0.9924
BET	q_{max}	64.9	58.9	67.2	72.6	35.7	58.8	43.4	66.4	159.9	229.7	153.7	n/a[1]
	K_L	0.0024	0.0023	0.0023	0.0027	0.0032	0.0003	0.0026	0.0023	0.0010	0.0000	0.0007	n/a
	K_S	0.0170	0.0191	0.0167	0.0203	0.0248	0.0165	0.0229	0.0232	0.0041	0.0027	0.0051	n/a
	r^2	0.9862	0.9578	0.9939	0.9488	0.9545	0.9791	0.9634	0.9145	0.9959	0.9876	0.9814	n/a
Loam		Below 100 µm				100 to 200 µm				200 to 400 µm			
		BPA	PPA	EPA	MPA	BPA	PPA	EPA	MPA	BPA	PPA	EPA	MPA
Lang-muir	q_{max}	167.7	331.8	108.7	435.3	125.2	199.1	90.0	368.7	61.6	86.6	59.9	229.4
	K_a	0.0028	0.0008	0.005	0.0014	0.0046	0.0013	0.0079	0.002	0.0085	0.0035	0.0096	0.0027
	r^2	0.9871	0.9673	0.8948	0.9805	0.8258	0.9584	0.9797	0.9886	0.9253	0.9643	0.8089	0.9244
Freund-lich	n_F	1.0132	0.3921	1.834	1.1518	2.0919	0.3123	1.9376	0.9902	2.2886	0.7218	2.7946	1.7001
	K_F	1.2983	1.1093	1.5672	1.1988	1.6124	1.0709	1.5453	1.1162	1.8659	1.351	1.9951	1.3879
	r^2	0.991	0.9691	0.9171	0.9762	0.8534	0.9342	0.9544	0.9581	0.9583	0.9714	0.8584	0.919
Redlich-Peterson	K_R	0.2844	0.1899	0.4067	0.2224	0.4218	0.1001	0.3956	0.1502	0.4906	0.3117	0.5303	0.3165
	a_R	2.1268	0.9382	3.8715	2.4948	4.3833	0.6155	3.8379	1.9644	4.5442	1.4922	5.8916	3.5245
	b_R	1.3290	1.2091	1.5018	1.2491	1.5247	1.1052	1.4852	1.1621	1.6333	1.3658	1.6995	1.3723
	r^2	0.9911	0.9542	0.9181	0.9788	0.8545	0.9373	0.9582	0.9655	0.9590	0.9713	0.8571	0.9454
BET	q_{max}	40.6	79.4	21.8	45.7	23.4	n/a	n/a	n/a	24.3	37.6	19.5	27.6
	K_L	0.0023	0.0009	0.0033	0.0029	0.0033	n/a	n/a	n/a	0.0023	0.0013	0.0028	0.0034
	K_S	0.0163	0.0039	0.0631	0.0222	0.0586	n/a	n/a	n/a	0.0377	0.0100	0.0762	0.0590
	r^2	0.9949	0.9931	0.9960	0.9740	0.9821	n/a	n/a	n/a	0.9968	0.9965	0.9921	0.9359

ACKNOWLEDGEMENTS

This research was carried out at the Chair of Analytical Chemistry of the Department of Chemistry at Tallinn University of Technology.

I would like to express my gratitude to the supervisor of my thesis Prof. Mihkel Kaljurand for his excellent guidance, advice, ideas, and encouragement during the years I have been part of the Chair of Analytical Chemistry.

My special thanks belong to Dr. Merike Vaher for providing me with ideas, supporting with solutions, having faith in me, and, of course, for countless, yet fruitful coffee breaks in the last four years.

In addition, I would like to thank Martin Jaanus from the Department of Circuit Theory and Design, Tallinn University of Technology, for the development of electronics for CE equipment. The contribution by Edur Kuuskmäe to preparing portable CE instruments is more than appreciated. I also thank my co-authors Natalja and Petr who survived, together with me, experiments with chemical weapons.

My sincere thanks go to my colleagues, fellow PhD students, and the rest of the people at the Chair of Analytical Chemistry at the Department of Chemistry for providing a pleasant working atmosphere, as well as for all their help during the research.

I thank close friends of mine – Hannes, Siim, Priit, Valter, and the others who never let me forget that there is a lot of interesting to do out of the lab, too.

Above all, I thank my family – Mammu, Mann, Mom and Dad – for being understanding, supportive, loving.

The Estonian Ministry of Education and Research and the Estonian Ministry of Defence are acknowledged for financial support. Financial support has also been provided by the Estonian Science Foundation grants no. 6166 and 7818. This work has been partially supported by a graduate school „Functional materials and processes“, which is funded by the European Social Fund under project 1.2.0401.09-0079 in Estonia.

ABSTRACT

A certain type of analytical problems whenever quick response is needed, like the detection of toxic industrial chemicals, environmental pollutants, or chemical warfare agents, *etc*., would take advantage of portable instruments. Analyses performed at the site reduce the time between the sample collection and interpretation of the results when an appropriate counter action should be taken.

This thesis has been devoted to the development of portable capillary electrophoresis (CE) equipment designed for field experiments. CE is an excellent method for field experiments as due to simplicity, it could easily be implemented into portable instruments, especially when compared to its main competitor, high-performance liquid chromatography (HPLC), which employs complex high-pressure pumps. The aim of the portable CE instrument developed in this thesis is to enable analysis of nerve agents. CE is a superb alternative to portable analyzers (IMS, etc.) available today for the detection of nerve agents.

The CE instrument developed in this work employs a capacitively-coupled contactless-conductivity detector (C^4D) which, due to its low power consumption and simple cell construction, is a brilliant alternative to the common UV detection. Moreover, C^4D offers good sensitivity for the detection of nerve agent hydrolysis products as these do not contain UV absorbing groups.

As the operation of a CE instrument in a contaminated environment could impose hazard to the operator, wearing personal protective equipment (PPE) and keeping the time in the zone as short as possible to reduce the risk of potential damage are highly recommendable. These aspects have been taken account in the design of the portable CE system in which a fast and simple sample injection system has been implemented. The manual sample injection with the cross-sampler using plastic syringes have demonstrated a relatively good reproducibility for CE (RSD<8.8%). Sample collection and extraction procedures have been developed using harmless degradation products of nerve agents. Simple procedures for sampling from soil, vegetation material, and hard surface matrices have been confirmed by experiments with genuine nerve agents. CE results have been verified using GC-MS as a reference method.

The second part of the thesis has been dedicated for signal processing as an important constituent of CE analysis which is capable of improving reproducibility and decreasing the time needed for the interpretation of the results. Algorithms covering everything starting from baseline correction and electropherogram alignment, to peak matching and identification have been developed. An innovative approach has been applied to correcting the irreproducibility of migration by adjusting changes in the EOF by monitoring thermal marks, *i.e*. small disturbances in the capillary created by a punctual heating that move with the velocity of the EOF.

KOKKUVÕTE

Kaasaskantavatel analüsaatoritel on suur eelis teatud tüüpi keemilistes analüüsides nagu mürgiste tööstuskemikaalide, keskkonna reostuse või keemilise ründerelva tuvastamine, sest kohapeal saadud tulemused säästavad oluliselt aega proovi võtmise ja tulemuste interpreteerimise vahel võimaldades kiiremini rakendada vastumeetmeid.

Antud doktoritöö on pühendatud kaasaskantava kapillaarelektroferograafi väljatöötamisele pidades silmas just välikatseid. Tänu oma lihtsusele on kapillaarelektroforees (KE) suurepärane meetod välikatseteks võrreldes näiteks oma põhilise konkurendi vedelik-kromatograafiaga, mis kasutab keerukaid kõrgrõhu pumpasid. Välja töötatud kaasaskantava analüsaatori põhiliseks rakenduseks on keemiliste ründerelvade detekteerimine.

Väljatöötatud kapillarelektroferograaf kasutab uudset kontaktita juhtivusdetektorit, mis tänu oma madalale energiatarbimisele ja lihtsale ehitusele on suurepäraseks alternatiiviks laialt levinud UV-detektorile. Enamgi veel, juhtivusdetektoril on hea tundlikkus määratavate närvi agentide laguproduktide suhtes võrreldes UV-detektoriga, mis näiteks ei sisalda UV-valgust neelavaid rühmi.

Sellise seadmega töötamine võib toimuda tingimustes, mis võivad kujutada ohtu operaatori tervisele, siis on oluline silmas pidada, et vajadusel tuleb kasutada isikukaitsevahendeid ja piirata ohupiirkonnas viibist. Neid nõudmisi arvestades on töötatud välja instrumendi disain rakendades väga lihtsalt ja kiirelt kasutatavat proovisisestuse seadet. Rakendatud ristsisendseade võimaldab kasutada tavalisis süstlaid proovisisestuseks andes kapillaarelektroforeesi kohta suhteliselt hästi korratavaid tulemusi (suhteline standardhälve vähem kui 8,8%).

Proovi kogumise ja ekstraktsiooni protseduurid on välja töötatud kasutades ohutuid närviagentide laguprodukte. Lihtsad proovi ettevalmistamise protseduurid võimaldavad otsida keemilist ründerelva pinnasest, taimsetelt materjalidelt ja kõva kattega maatriksitelt nagu näitasid katsed tõeliste närvi agentidega (sariin, somaan, VX). Mass-spektromeetriga ühendatud gaasikromatograafiga saadud võrdlustulemused kinnitasid KE tulemusi.

Osa doktoritööst on pühendatud signaali töötlusele kui olulisele osale KE analüüsist, mis võimaldab parandada tulemuste korratavust ja lühendada märgatavalt tulemuste interpreteerimiseks kuluvat aega. Väljatöötatud algoritmid hoolitsevad nulljoone triivi eemaldamise, halvasti kattuvate signaalide reastamise ning ainete automaatse identifitseerimise eest. Unikaalne signaalide reastamise algoritm korrigeerib kõikuvad migratsiooni ajad rakendades selleks elektroosmootse voo triivi kohta termomarkeritega saadud andmeid. Termomarkerid on väikesed kontsentratsiooni häiritused, mida tekitatakse kapillaari kuumutamisel mingis punktis.

ORIGINAL PUBLICATIONS

Publication I

Seiman, A., Jaanus, M., Vaher, M., Kaljurand, M., A portable capillary electropherograph equipped with a cross-sampler and a contactless-conductivity detector for the detection of the degradation products of chemical warfare agents in soil extracts. *Electrophoresis* **2009**, *30*, 507-514.

Andrus Seiman[1]
Martin Jaanus[2]
Merike Vaher[1]
Mihkel Kaljurand[1]

[1]Department of Chemistry, Tallinn University of Technology, Tallinn, Estonia
[2]Department of Circuit Theory and Design, Tallinn University of Technology, Tallinn, Estonia

Received June 2, 2008
Revised August 13, 2008
Accepted August 13, 2008

Research Article

A portable capillary electropherograph equipped with a cross-sampler and a contactless-conductivity detector for the detection of the degradation products of chemical warfare agents in soil extracts

A fully portable CE device equipped with a capacitively coupled contactless-conductivity detector and a cross-injection device is put to the test in laboratory conditions. The portable device is capable of working on batteries for at least 4 h. After that, its performance is strongly affected by the drop in the high-voltage output and analysis may be interrupted if its length exceeds a reasonable time. The concentration of the BGE affects both ionic strength and conductivity. Choosing an optimal concentration of BGE is therefore about finding a good compromise between selectivity and sensitivity. All experiments were performed using a mixture of histidine and MES with a concentration of 15 mM as BGE. The performance of the cross-injection device is optimized by the use of internal standards. Satisfactory reproducibility is gained as the RSD of peak areas is reduced to 8% or less. LODs for different phosphonic acids are in the range of 2.5–9.7 μM. For the analysis of adsorption of phosphonic acids in sand and loamy soil samples, calibration curves are constructed. Linearity in a measured concentration range of 10–100 μM is excellent, as the squares of correlation constants are ~1. The concentration analysis of phosphonic acids in soil extracts demonstrates that their adsorption curves in sand and loamy soil follow different adsorption isotherms.

Keywords:
CE / Chemical warfare agents / Contactless-conductivity detection / Portable instrument / Sample injection DOI 10.1002/elps.200800341

1 Introduction

The detection of chemical, biological, radiological and explosive material that may be used to do harm poses analytical challenges that are exceptional in both quantitative and qualitative terms [1]. Portable devices could resolve stringent requirements for fast and efficient chemical, biological, radiological and explosive detection to identify and quantify unknown entities. The transport and handling of the portable equipment must be addressed at an early stage in the system design to ensure maximum usability. Weight and size, number of personnel required to operate the equipment, vehicle mounting, impact on deployment and response time, *etc.* are all key aspects to be considered in the system design stage [2].

Miniaturization is often a key way of developing a technology to make an instrument truly portable. This works well in a number of applications. It is not always possible, however, to miniaturize devices without compromising one or more factors. CE has many advantages over chromatographic separation techniques in terms of potential miniaturization. To name just a few, the CE device consists only of a high-voltage supply, a capillary, small BGE vessels and a detection system. What is most important is that CE requires no use of complex mechanical high-pressure pumps as liquid chromatography does.

For portable CE instruments the most challenging task is to find an appropriate detection system as the most widely used UV absorption detection is not suitable to be used in portable devices owing to their high power consumption of light sources. The most popular alternatives to UV detection may be found among electrochemical detection techniques.

Correspondence: Andrus Seiman, Department of Chemistry, Tallinn University of Technology, Akadeemia tee 15, 12618 Tallinn, Estonia
E-mail: andrusseiman@gmail.com
Fax: +372-620-2828

Abbreviations: **1-BPA,** 1-butylphosphonic acid; **C^{4}D,** capacitively coupled contactless-conductivity detector; **CWA,** chemical warfare agents; **EPA,** ethylphosphonic acid; **His,** histidine; **MPA,** methylphosphonic acid; **PMPA,** pinacolyl MPA; **PPA,** propylphosphonic acid

Amperometric [3–6], potentiometric [3, 7–9] and conductometric [10, 11] detection systems may all be used in portable capillary or microchip electrophoresis devices. In recent years capacitively coupled contactless-conductivity detection has become the most widely used electrochemical detection technique. Its detection cell is of a very simple construction compared with those of amperometric and potentiometric detections, though amperometric detection demonstrates a better LOD.

The capacitively coupled contactless-conductivity detector (C^4D) is a universal and sensitive tool that was first introduced independently in 1998 by da Silva and do Lago [12] and Zemann and colleagues [13]. The C^4Ds are basically constructed of two axially placed tubular electrodes that encompass the separation capillary. This means that the signal of C^4D is gathered longitudinally along the capillary instead of the transversal mode of conventional absorbance detection schemes. One of the two electrodes is excited with an alternating current signal and the other electrode is used to register the same signal after it has passed through the cell.

In recent years capacitively coupled contactless-conductivity detection has been implemented in a miniaturized electrophoresis microchip and portable CE systems. For instance, the portable CE system with capacitively coupled contactless-conductivity detection developed by Kubáň and colleagues [14] can run the detector and the data acquisition system from the batteries for 9 h. High-voltage power supply with both polarities has an output of 15 kV. The excitation sine wave is in the frequency range between 100 and 1000 kHz and in the voltage range between 2 and 20 V_{pp}. The samples are introduced in an electrokinetic or hydrodynamic mode by manual turning or moving of the sample tray. A specific device runs on four 12 V batteries. The detection system uses two batteries of four. The high-voltage power supply and data acquisition system use one battery each.

Xu and colleagues [15] have published a description of their portable CE instrument that is about the same size as the instrument developed by Kubáň and colleagues [14], but lighter, and its batteries last for only a couple of hours. The detector works at a constant excitation frequency of 125 kHz and a signal voltage of 240 V_{pp}. The design of the detection cell is completely different from the cell used by two commercially available C^4D instruments (http://www.istech.at/product.htm and http://www.edaq.com/C4D_intro.html), where tubular electrodes are placed in a rectangular aluminum case. It consists of a capillary, a copper electrode and shielding with insulator layers screwed together between a circular-shaped aluminum cover and base plates. The separation of 11 low-molecular-weight organic acids and 16 chlorinated acid herbicides took place in single analysis, which lasted for 35 min.

Wang and Fu [16] developed a miniaturized CE system with contactless-conductivity detection and flow-injection sample introduction. A 5.5 cm fused-silica capillary was fixed to the detection cell consisting of two 2 mm tubular electrodes in between the glass slide and the silicone elastomer layer. The performance of the device was studied by analysis of cations in surface water.

Nerve agents belong to the most toxic compounds ever produced. Three such agents, Sarin, Soman and VX, contain a functional group of alkyl methylphosphonate. In aqueous environments these organophosphorus nerve agents easily hydrolyze to produce nontoxic and more stable alkyl methylphosphonic acids (MPAs). The identification of these alkyl MPAs is therefore very suitable for determining the use of nerve agents even if the nerve agents themselves have already been degraded. Analysis of the breakdown products of nerve agents could be done by various methods, such as gas and liquid chromatography, mass spectrometry and CE. The pros and cons of different methods have been reviewed in [17].

In the case of CE, both direct [18] and indirect UV detections [19] may be used to detect the degradation products of organophosphorous nerve agents; however, the indirect UV detection mode is preferred, because it is more sensitive as alkyl phosphorous acids do not contain any chromophoric groups. In [20] it was shown that reversing the EOF combined with an electrokinetic sample injection can provide more than a 100-fold improved LOD compared with the hydrodynamic injection. The breakdown products of organophosphorous nerve agents can easily be detected with contactless-conductivity detection as they are strong acids and therefore dissociate completely in aqueous environments. Although the selectivity and sensitivity of the conductivity and indirect UV detections are rather similar, as reported in [21, 22], the former has one advantage over the latter, and this is its potential use in portable devices, as reported in the last paragraph.

The portable CE devices reported earlier by several different groups [14, 15, 23–25] typically apply the electrokinetic or hydrodynamic sample injection familiar from bench-top CE systems. This kind of sample injection involves a lot of repeated manipulations with buffer and sample vessels. These manipulations are automated in bench-top CE instruments, but have to be carried out manually in portable devices. For portable devices a simple, robust and quick sample injection is always favorable, especially when field analyses of toxic pollutants, nerve agents, *etc.* are performed.

One such candidate for a robust sampling device for a portable instrument could be a cross-sampler. The cross-sampler [26] and its modifications – the T [27] and double-T [28] injection – have been used in microchip electrophoresis ever since the first electrophoresis microchips were introduced. Electrophoresis microchips, in general, consist of at least two channels – one is for sample injection and the other for separation. In microchips, the electrophoretic separation process usually takes place in two discrete steps. First, the sample is loaded into the sample injection channel and the sample plug is formed. Second, the sample plug is loaded into the separation channel and the separation process begins. While separation is always driven by electrophoretic forces, the sample plug may be

formed by different forces, electrophoretic force and pressure being most common. Basically, the cross-sampler is also suitable for use for conventional CE. In practice, problems occur when crossing capillaries are connected, as the dimensions of capillaries make it mechanically extremely complicated. There are only a few publications on cross-sampler systems for conventional CE. Zare and Huang [29] have patented a cross- or T-shaped device for CE. One makes the device by boring two holes in the separation capillary at the selected location, then introducing elongate guide members into the holes and threading members into the sample injection capillaries until the separation capillary contacts the sample injection capillaries. The way the device is operated is not defined in the patent, making both the hydrodynamic and electrokinetic injections possible. Tsukagoshi and colleagues [30] demonstrated a rather simple cross-sampler, as capillaries were fixed to the holes that were drilled into a Tygon tube. Their device was operated in multiple steps. First, the sample was electrokinetically driven from the sample reservoir to the sample waste reservoir so that it filled the cross-section of the sampler. Second, the sample in the cross-section was separated by the application of high voltage between the buffer and waste reservoirs.

In this paper the use of a portable CE device with capacitively coupled contactless-conductivity detection for the analysis of the degradation products of nerve agents is described. The goal was to construct a very simple sampler so that the CE device could be operated by nonqualified personnel. The idea was to use syringes to inject a sample. The sampler used is a modification of the one employed for chemical reaction monitoring in [31]. A cross-sampler automated by pressure was redesigned for use in the field analyses, where pressurized control of the cross-sampler is complicated. The portable CE is used for the separation and determination of various phosphonic acids extracted from soil samples. A new cross-sampler has been put to the test. In this paper we demonstrate that the cross-sampler is an attractive option for use in portable CE devices as the sample introduction is simpler than in hydrodynamic or electrokinetic injections, as reported in last paragraph.

2 Materials and methods

2.1 Chemicals

During experiments, five phosphonic acids, MPA, ethylphosphonic acid (EPA), 1-butylphosphonic acid (1-BPA), propylphosphonic acid (PPA) and pinacolyl MPA (PMPA), were subjected to analysis. The first three were purchased from Alfa Aesar, Lancaster Synthesis (Windham, NH, USA), and the last two from Sigma-Aldrich (Steinheim, Germany). Histidine (His) and MES were purchased from Merck (Darmstadt, Germany). Sodium hydroxide was purchased from Chemapol (Prague, Czech Republic).

BGE was prepared by dissolving MES and His in deionized water. The stock solution containing all five phosphonic acids at a concentration of 10 mM was prepared by dissolving an exact amount of analytes in deionized water. All chemicals were used without further purification.

2.2 Portable CE instrument with C^4D

The portable CE instrument with C^4D and the cross-sampler tested in this work were made entirely in-house. The dimensions of the whole system are $330 \times 180 \times 130$ mm and it weighs less than 4 kg. The CE system employs EMCO DX250 (Sutter Creek, CA, USA) high power supplies. High-voltage output of the system is up to 25 kV. The operating time of the system running on batteries is at least 4 h. This should be enough as it is comparable to the battery supply of a standard laptop computer. The system uses ten commonly available AA-type rechargeable batteries with an overall output of 15 V.

The detection cell used in the portable CE device is similar to those used in commercial devices. The cell itself has been built into a rectangular piece of alumina where three holes have been milled for two tubular electrodes and an operational amplifier. Two tubular electrodes made of syringe needles with a length of 8 mm and a gap of 0.8 mm between them are located in separate chambers and the alumina between and around them is grounded and acts as a shielding. One of the electrodes was excited with a 60 V peak-to-peak sine wave oscillating in a frequency range of 50–300 kHz. The signal was picked up by the second electrode and further amplified. The exciting frequency and amplification amount are controlled by an external computer using software written in-house. In all experiments the default frequency was 200 kHz. Data acquisition was carried out with the in-house built 16-bit analog-to-digital converter integrated inside the portable CE system detector electronics. An RS-232 port is used to communicate with the computer.

2.3 Cross-sampler

The cross-sampler used in the CE instrument is built according to ideas familiar from microchip electrophoresis. It is made of two pieces of a capillary, teflon tubing and necessary fittings, which all have been connected to a rectangular PMMA block. The dimensions of the sampler (Fig. 1A) are $22 \times 22 \times 8$ mm. There are drilled sample injection and separation channels in the device. At different endings of the separation channel two capillaries with horizontally smooth endings are inserted. The capillaries are fixed so that their endings meet at the crossing channel. The device uses fused-silica capillaries with a length of 6 and 48 cm. A longer capillary serves as a separation capillary (Fig. 1B). The effective length between the crossing point and the detection cell is 42 cm. The fused-silica capillaries

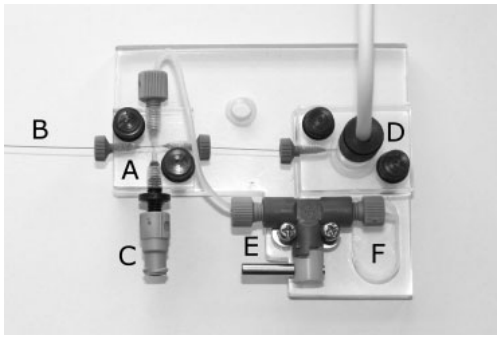

Figure 1. Cross-sampler with its surroundings: (A) cross-sampler; (B) separation capillary; (C) socket for syringe; (D) BGE vessel with electrode lead; (E) shut-off valve; and (F) waste reservoir.

(id 75 μm × od 365 μm) were obtained from Polymicro Technologies (Tucson, AZ, USA). The size of the gap between the two endings of the capillaries is extremely important as it defines the amount of the sample to be injected into the separation channel. An optimal gap size seems to be about that of the inner diameter of the capillaries used. The capillaries are put in place under the microscope to ensure that they are in line and the gap between them is not too wide, as otherwise the laminar flow of the liquids may be interrupted and a higher amount of the sample is inserted into the separation capillary than is the gap between the capillaries. The gap width is estimated to be about 30 μm. The capillaries and tubes are fixed with 10/32″ threaded *Upchurch Scientific Nanoport* (Oak Harbor, WA, USA) fittings.

A special socket (Fig. 1C) to be used with threaded or conventional syringes is inserted into one side of the sample injection channel crossing the separation channel. The teflon tube with an outer diameter of 1/16″ is inserted into the other side of the sample injection channel and connected to the waste reservoir (Fig. 1F). The sample is injected by syringes. A syringe is inserted into the socket and the BGE solution in the cross-section of the sampler is replaced by the sample solution as the sample solution is pushed into the sample introduction channel by the injection. At the same time the rest of the sample exits through the waste channel. The sample solution between the capillaries in the cross-section of the sampler is inserted into the separation channel by laminar EOF, which carries the sample to the separation capillary and replaces the junction between two capillaries with BGE as soon as the high voltage is turned on. Obviously, there is continuous diffusion of the sample into the separation channel during the analysis run, which will affect the baseline level. The amount of the sample inserted into the separation capillary is determined both by the length of the gap between capillaries and by the amount of the sample flushed through the cross during the sampling. Sample injection in the case of the cross-sampler, however, is definitely not a pressurized injection as the waste channel has a much larger inner diameter than the capillaries and is relatively short. This means that the resistance that the waste channel offers is much smaller than the resistance the capillaries offer.

In the middle of the waste channel there is a shut-off valve (Fig. 1E, *Upchurch Scientific* part no. P-782). For sampling and analysis the valve is opened and the excess sample exits through the waste channel. When the valve is closed, it is possible to wash the capillaries as the liquid injected into the device cannot exit through the waste channel and is pushed into the capillaries instead. With this construction it is possible to reconfigure the device from the sampling mode to the washing mode just by changing the position of the waste channel valve.

2.4 Sample preparation

The environmental samples used in the experiments reported here were prepared from natural sand and natural loamy soil collected from two different locations in Estonia – loamy soil from Southern Estonia (Viljandi area) and sand from Northern Estonia (Tallinn). For sample preparation, first 2 g of soil material were weighed into plastic vials. Second, soil materials were spiked with the stock solution of phosphonic acids. After a 1 h exposure to phosphonic acids, 10 mL of deionized water was added to the soil samples. At first a 24 h exposure was used, but preliminary experiments were not indicative of any difference in electropherograms of a 1 and 24 h exposure. Thirty minutes after the addition of water, the samples were sonicated for 10 min, followed by filtration with 0.45 μm filters.

The volumes of the stock solution added to the soil material were 10, 25, 50 and 100 μL. The added amount of phosphonic acids with 10 mL of added water corresponds to the concentrations of 10, 25, 50 and 100 μM. In practice, as shown below, these concentrations were lower, as some portion of phosphonic acids was adsorbed in the soil material. For the calibration curve the sample preparation was basically the same, except that phosphonic acids were added to soil samples at the end of the sample preparation right after the filtration. This means that in the beginning, pure water was added to the soil samples and the rest of the operations were performed as described in previous paragraph.

3 Results and discussion

3.1 Separation optimization and basic performance of the cross-injection device

The choice of the right BGE for conductivity detection is challenging as BGE must have a very low conductivity to achieve maximum sensitivity and, at the same time, have sufficient ionic strength. Finding a suitable BGE is a major drawback of conductivity detection as the list of possible

BGEs is short. For the experiments reported here, MES/His, one of the most commonly used BGEs for conductivity detection, was chosen. Its different concentrations were tested to find an optimal one, as higher sensitivity is obtained by use of buffers with a lower conductivity, and higher selectivity is obtained with a higher ionic strength. The influence of three different concentrations of BGE is shown in Fig. 2. A minimum concentration of 15 mM of BGE is required to achieve sufficient separation although the signal-to-noise ratio for lower-concentration BGEs is higher as the difference in conductivity between phosphonic acids and BGE is more noticeable. The electropherograms also reveal a system peak appearing at the detection point right after the EOF. The size, the shape and even the direction of the system peaks are not stable and can change from experiment to experiment, though the migration time of the system peaks is reproducible. There are a few peaks before EOF that probably belong to metals like sodium, potassium, *etc*. although none of them were added to the solutions. It is almost impossible to avoid the appearance of these peaks as the LOD of these metals is very low owing to the high conductivity of the latter.

A cross-sampler is convenient for inserting a sample into capillaries as changing and lifting BGE and sample vessels of bench-top CE instruments are replaced by a simple injection with plastic syringes. A drawback of the cross-sampler is that high amounts of the sample solution are consumed, which considerably exceed those used in conventional hydrodynamic and electrokinetic sample injections. Moreover, most of the sample solution is discarded into the waste reservoir, as every time the sample is injected it has to replace the old solution from the last injection filling the cross-injection device. Of course, when multiple analyses with the same sample solution are performed, the waste is less. Experiments demonstrated the sample volumes of 0.05–0.10 mL *per* experiment to be optimal.

In an ideal case the amount of the sample injected into the separation capillary should be determined only by the configuration of the capillaries and the injection device and not by the injection itself. This means that how hard or how long a syringe is pushed should not affect the amount of the sample injected. In practice, it is extremely difficult to control hand movements and make reproducible injections in experiment after experiment. If one pushes a syringe too hard, it is possible to introduce huge amounts of the sample. It is therefore obvious that for the quantification of analytes some sort of internal standard should be used. Since in our case the sample matrix is water, the neutral peak of the EOF could be used as an internal standard, as the area of the water peak directly represents the size of the injected sample plug. The size of the water peak is enormous, however, compared with the small peaks of dilute analytes. This leads to the situation where the detector amplification should be reduced, to ensure that the full water peak would stay in a narrow measurement range of a 16-bit analog-to-digital converter. The reduction of the detector amplification means that as well as the water peak the analyte peaks are also reduced and this results in lower sensitivity, which is not acceptable. For the analysis of sand samples citric acid was therefore used as an internal standard. As citric acid seemed to degrade quite easily, new solutions were made quite often, every day or two. Immediately before experiments, 4 μL of a 20 mM citric acid solution was added to 1 mL of the sample. This amount of the sample solution was enough to perform 10 or 20 experiments.

The first electropherograms (Fig. 3A) revealed that besides the six peaks belonging to five phosphonic acids and citric acid, there were two unknown peaks. The study of blank samples (Fig. 3B) – water extracted from sand without

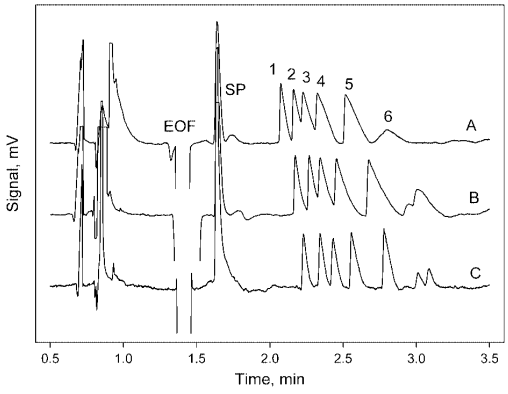

Figure 2. Effect of the BGE concentration on the separation of five phosphonic acids. The BGE solution is MES/His with a concentration of (A) 5 mM, (B) 10 mM, (C) 15 mM. Separation voltage: 20 kV; sample solution: 100 μM phosphonic acids dissolved in sand extraction water. 1, PMPA; 2, 1-BPA; 3, PPA; 4, EPA; 5, MPA; 6, peaks extracted from soil; SP, system peak.

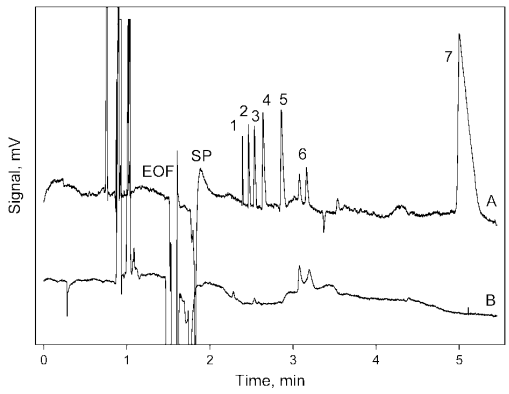

Figure 3. Electropherograms of sand extracts. The BGE solution is 15 mM MES/His. Separation voltage: 20 kV. Sample solution: 75 μM phosphonic acids dissolved in sand extraction water; (A) sample, (B) pure sand extraction water. 1, PMPA; 2, 1-BPA; 3, PPA; 4, EPA; 5, MPA; 6, peaks extracted from soil; 7, citric acid; SP, system peak.

the addition of any phosphonic acids – verified that these two peaks belong to substances that have been extracted from pure sand samples. These two peaks also exist in the loamy soil extracts. Although those two peaks were never identified, as this was not the goal of this paper, they could be used as an internal standard.

As mentioned in previous paragraph, it is quite difficult to control the cross-injection device manually to make reproducible sample injections and therefore the use of some sort of internal standard is recommended. Without any internal standard, at some concentrations of phosphonic acids the RSD of peak areas varies up to 50%. Use of an internal standard, *i.e.* division of the peak area of the analyte by the peak area of the internal standard, means that reproducibility will be immediately improved. The RSD achieved using internal standards is 8% or better. Reproducibility of migration times is excellent as the RSD is below 5%.

3.2 Analyses of soil extracts

For analyses of soil extracts the calibration curve of five concentrations of phosphonic acids in the region between 10 and 100 μM was created. First, the sand samples were taken for examination. For sand samples two competitive calibration curves were constructed where citric acid or an unidentified peak extracted from sand was used as an internal standard. The linearity of the curve obtained with an unknown peak extracted from sand as an internal standard was somewhat better, as the square of the correlation coefficient was closer to one (R^2>0.99). Only in the case of PMPA was the linearity less than perfect ($R^2 = 0.9688$). The results obtained by use of the calibration curve of citric acid are the opposite, as the linearities in general were not so good, being in the range of $R^2 = 0.95$–0.98. Only PMPA had an excellent linearity (R^2>0.99). No citric acid was added to loamy soil samples, as the results of the experiments with sand samples demonstrated that the peak of the unidentified compound extracted from the soil samples is a better internal standard than citric acid. The linearities of loamy soil samples were excellent (R^2>0.99), except for PPA ($R^2 = 0.98$). Specific performance data for phosphonic acids including LODs are presented in Table 1. LOD of phosphonic acids in soil extracts is calculated by interpolation of the calibration curves. LOD for different phosphonic acids is in the range of 2.5–9.7 μM. In the case of real chemical warfare agent (CWA) samples it is difficult to predict which concentrations should be detected as this kind of information is not freely available. The concentration of degradation products in real samples depends on many aspects such as the type of a CWA attack, the time of exposure to CWA, half-time of specific nerve agent, *etc.* All experiments here have been performed under conditions of sample stacking as all samples are dissolved in water. In the case of very low concentration of real samples, however, some additional pre-concentration could be needed.

The soil extracts were prepared with four different amounts of the mixture of phosphonic acids. These amounts should correspond to the concentrations of 10, 25, 50 and 100 μM if phosphonic acids are not adsorbed in the soil and are fully extracted with water. The soil extracts were analyzed under the same conditions as all experiments performed in this work. The amount of the phosphonic acids extracted was calculated according to the calibration curves with the soil peak as an internal standard, because the linearity of the curves was better. The difference in concentration between the spiked and extracted phosphonic acids corresponded to the amount of phosphonic acids adsorbed in soil. In the case of different phosphonic acids the results were comparable as the acids were adsorbed in

Table 1. Performance data for phosphonic acids

	LOD (μM)	RSD[a] (%)	$(a \pm s_a)$[b]	$(b \pm s_b)$[b]	(R^2)[c]	$(A \pm s_A)$[d]	$(K \pm s_K)$[d] $(\mu M)^{-1}$
Sand							
PMPA	6.7	3.3	−0.107 ± 0.18	0.028 ± 0.003	0.969		
1-BPA	4.2	8.5	0.147 ± 0.08	0.027 ± 0.001	0.993		
PPA	2.5	6.5	0.039 ± 0.15	0.035 ± 0.002	0.986		
EPA	3.0	6.0	0.028 ± 0.03	0.028 ± 0.001	0.999		
MPA	3.7	6.6	0.043 ± 0.10	0.043 ± 0.002	0.996		
Loamy soil							
PMPA	6.7	6.5	0.031 ± 0.06	0.014 ± 0.001	0.987	0.91 ± 0.05	0.015 ± 0.002
1-BPA	7.4	5.2	−0.067 ± 0.07	0.019 ± 0.001	0.990	0.74 ± 0.03	0.008 ± 0.001
PPA	9.2	8.8	−0.135 ± 0.11	0.024 ± 0.002	0.982	0.60 ± 0.04	0.004 ± 0.001
EPA	5.3	6.1	−0.013 ± 0.09	0.026 ± 0.002	0.990	0.75 ± 0.04	0.008 ± 0.001
MPA	4.1	6.5	−0.011 ± 0.12	0.035 ± 0.002	0.990	1.02 ± 0.03	0.012 ± 0.001

a) RSD of peak areas.

b) Calibration line equation $y = a + bc$ parameters: a, intercept; s_a, its standard deviation; b, slope; s_b, its standard deviation; y, detector response and c, concentration.

c) Square of correlation coefficient of calibration line.

d) Langmuir isotherm $c_{ad} = Ac_{ip}/(1+Kc_{ip})$ parameters with their standard deviations; c_{ad}, adsorbed concentration; c_{ip}, input concentration.

the soil at a similar rate. This means that their adsorbance in the soil samples is not structure-dependent or their structures are very similar. Since sand and loamy soil have different structure, however, their adsorption behavior may be different. Figure 4 presents the average concentration of adsorbed phosphonic acids found in sand and loamy soil plotted against the spiking concentration. The results are truly fascinating as they reveal a totally different behavior of sand and loamy soil samples. In the measured range of 10 and 100 μM the sand samples adsorb phosphonic acids linearly ($R^2 = 0.9904$) as around 70% of the spiked phosphonic acids are adsorbed in sand, while only 30% could be extracted. The behavior of phosphonic acids in loamy soil in the measured concentration range is completely different, as their adsorption curve is nonlinear.

From the shape of the adsorption curve we can assume that the adsorption of phosphonic acids in loamy soil follows the Langmuir isotherm. At low concentration the adsorption curve is linear as no molecules have been adsorbed on the surface. Later the adsorption curve will decrease until it reaches constant value, when all adsorption sites are filled and monolayers of phosphonic acids have been formed on the surface. Although the measured concentrations covered only a part of the adsorption isotherm, the parameters of Langmuir's isotherm can still be calculated (Table 1) for loamy soil. No Langmuir's isotherm parameters for adsorption curve of phosphonic acids in sand samples have been calculated as the curve cannot be fitted into a simple Langmuir's isotherm. Adsorption of phosphonic acids in sand must follow some more complex equation that is capable of describing adsorption in multiple layers.

3.3 Battery-powered analyses

Energy is extremely important for portable devices as its lack may interrupt the performance of analyses in the field when batteries run empty. The simplest CE devices consist of three energy-consuming parts. These are a detector, a data acquisition system and a high-voltage power supply. The consumption of energy by the data acquisition system is rather low as it usually consists of low-power microelectronics. The consumption of energy by the C^4D is determined by the generator used for the excitation of one of the two electrodes. The electrode can be excited with a lower voltage, though higher voltages usually give better results if sensitivities are observed. This leads to the conclusion that the high-voltage power supply is probably the major consumer of power in the system. This has been proven by a simple test in which the data acquisition system and the C^4D are capable of working for 8 h, while the whole system, including the high-voltage power supply, started facing problems with high voltage switched on after 4 h of constant working. The data acquisition system and the detector continued their work, however, without any problems; 3 or 4 h are enough given the capacities of laptop computer batteries. As the experiments were carried out in laboratory conditions, the influence of the temperature on the viscosity of solutions, and hence on the analysis time, was not investigated. In field analyses, temperature plays a crucial role. The higher viscosities caused by lower temperature will increase analysis time. This means that analysis may last a long time or is impossible to perform even though the batteries are fully charged.

As batteries contribute heavily to the weight of the device, it should be possible to replace them to find a compromise between the weight of the instrument and the capacity of the batteries.

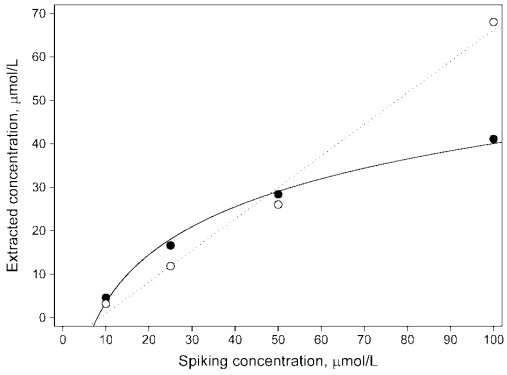

Figure 4. An average adsorption of phosphonic acids in sand (open circle) and loamy soil (closed circle) samples *versus* the spiking concentration of phosphonic acids.

4 Concluding remarks

The portable CE device equipped with capacitively coupled contactless-conductivity detection and a cross-sampler is a small and comfortable analytical system that may be carried easily into the field. The cross-injection device makes sample introduction simple compared with manual hydrodynamic or electrokinetic injections. Quantitative analyses are possible with the aid of an internal standard. Inaccurate sample injections can be rendered numerically reproducible by use of the relation between the analyte and internal standard peak areas. It is possible to reach an RSD of 8%, though it is more difficult to achieve at lower concentrations. Reproducibility of migration times is good as RSD is less than 5%. Calculated LOD for phosphonic acids is in the range of 2.5–9.7 μM. These results can be considered acceptable, however, as they have been achieved with the portable device constructed primarily to do field analyses. Performing field analyses outside may be complicated as the temperature is not under control and may affect the viscosity of the solutions used. If the viscosity poses no problem, the fully charged batteries save at least 3–4 h of analysis time.

The authors have declared no conflict of interest.

5 References

[1] Bell, A., Vadgama, P., *Analyst* 2008, *133*, 557.

[2] Turl, D. E. P., Wood, D. R. W., *Analyst* 2008, *133*, 558–562.

[3] Huang, X., Zare, R. N., Sloss, S., Ewing, A. G., *Anal. Chem.* 1991, *63*, 189–192.

[4] Kappes, T., Schnierle, P., Hauser, P. C., *Anal. Chim. Acta* 1999, *393*, 77–82.

[5] Chen, D.-C., Chang, S.-S., Chen, C.-H., *Anal. Chem.* 1999, *71*, 3200–3205.

[6] Kappes, T., Hauser, P. C., *Analyst* 1999, *124*, 1035–1039.

[7] De Backer, B. L., Nagels, L. J, *Anal. Chem.* 1996, *68*, 4441–4445.

[8] Kappes, T., Hauser, P. C., *Anal. Comm.* 1998, *35*, 325–329.

[9] Li, F. Y., Wei, H., Wang, T., Wu, Y., *Proc. SPIE* 2001, *4199*, 51–58.

[10] Zemann, A. J., *Electrophoresis* 2003, *24*, 2125–2137.

[11] Kubáň, P., Hauser, P. C., *Anal. Chim. Acta* 2008, *607*, 15–29.

[12] da Silva, J. A. F., do Lago, C. L., *Anal. Chem.* 1998, *70*, 4339–4343.

[13] Zemann, A. J., Schnell, E., Volgger, D., Bonn, G. K., *Anal. Chem.* 1998, *70*, 563–567.

[14] Kubáň, P., Nguyen, H. T. A., Macka, M., Haddad P. R. *et al.*, *Electroanalysis* 2007, *19*, 2059–2065.

[15] Xu, Y., Wang, W., Li, S. F. Y., *Electrophoresis* 2007, *28*, 1530–1539.

[16] Wang, L., Fu, C., *Instrum. Sci. Technol.* 2004, *32*, 303–309.

[17] Hooijschuur, E. W. J., Kientz, C. E., Brinkman, U. A., *J. Chromatogr. A* 2002, *982*, 177–200.

[18] Pianetti, G. A., Taverna, M., Baillet, A., Mahuzier, G. *et al.*, *J. Chromatogr.* 1992, *630*, 371–377.

[19] Nassar, A.-E. F., Lucas, S. V., Myler, C. A., Jones W. R. *et al.*, *Anal. Chem.* 1998, *70*, 3598–3604.

[20] Melanson, J. E., Wong, B. L.-Y., Boulet, C. A., Lucy, C. A., *J. Chromatogr. A* 2001, *920*, 359–365.

[21] Nassar, A.-E. F., Lucas, S. V., Jones, W. R., Hoffland, L. D., *Anal. Chem.* 1998, *70*, 1085–1091.

[22] Rosso, T. E., Bossle, P. C., *J. Chromatogr. A* 1998, *824*, 125–133.

[23] Hutchinson, J. P., Evenhuis, C. J., Johns, C., Kazarian, A. A. *et al.*, *Anal. Chem.* 2007, *79*, 7005–7013.

[24] Xu, Y., Qin, W. Li, S. F. Y., *Electrophoresis*, 2005, *26*, 517–523.

[25] Kappes, K., Galliker, B., Schwarz, M. A., Hauser, P. C., *Trends. Analyt. Chem.* 2001, *20*, 133–139.

[26] Jacobson, S. C., Hergenröder, R., Koutny, L. B., Warmack, R. J. *et al.*, *Anal. Chem.* 1994, *66*, 1107–1113.

[27] Harrison, D. J., Manz, A., Fan, Z., Lüdi, H. *et al.*, *Anal. Chem.* 1992, *64*, 1928–1932.

[28] Effenhauser, C. S., Manz, A., Widmer, H. M., *Anal. Chem.* 1997, *65*, 2637–2642.

[29] Zare, R., Huang, X., US Patent 5, 298, 134, 1994.

[30] Tsukagoshi, K., Suzuki, T., Nakajima, R., *Anal. Sci.* 2002, *18*, 1279–1280.

[31] Kulp, M., Vaher, M., Kaljurand, M., *J. Chromatogr. A* 2005, *1100*, 126–129.

Publication II

Seiman, A., Makarõtševa, N., Vaher, M., Kaljurand, M., Detection of nerve agent degradation products in different soil fractions using capillary electrophoresis with contactless conductivity detection. *Chemistry and Ecology* **2010**, *26*, 145-155.

Chemistry and Ecology
Vol. 26, Supplement, October 2010, 145–155

Taylor & Francis
Taylor & Francis Group

The detection of nerve agent degradation products in different soil fractions using capillary electrophoresis with contactless conductivity detection

Andrus Seiman*, Natalja Makarõtševa, Merike Vaher and Mihkel Kaljurand

Department of Chemistry, Tallinn University of Technology, Tallinn, Estonia

(*Received 31 October 2009; final version received 28 May 2010*)

The adsorption of various phosphonic acids in sand and loam was studied. Samples of both soil types were sieved into three different fractions according to particle size. The fractions used were in the range 0–100, 100–200 and 200–400 μm. The performance of the capillary electrophoresis equipped with contactless conductivity detection was investigated. The limit of detection for the phosphonic acids tested was in the range 0.11–1.4 ppm. Different isotherms were constructed for all adsorption curves. Adsorption was found to be higher in sand than in loam when the Langmuir adsorption isotherm was used. The adsorption of methylphosphonic acid was higher than that of other phosphonic acids due to the smaller molecular size of the former.

Keywords: adsorption; capillary electrophoresis; chemical warfare agents; contactless conductivity detection; soil fraction

1. Introduction

Organophosphorous nerve agents are one of the most toxic substances ever synthesised. Although having found limited use so far, determination of these substances or their degradation products is still an important field of research, especially in the last 10 years, which have seen terrorist activity increase. Therefore, there is a continuous need for rapid and reliable methods for the detection of nerve agents and their degradation products. Nerve agents are categorised according to structure into two groups: G- and V-type. Both types have several similar structural features, such as the existence of a double bond between the terminal oxygen and phosphorous or two lipophilic groups and one leaving group bound to the phosphorous. These features make nerve agents unique and distinct from the large group of organophosphates, such as the herbicides, pesticides, and insecticides widely found in soil due to their use in agriculture. In aqueous environments, these organophosphorous nerve agents hydrolyse more or less easily to produce non-toxic and more stable compounds. The most important degradation products of nerve agents are alkyl alkylphosphonic acids, which are suitable for verifying the presence or use of organophosphorous

*Corresponding author. Email: andrusseiman@gmail.com

ISSN 0275-7540 print/ISSN 1029-0370 online

DOI: 10.1080/02757540.2010.497761
http://www.informaworld.com

nerve agents. Moreover, being specific to particular nerve agents, these acids can be used to identify their parental nerve agents.

Various separation methods such as gas (GC) [1] and liquid chromatography [2] and capillary electrophoresis (CE) [3] can be used to analyse the degradation products of nerve agents. Nowadays, the chromatographic methods developed for this purpose are mostly coupled to mass spectrometry [4,5]. GC is a suitable tool for analysing easily volatile nerve agents whose degradation products, however, cannot be directly applied to GC analysis because of their high polarity and low water solubility. Therefore, a derivatisation procedure for conversion of the degradation products into more volatile compounds is needed. A detailed review of possible separation techniques for the analysis of nerve agents is given in Hooijschuur et al. [6]. In view of the fact that phosphonic acids need no derivatisation, the fast, simple and relatively inexpensive CE is often preferred. CE analysis requires simple sample preparation involving dilution and filtration, and easy equipment operations and maintenance. CE is less sensitive to sample matrix and, therefore, real samples such as aqueous soil extracts and river water can be subjected to CE analysis [3,7,8]. It is possible to use direct [3] and indirect UV [9] to detect nerve agents and their degradation products in CE. The indirect mode of UV detection is preferred as it is more sensitive because phosphonic acids do not contain any chromophoric groups. Lately, a contactless conductivity detection (CCD) has also been used to detect nerve agent degradation products [10–12].

Basic principles of CCD and a more detailed description of the current set-up are available as supplementary material S1 (available online only). In this work, a CCD–CE system was used to study the adsorption of phosphonic acids in different fractions of soil.

The adsorption curves can be fitted to different types of isotherms, the Langmuir and Freundlich types being the most common. Kothawala et al. fitted their experimental data for the adsorption of organic carbon onto mineral soils to four different types of adsorption isotherms [13]. The Langmuir isotherm was found to produce more robust results. Fitting the Freundlich and Langmuir isotherms to the same data has been compared in Vasanth Kumar and Sivanesan [14]. Again, the latter was more advantageous. In this study, a linear least squares method was used to estimate the performance of the Langmuir and Freundlich adsorption isotherms. In addition to the Langmuir and Freundlich adsorption isotherms, the Redlich–Peterson and BET-isotherms were also calculated. An introduction to the theoretical background of these adsorption isotherms is available as supplementary material S2 (available online only).

2. Materials and methods

2.1. *Soil samples*

Environmental soil samples were collected from two different locations in Estonia. The sand sample was taken from a park in the city of Tallinn (latitude: 59°23′42.13″, longitude: 24°40′37.02″) and the loam sample from a forest in the Kõpu rural municipality, Viljandi county (latitude: 58°19′34.72″, longitude: 25°17′45.19″). Samples were collected from the surface layer of soil at a maximum depth of 5 cm. Sand and loam samples had not been exposed to nerve agents or their degradation products before. The sampling sites were chosen far away from agricultural areas to avoid possible contamination of samples with the other types of organophosphates used in agriculture, such as herbicides or insecticides.

Gravimetric analysis was used to determine the organic content of the soil samples. First, the crucibles used for the analysis were heated to 550 °C for 4 h in a muffle furnace to gain constant weight. Second, after cooling for 30 min, the crucibles were weighed and $\sim$ 1 g of a particular soil sample was added to the crucibles. The soil samples were treated for 4 h at a temperature of 550 °C. After a 30 min cooling period, the crucibles with temperature-treated samples were

Table 1. Organic matter in different soil fractions.

Size of fraction, μm	Amount of organic matter, %	
	Sand	Loam
<100	1.24	5.64
100–200	0.55	7.03
200–400	0.50	6.05

weighed again. The organic content of the soil samples was calculated using the difference between the two masses. Four hours was long enough for all the samples to lose their organic part.

The adsorption of phosphonic acids in soil may be considered as a sum of physicosorption and chemisorption. A simple explanation for this could be as follows. Phosphonic acids are adsorbed onto inorganic soil particles by undergoing physicosorption, whereas their adsorption onto the organic part of a soil sample takes place under the mechanism of chemisorption. This simplified theory may be applied to explaining the adsorptive behaviour of phosphonic acids in different types of soil. Therefore, the organic content of soil samples was determined using gravimetric analysis and muffle furnaces.

Data on the organic content of soil samples are presented in Table 1. The organic content of the loam samples (5.64–7.03%) was 10 times as high as that of the sand samples (0.50–1.24%). The organic content of the finest fraction of the sand sample was $\sim$ 2.5 times as high as that of the other two fractions. This means that the organic matter of the sample contained small fractions of clay, silt and very fine sand. However, in the case of loamy soil, the respective figures were slightly different. So, the organic content of its medium fraction was the highest and that of the finest fraction the lowest.

2.2. *Preparation of soil extracts*

Loam and sand samples were first dried at room temperature until the mass of both samples was constant. The procedure took three to four days. After that, the samples were fractionated by particle size using three sieves with different hole sizes. The sand and loam samples were sieved into three fractions: <100, 100–200 and 200–400 μm. Samples with a particle size >400 μm were disposed of. Basically, the fractions represented very fine, fine and medium-grained sand. Clay and silt were not thoroughly dealt with because Estonian soils are mainly sand-based. Silt and clay were the components of the finest fraction of samples.

For sample preparation, 0.5 g of the fractionated soil material was weighed into 2 mL plastic vials. The samples were spiked with a 2 mM stock solution of five phosphonic acids. The added amounts of phosphonic acids were 12.5, 25, 37.5, 50, 75 or 100 μL. After a 50 min exposure to phosphonic acids, MilliQ water was added to the soil samples to obtain a total volume of 1 mL. This means that the concentration of phosphonic acids in the samples was 25, 50, 75, 100, 150 or 200 μM, respectively. The samples were then shaken for 10 min and also centrifuged for 10 min. A 500 μL aliquot of an unfiltered supernatant was placed into 0.5 mL plastic vials and 2-aminoethyl dihydrogenphosphate (AEDHP) was added as an internal standard. The concentration of the internal standard was 500 μM. The unfiltered samples were subjected to CE analysis.

2.3. *CCD–CE experiments*

2.3.1. *Instrumentation*

All experiments were carried out using a commercially available Agilent Technologies CE instrument (Waldbronn, Germany) equipped with a diode array detector. For detection a CCD detector

was used instead of a UV detector. The CCD detector was made in-house. A detailed description of this detector is given in Seiman et al. [15] and supplementary material S1 (available online only). The combination of the in-house CCD detector and the conventional bench-top Agilent instrument enabled application of the detection schemes developed for CCD to a large number of samples because the Agilent instrument provides possibilities for programming long sequences of separate analyses.

The uncoated fused-silica capillary (i.d., 75 μm; o.d., 360 μm) with a total length of 55 cm was purchased from Agilent Technologies (Santa Clara, CA, US). The length of the capillary to the CCD cell was 45 cm and to the DAD cell, 49 cm.

2.3.2. *Standards*

For analysis of the degradation products of toxic organophosphates the following phosphonic acids were used: methylphosphonic acid (MPA), ethylphosphonic acid (EPA), 1-butylphosphonic acid (1-BPA), propylphosphonic acid (PPA) and pinacolyl metylphosphonic acid (PMPA). MPA, EPA and 1-BPA were purchased from Alfa Aesar, Lancaster Synthesis (Windham, NH, USA) and PPA and PMPA were from Sigma-Aldrich (Steinheim, Germany). AEDHP used as the internal standard, and BGE components, L-histidine (His) and 2-(*N*-morpholino)ethanesulphonic acid hydrate (MES hydrate), were also purchased from Sigma-Aldrich (Steinheim, Germany). Sodium hydroxide was purchased from Chemapol (Prague, Czech Republic).

Standard stock solutions were prepared by dissolving an exact amount of each phosphonic acid in MilliQ water to a concentration of 10 mM. This was followed by a further mixing of all five analytes into a standard solution of a total concentration of 2 mM.

BGE for capillary electrophoresis analysis was prepared by dissolving an exact amount of His and MES in MilliQ water.

2.3.3. *Procedures*

A new capillary was flushed with a 1 M NaOH for 10 min and then with water for 10 min and with BGE for 10 min. Before starting the experiments, the capillary was flushed with a 0.1 M NaOH for 3 min, with water for 10 min and with BGE for 10 min every day. Between each run it was rinsed with water for 2 min and with BGE for 3 min. The BGE was a 15 mM Mes/His buffer. The sample was injected hydrodynamically for 10 s (50 mBar). In all experiments, the cartridge with the separation capillary was thermostated at 25 °C. The separation voltage was 20 kV.

3. Results and discussion

3.1. *Performance of the CCD-CE system*

For the analysis of adsorption of phosphonic acids in soil, first, calibration curves had to be constructed. This was a suitable opportunity to evaluate the performance, including the reproducibility, sensitivity, etc., of the combined CCD–CE equipment. The calibration curve of seven points was constructed in the region 10–200 μM. An internal standard AEDHP was added to every sample at a concentration of 500 μM. The constructed calibration curve demonstrated good linearity in the measured range as the coefficient of determination between experimental data and the constructed calibration curve was close to one ($R^2 > 0.99$ for all phosphonic acids). Multiple repetitive analyses needed for the construction of the calibration curve were performed to calculate the reproducibility of the CCD–CE system. Detailed performance data are given in Table 2. The reproducibility of the system was acceptable as the relative standard deviations (RSD) of

Table 2. Performance data for phosphonic acids.

	LOD* (μM)	RSD† (%)	$b_0^{\ddagger}$	$b_1^{\ddagger}$	$(R^2)^{\S}$
PMPA	7.56	5.68	−0.0514	0.0068	0.9915
1-BPA	5.96	3.48	−0.0572	0.0096	0.9977
PPA	5.45	4.23	−0.0605	0.0111	0.9974
EPA	5.84	2.58	−0.0847	0.0145	0.9952
MPA	1.20	6.92	−0.0236	0.0196	0.9984

Notes: *Limit of detection. †Relative standard deviation of peak areas. ‡Calibration line equation $y = b_0 + b_1 c$ parameters: b_0, intercept; b_1, slope; y, detector response; c, concentration. §Square of correlation coeficient of calibration line.

peak areas were in the region 2.6–6.9%. To estimate the sensitivity of the CCD detector, LODs for all the phosphonic acids analysed were calculated by interpolating the calibration curves. The LODs were in the range of 1.2 (0.11) and 7.6 (1.4) μM (ppm).

3.2. *Analysis of blank soil extracts*

When developing procedures for the extraction of nerve agent degradation products from soil, all possible unknown substances that could have been extracted from soil had to be separated from phosphonic acids using CCD–CE analysis. Otherwise it would have been impossible to estimate the adsorption of nerve agent degradation products in soil. Blank extracts of loam and sand samples were examined first to discover all unknown peaks belonging to substances which extracted from soil under the current extraction procedures. A comparison of blank soil extracts and extracts containing phosphonic acids was necessary to find out if peaks of the latter were separated from each other and from all unknown peaks belonging to soil extracts.

Blank samples (Figure 1(B)) had two peaks that were observed in case of all loam and sand samples. Only the height of the peaks in different fractions varied. All unknown peaks migrated slower

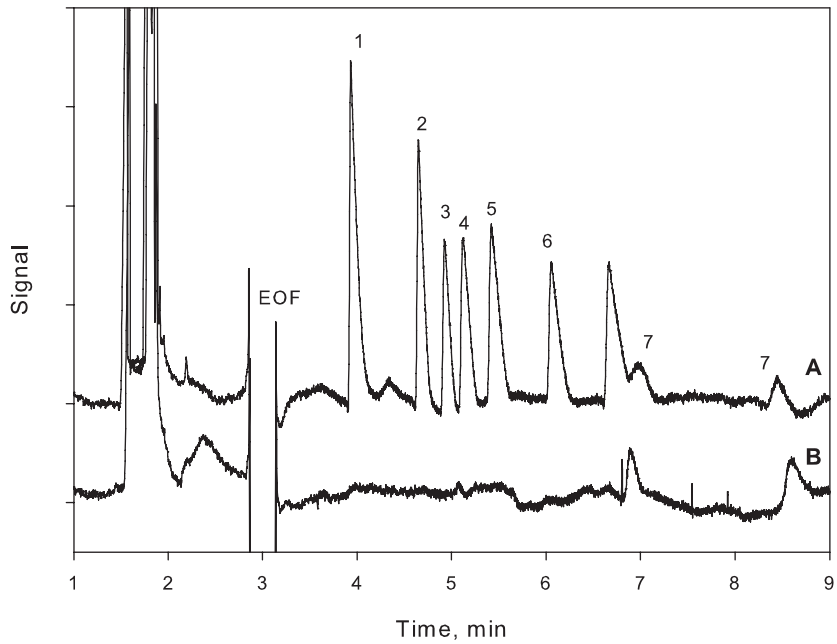

Figure 1. Separation of blank soil extract and phosphonic acids. (A) Blank extract from sand, fraction 100–200 μm; (B) extract of 100 μM phosphonic acids from sand, fraction 100–200 μm. EOF, electroosmotic flow; 1, AEDHP; 2, PMPA; 3, BPA; 4, MPA; 5, EPA; 6, MPA; 7, unknown peaks.

than phosphonic acids (Figure 1(A)). It may be assumed that these unknown peaks corresponded to some small anions, though they were not identified as it was not the goal of this article.

3.3. *Adsorption isotherms of different soil samples*

Sand and loam extracts were prepared using six different concentrations of phosphonic acids by spiking a particular sample with a certain amount of the standard mixture of phosphonic acids. Spiked samples were extracted with water after a certain time. With no adsorption at all the concentration of phosphonic acids in these extracts would have been 25, 50, 75, 100, 150 and 200 μM. In reality, all these concentrations were lower as some amount of phosphonic acids was adsorbed into the soil. The difference between these two concentrations was well suited for estimating the degree of adsorption of phosphonic acids in a particular soil sample. All together, adsorption curves were constructed for two types of soil and three fractions of each. Six concentrations of phosphonic acids were measured to construct one adsorption curve. With three parallel experiments for every sample, 108 soil extracts were analysed in total.

On the basis of the experimental data, four different types of adsorption isotherms were constructed. A comparison of the determination coefficients of experimental data and fitted isotherms enables an assumption to be made about which isotherm of the four is the closest to the performance of real soil. The parameters and determination coefficients for all calculated isotherms are given in Table 3. The parameters of the Langmuir and Freundlich isotherms were calculated using a least square method in a linearised form. The parameters of the Redlich–Peterson and BET-isotherms could not be found using a linear form of the method because they contain three unknown parameters. Instead, a nonlinear trial and error procedure was used to determine all three parameters. The coefficients of determination of calculated isotherms and experimental data were used to compare different adsorption models.

A comparison shows no significant difference to exist in determination coefficients between the Langmuir, Freundlich and Redlich–Peterson isotherms in the measured concentration region. The isotherms follow closely each other's path when plotted on the same graph. When extrapolated to higher concentrations, the Langmuir isotherm levels out at $q_{\max}$, while the other two isotherms continue to grow. The Redlich–Peterson isotherm would have been expected to have superior fitting because it is described with the aid of three adjustable parameters, instead of two as is the case with the Langmuir and Freundlich isotherms. Apparently, there is no significant difference in determination coefficients (R^2) between the above adsorption isotherms, and the type of the best fitting isotherm varies from sample to sample. Therefore, the Langmuir isotherm may be considered to be no worse in performance than the other two and its parameter, $q_{\max}$, which is a maximum adsorption on the monolayer coverage, could be used to compare the adsorptive capacity of various samples.

At a low concentration of phosphonic acids, the Langmuir adsorption isotherm is linear because no molecules were adsorbed on the surface. At higher acid concentrations, the adsorption curve decreases until it reaches a constant value, the maximum adsorption, when all adsorption sites are filled and the monolayer of phosphonic acids is formed on the surface of soil particles.

The results obtained demonstrate the adsorption capacity of sand to be higher than that of loam. The adsorption capacity of smaller fractions of sand samples is higher. However, the difference in adsorption capacity between the smallest fractions (below 100 μm) of sand and loam samples is not as significant as that between their larger fractions (200–400 μm).

Figure 2 illustrates the adsorption of EPA in different soil samples. EPA was chosen as an example to illustrate the adsorptive behaviour of all the phosphonic acids tested in this work, with the exception of PMPA. In case of the sand sample, adsorption was lowest in the medium-sized fraction and highest in the smallest fraction. In case of the loam sample, two smaller fractions

Table 3. Parameters of various adsorption isotherms for sand and loam samples.

		< 100 μm				100–200 μm				200–400 μm			
		BPA	PPA	EPA	MPA	BPA	PPA	EPA	MPA	BPA	PPA	EPA	MPA
Sand													
Langmuir	q_{max}	238.3	205.5	252.8	495.2	323.6	62.2	193.4	282.6	581.4	241.7	268.9	339.9
	K_a	0.0036	0.0042	0.0035	0.0022	0.0017	0.0162	0.0035	0.0038	0.001	0.0026	0.0027	0.0033
	r^2	0.9681	0.937	0.9808	0.9837	0.8856	0.9191	0.9376	0.9735	0.9971	0.9867	0.9804	0.9967
Freundlich	n_F	1.9377	2.1648	1.9888	2.0327	1.1653	3.983	1.5924	2.6812	0.8138	1.0074	1.3423	2.1561
	K_F	1.3332	1.4033	1.3302	1.2281	1.2679	2.071	1.3598	1.3877	1.0992	1.1915	1.235	1.2702
	r^2	0.9795	0.9494	0.9912	0.9902	0.8872	0.8938	0.9474	0.9842	0.997	0.9728	0.98	0.9914
Redlich–Peterson	K_R	0.3013	0.3362	0.2941	0.2398	0.2076	0.5458	0.3169	0.3306	0.1360	0.2126	0.2426	0.2657
	a_R	3.9656	4.4092	3.9590	4.2556	1.8591	8.1942	3.3096	5.5674	1.6945	2.0340	2.7244	4.3811
	b_R	1.3516	1.3996	1.3419	1.2711	1.2307	1.7260	1.3729	1.3917	1.1457	1.2369	1.2746	1.3043
	r^2	0.9790	0.9491	0.9912	0.9903	0.8921	0.8970	0.9474	0.9838	0.9970	0.9749	0.9805	0.9924
BET	q_{max}	64.9	58.9	67.2	72.6	35.7	58.8	43.4	66.4	159.9	229.7	153.7	n.a.*
	K_L	0.0024	0.0023	0.0023	0.0027	0.0032	0.0003	0.0026	0.0023	0.0010	0.0000	0.0007	n.a.
	K_S	0.0170	0.0191	0.0167	0.0203	0.0248	0.0165	0.0229	0.0232	0.0041	0.0027	0.0051	n.a.
	r^2	0.9862	0.9578	0.9939	0.9488	0.9545	0.9791	0.9634	0.9145	0.9959	0.9876	0.9814	n.a.
Loam													
Langmuir	q_{max}	167.7	331.8	108.7	435.3	125.2	199.1	90.0	368.7	61.6	86.6	59.9	229.4
	K_a	0.0028	0.0008	0.005	0.0014	0.0046	0.0013	0.0079	0.002	0.0085	0.0035	0.0096	0.0027
	r^2	0.9871	0.9673	0.8948	0.9805	0.8258	0.9584	0.9797	0.9886	0.9253	0.9643	0.8089	0.9244
Freundlich	n_F	1.0132	0.3921	1.834	1.1518	2.0919	0.3123	1.9376	0.9902	2.2886	0.7218	2.7946	1.7001
	K_F	1.2983	1.1093	1.5672	1.1988	1.6124	1.0709	1.5453	1.1162	1.8659	1.351	1.9951	1.3879
	r^2	0.991	0.9691	0.9171	0.9762	0.8534	0.9342	0.9544	0.9581	0.9583	0.9714	0.8584	0.919
Redlich–Peterson	K_R	0.2844	0.1899	0.4067	0.2224	0.4218	0.1001	0.3956	0.1502	0.4906	0.3117	0.5303	0.3165
	a_R	2.1268	0.9382	3.8715	2.4948	4.3833	0.6155	3.8379	1.9644	4.5442	1.4922	5.8916	3.5245
	b_R	1.3290	1.2091	1.5018	1.2491	1.5247	1.1052	1.4852	1.1621	1.6333	1.3658	1.6995	1.3723
	r^2	0.9911	0.9542	0.9181	0.9788	0.8545	0.9373	0.9582	0.9655	0.9590	0.9713	0.8571	0.9454
BET	q_{max}	40.6	79.4	21.8	45.7	23.4	n.a.	n.a.	n.a.	24.3	37.6	19.5	27.6
	K_L	0.0023	0.0009	0.0033	0.0029	0.0033	n.a.	n.a.	n.a.	0.0023	0.0013	0.0028	0.0034
	K_S	0.0163	0.0039	0.0631	0.0222	0.0586	n.a.	n.a.	n.a.	0.0377	0.0100	0.0762	0.0590
	r^2	0.9949	0.9931	0.9960	0.9740	0.9821	n.a.	n.a.	n.a.	0.9968	0.9965	0.9921	0.9359

Note: *Not available, statistically best fitted isotherm does not correspond to real life expectations having negative q_{max}, etc.

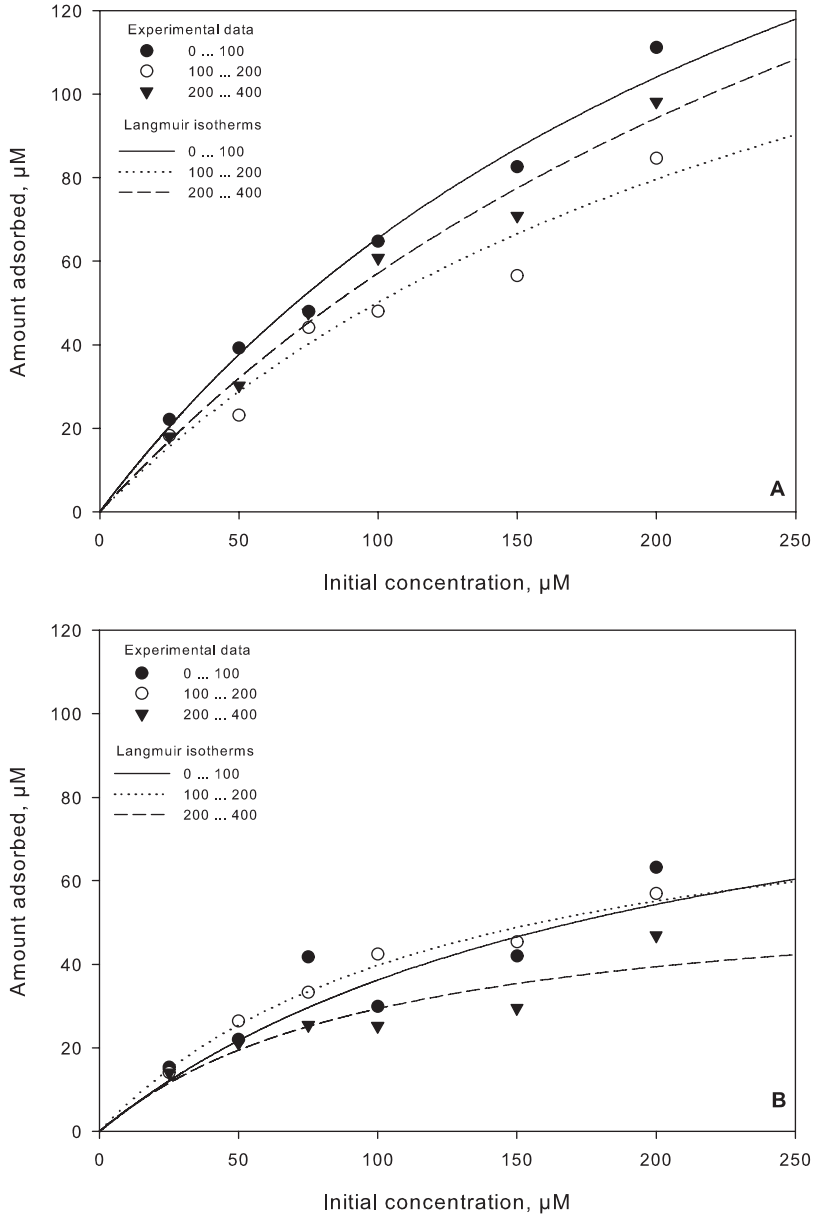

Figure 2. Adsorption data with fitted Langmuir isotherm of EPA in different soil fractions. (A) Sand samples, (B) loamy soil samples.

demonstrated a similar adsorption, while the largest fraction had an adsorption isotherm which was significantly higher than that of the other fractions.

The adsorption of different phosphonic acids in different fractions of sand and loamy soil samples was rather similar. On the basis of the adsorption isotherms of 200–400 µm fractions (Figure 3), some general conclusions can be drawn. First of all, adsorption was highest in the case of MPA. This could be explained by the different sizes of the various phosphonic acid molecules. Of the four phosphonic acids, the molar mass of MPA was by far the lowest. The other three acids had a similar adsorption rate in both sand (Figure 3(A)) and loamy soil (Figure 3(B)). From the two figures it can be seen that the Langmuir adsorption isotherm in the case of the loam sample

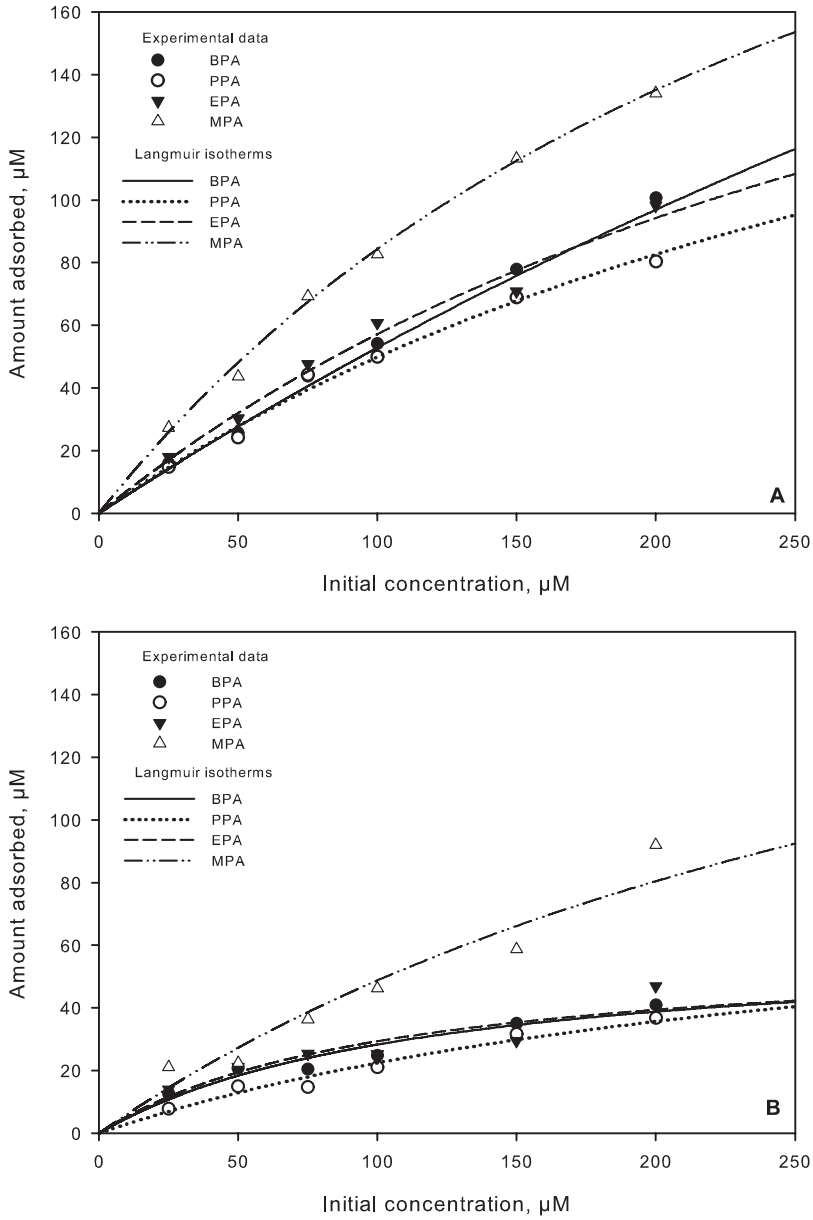

Figure 3. Adsorption data with fitted Langmuir isotherm of different phosphonic acids in soil fractions. (A) Phosphonic acids in sand, fraction 200–400 µm; (B) phosphonic acids in loamy soil, fraction 200– 400 µm.

achieved its constant value at an acid concentration of 200 mM, whereas in the case of the sand sample, the adsorption isotherm at this concentration, except for MPA, was still in the linear region. Therefore, one could expect that the adsorption of phosphonic acids in the sand sample would be higher, which was also confirmed by q_{max} values.

An alternative explanation for the adsorptive behaviour of nerve agent degradation products in soil could be given using the BET-isotherm. While the Langmuir isotherm treats adsorption in one monolayer, the BET-isotherm, on the contrary, assumes that the adsorption of phosphonic acids on the surface of soil particles takes place in several layers. Statistically it is not possible to tell which

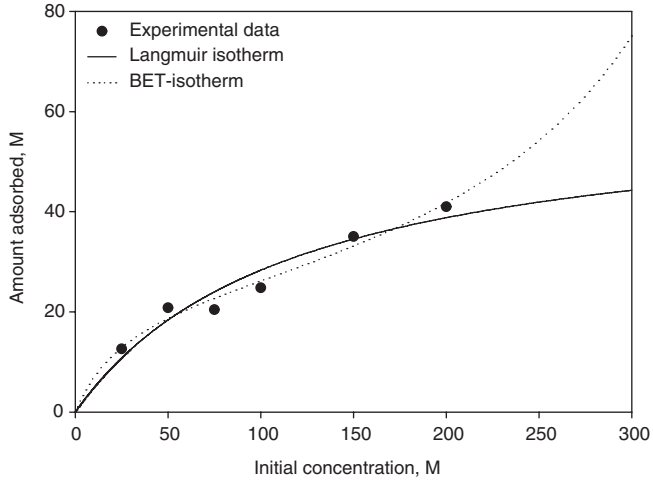

Figure 4. Comparison of fitting Langmuir and BET-isotherm to the same experimental data. Experimental conditions: MPA in soil fraction sized 200–400 μm.

model is more likely as there is no significant difference in determination coefficients between the Langmuir and BET-isotherms, i.e. the quality of fitting both isotherms to experimental data is almost similar. A comparison of two isotherms is given in Figure 4. Both isotherms follow the same path until the point where the second layer of the adsorbent starts to form in the BET-isotherm or the Langmuir isotherm starts to level as the monolayer around the soil particle is filling up. One of the three parameters describing the BET-isotherm is q_{max}, which is the concentration corresponding to a complete monolayer adsorption. The definition of this parameter is exactly the same as in the case of the Langmuir isotherm equation. Apparently, the values of q_{max} of the Langmuir isotherm are 3–10 times higher than those of the BET-isotherm.

For all the phosphonic acids tested, the adsorption mechanism is the same because their molecular structures are very similar. Therefore, it is unlikely that the adsorption concentration corresponding to a complete monolayer of one particular phosphonic acid could vary in such a wide range. Hence, the adsorption mechanism of nerve agent degradation products must be either Langmuir's or BET's. The concentration range under study is apparently too narrow to tell us which of the two mechanisms is more likely, because the measured points are in the range where only the first monolayer is filling up. Unfortunately, in a particular BGE system, much higher concentrations cannot be measured with CE because separation between high concentration phosphonic acid peaks is not sufficient. It is possible to use CE to measure the adsorption of every phosphonic acid separately at higher concentrations, but this may lead to different results compared with the situation when they are detected together because it is very likely that phosphonic acids with highly similar molecular structures compete for the same adsorption sites around a soil particle.

4. Conclusions

Phosphonic acids as degradation products of their parental nerve agents may serve as excellent fingerprint markers for the verification of the use of nerve agents. The adsorption of different phosphonic acids in different fractions of loam and sand samples was studied. The results demonstrated that the difference in adsorption between loam and sand samples was more significant than that between individual fractions. A comparison showed the adsorption of MPA in different soil samples to be relatively higher than that of other phosphonic acids.

CE has proven to be a suitable tool for separating phosphonic acids and could therefore easily be used for the analysis of adsorption. Moreover, it enables analysis of the adsorption of several components on the same adsorbent simultaneously. This offers a great opportunity to study a competitive adsorption of similar molecules on the same adsorption sites. In CE, the use of minimum concentrations of substances is restricted by the sensitivity of CCD–CE, while application of maximum concentrations is restricted by the separation system because separation is insufficient above certain concentrations.

Acknowledgements

We acknowledge the Estonian Science Foundation (Grant No. 7818) for financial support. We thank Edur Kuuskmäe for assistance with the preparation of CCD–CE equipment.

References

[1] G.A. Sega, B.A. Tomkins, and W.H. Griest, *Analysis of methylphosphonic acid, ethyl methylphosphonic acid and isopropyl methylphosphonic acid at low microgram per liter levels in groundwater*, J. Chromatogr. A 790 (1997), pp. 143–152.

[2] E.W.J. Hooijschuur, C.E. Kientzb, and U.A.Th. Brinkmana, *Application of microcolumn liquid chromatography and capillary electrophoresis with flame photometric detection for the screening of degradation products of chemical warfare agents in water and soil*, J. Chromatogr. A 928 (2001), pp. 187–199.

[3] A.-E.F. Nassar, S.V. Lucas, C.A. Myler, W.R. Jones, M. Campisano, and L.D. Hoffland, *Quantitative analysis of chemical warfare agent degradation products in reaction masses using capillary electrophoresis*, Anal. Chem. 70 (1998), pp. 3058–3604.

[4] R.-S. Zhao, J.-P. Yuan, H.-F. Li, X. Wang, T. Jiang, and J.-M. Lin, *Nonequilibrium hollow-fiber liquid-phase microextraction with in situ derivatization for the measurement of triclosan in aqueous samples by gas chromatography–mass spectrometry*, Anal. Bioanal. Chem. 387 (2007), pp. 2911–2915.

[5] R.M. Black and R.W. Read, *Application of liquid chromatography–atmospheric pressure chemical ionisation mass spectrometry, and tandem mass spectrometry, to the analysis and identification of degradation products of chemical warfare agents*, J. Chromatogr. A 759 (1997), pp. 79–92.

[6] E.W.J. Hooijschuur, C.E. Kientz, and U.A. Brinkman, *Analytical separation techniques for the determination of chemical warfare agents*, J. Chromatogr. A 982 (2002), pp. 177–200.

[7] R.L. Cheicante, J.R. Stuff, and H.D. Durst, *Separation of sulfur containing chemical warfare related compounds in aqueous samples by micellar electrokinetic chromatography*, J. Chromatogr. A 711 (1995), pp. 347–352.

[8] J.-P. Mercier, P. Morro, M. Dreux, and A. Tambute, *Capillary electrophoresis analysis of chemical warfare agent breakdown products. I. Counterelectroosmotic separation of alkylphosphonic acids and their monoester derivatives*, J. Chromatogr. A 741 (1996), pp. 279–285.

[9] G.A. Pianetti, M. Taverna, A. Baillet, G. Mahuzier, and D. Baylocq-Ferrier, *Determination of alkylphosphonic acids by capillary zone electrophoresis using indirect UV detection*, J. Chromatogr. A 630 (1992), pp. 371–377.

[10] T.E. Rosso and P.C. Bossle, *Capillary ion electrophoresis screening of nerve agent degradation products in environmental samples using conductivity detection*, J. Chromatogr. A 824 (1998), pp. 125–134.

[11] L. Xu, P.C. Hauser, and H.K. Lee, *Electro membrane isolation of nerve agent degradation products across a supported liquid membrane followed by capillary electrophoresis with contactless conductivity detection*, J. Chromatogr. A 1214 (2008), pp. 17–22.

[12] L. Xu, P.C. Hauser, and H.K. Lee, *Determination of nerve agent degradation products by capillary electrophoresis using field-amplified sample stacking injection with the electroosmotic flow pump and contactless conductivity detection*, J. Chromatogr. A 1216 (2009), pp. 5911–5916.

[13] D.N. Kothawala, T.R. Moore, and W.H. Hendershot, *Adsorption of dissolved organic carbon to mineral soils: a comparison of four isotherm approaches*, Geoderma 148 (2008), pp. 43–50.

[14] K. Vasanth Kumar and S. Sivanesan, *Comparison of linear and non-linear method in estimating the sorption isotherm parameters for safranin onto activated carbon*, J. Hazard. Mater. B 123 (2005), pp. 288–292.

[15] A. Seiman, M. Jaanus, M. Vaher, and M. Kaljurand, *A portable capillary electropherograph equipped with a cross-sampler and a contactless-conductivity detector for the detection of the degradation products of chemical warfare agents in soil extracts*, Electrophoresis 30 (2009), pp. 507–514.

Publication III

Kuban, P., Seiman, A., Makarõtševa, N., Vaher, M., Kaljurand, M. In situ determination of sarin, soman and VX nerve agents in various matrices by portable capillary electropherograph with contactless conductivity detection, *Journal of Chromatography A* **2011**, *1218*, 2618-2625.

Journal of Chromatography A, 1218 (2011) 2618–2625

Contents lists available at ScienceDirect

Journal of Chromatography A

journal homepage: www.elsevier.com/locate/chroma

In situ determination of nerve agents in various matrices by portable capillary electropherograph with contactless conductivity detection

Petr Kubáň*, Andrus Seiman, Natalja Makarõtševa, Merike Vaher, Mihkel Kaljurand

Department of Chemistry, Tallinn University of Technology, Akadeemia tee 15, 12618 Tallinn, Estonia

ARTICLE INFO

Article history:
Received 28 January 2011
Received in revised form 3 March 2011
Accepted 7 March 2011
Available online 12 March 2011

Keywords:
Capillary electrophoresis
Capacitively coupled conductivity detection
Genuine nerve agents
Aqueous extraction

ABSTRACT

Rapid, efficient and robust methods for sampling and extracting genuine nerve agents sarin, soman and VX were developed for analyzing these compounds on various solid matrices, such as concrete, tile, soil and vegetation. A portable capillary electrophoretic (CE) system with contactless conductometric detection was used for the *in situ* analysis of the extracted samples. A 7.5 mM MES/HIS-based separation electrolyte accomplished the analysis of target analytes in less than 5 min. The overall duration of the process including instrument start-up, sample extraction and analysis was less than 10 min, which is the fastest screening of nerve agents achieved with liquid phase separation methods to date. The procedure can easily be performed by a person in a protective suit and is therefore suitable for real-life applications. The CE results were validated by an independent GC–MS method and a satisfactory correlation was obtained. The use of a proper sampling strategy with two internal standards and "smart" data-processing software can overcome the low reproducibility of CE. This has a significant impact on the potential acceptance of portable CE instrumentation for the detection and analysis of genuine chemical warfare agents (CWA).

1. Introduction

Chemical warfare agents (CWA) are chemical substances that are intended for use in military operations to kill, seriously injure or incapacitate people through their physiological effects. As a result of ongoing efforts to outlaw the production, stockpiling and use of chemical weapons, a Chemical Weapons Convention (CWC) [1] was enacted in 1997 and has been signed by 188 countries to date. According to the CWC definition, CWA are Schedule 1 substances, i.e. they can be used either as chemical weapons or in the manufacture of chemical weapons; they have very limited or no use outside of chemical warfare. A significant group of Schedule 1 substances are the so-called nerve agents (NA), which can be subdivided into two main classes – G-type and V-type. Nerve agents typically act as efficient acetylcholinesterase inhibitors and attack the human nervous system, resulting in eventual death if an appropriate antidote is not administered in time. Nerve agents were used during World War I, but also more recently in documented cases such as in the Kurdish village of Birjinni (1988) [2], the Matsumoto city incident (1994) [3] and the Tokyo subway attack (1995) [4]. The latter incidents led to several deaths and affected thousands of people.

These types of civil terrorism are probably the reason that nerve agents are being intensely studied and that the search for possible new methods of determining NA is still very active [5]. The quest for the development of an analytical method is targeted at the ability to identify the agents used in an attack as quickly as possible, so that appropriate antidotes can be administered in time. For such a method to be useful, several factors have to be considered, including the portability of the instrumentation, the instrument start-up time, the sampling and sample preparation time, and the actual analysis time.

A large number of analytical techniques have been developed to detect CWA or their degradation products. Simple colorimetric tests are available commercially for the protection of military personnel [6]. At the moment, however, the most popular instrumental technology seems to be ion mobility spectroscopy (IMS). It is an efficient tool for monitoring gaseous phase CWA and provides an effective and rapid method of detection [7]. Other interesting technologies are flame photometry (FPD), and surface acoustic wave (SAW) and surface plasmon resonance (SPR) [6]. Research and development in the field of CWA determination has produced many commercial products; portable instruments are available from large international corporations such as Dräeger, Smiths Detection, RAE Systems and Proengin. Most of these instruments use IMS, FPD or SAW technology platforms. The advantages and disadvantages of many off-the-shelf instruments were documented in a recent report [8]. One common drawback of gas phase detectors is that they are not very effective for detecting aqueous phase CWA. The agent is often deposited on a surface close to the attack site and is subject to hydrolysis due to atmospheric or soil humidity. The

* Corresponding author. Tel.: +372 6204322; fax: +372 6202828.
E-mail address: petr.kuban@gmail.com (P. Kubáň).

0021-9673/$ – see front matter © 2011 Elsevier B.V. All rights reserved.
doi:10.1016/j.chroma.2011.03.006

effectiveness of gas phase detectors is questionable under these circumstances.

Chromatographic separation techniques play a dominant role in many areas including NA detection. Usually, GC [9] and HPLC [10] are coupled to an element specific detector (FPD) [11–13] or to a mass spectrometer (MS) [14–16] because these detection techniques provide very reliable identification of separated compounds. Each of these techniques has advantages and drawbacks for on-site analysis. For instance, GC can be made portable and the separation times are relatively short [17]. However, the analysis typically requires derivatization steps because NA are not sufficiently volatile, and analysis from an aqueous environment presents a particular challenge. HPLC, on the other hand, can be used for the analysis of aqueous extracts, but it cannot readily be made portable and thus requires the sample to be delivered to an analytical laboratory. It is therefore not suitable for rapid on-site screening.

Electromigration methods such as capillary electrophoresis (CE) have attracted only academic interest as possible technological platforms for NA detection. No off-the-shelf instruments have yet appeared on the market, probably due to the perceived immaturity of the technique. However, CE has some distinct advantages, which have been demonstrated in many publications. It is arguably the technique that is best suited for field and on-site analysis of complex mixtures in complicated matrices. CE can easily be miniaturized, unlike GC or HPLC. CE, especially with electrochemical or optical (LED based) detection, does not consume large quantities of energy. CE startup time is significantly shorter than that of HPLC, because there is no requirement for lengthy equilibration of the separation column with an eluent. In addition, CE analysis times are unquestionably the shortest of the available separation techniques.

It is therefore not surprising that CE is very popular for the analysis and screening of nerve agents and their degradation products, as documented in several recent reviews [18–21]. The prevailing CE detection methods are UV and conductivity detection, but laser-induced fluorescence [22–25], MS [26–29] and element specific detectors [30,31] have also been used. CE separation with indirect UV detection of NA degradation products was first described by Pianetti et al. in 1993 [32]. Phenylphosphonic acid was used as the UV-absorbing probe, as most NA degradation products do not absorb in UV, and this technique was subsequently adopted by other authors [33–35]. Alternative electrolyte probes applied in indirect UV detection include sorbate [36,37], borate [38,39] and chromate [40]. Derivatization with sodium borate and direct UV detection at 214 or 254 nm was advanced by Robins and Wright [39]. All of the reported research on CE with UV detection relies on laboratory-based instruments with UV detectors that consume large quantities of energy. Although CE systems with diode-based UV detectors can easily be made portable, they have not yet been used for CWA detection.

Conductivity detection is probably best suited to an on-site, portable CE device, because it can be miniaturized, power consumption is minimal, and it is relatively sensitive to the compounds of interest, especially NA degradation products. Contact conductivity detection with CE for the detection of NA degradation products was first demonstrated by Rosso and Bossle [41] and later by Nassar et al. [33,34]. Due to the obvious advantages of the recently developed contactless conductivity detection (C4D) approach [42,43], contact conductivity detection has been replaced by C4D in CE. A separation electrolyte based on MES/HIS has been used in CE with C4D for NA separation. A negative [44–47] or positive [48–51] polarity mode was applied; polarity in this context refers to the polarity on the detection side. Some researchers added an electroosmotic flow modifier to the electrolyte to suppress or reverse the EOF [33,34,49–51], while others used no EOF modification [44–47]. The negative polarity mode offers some advantages over the positive, as the inorganic cations and anions are effectively separated from the NA degradation products. In the positive polarity mode, the small anions, if present in the samples in significant amounts, may influence the separation of the analytes of interest, and pretreatment steps are often needed to remove the small anions and the cations from these samples [40].

Of the approximately 40 publications in which the use of capillary electrophoresis for the detection of CWA is reported, only three applied it for the determination of genuine nerve agents [25,33,34] rather than their simulants or degradation products. The analyses were conducted in the laboratory, not in the field. This is understandable, because nerve agents are not freely available, even for research purposes. There are severe restrictions on their use (a license from state authorities is often needed), and NA require special attention during subsequent disposal/decontamination. Only a few sites in Europe, for example, are authorized to perform such research and have suitable disposal facilities. Research conducted with NA degradation products or simulants certainly has great importance, but the performance of CE with genuine nerve agents under real life conditions is largely unknown. This is especially relevant to information on NA sampling and extraction methods for CE analysis from different matrices in which NA might possibly be used.

To the knowledge of the authors, there are no reported cases of the use of CWA detectors in the battlefield or immediately following a terrorist attack. On the contrary, there are documented cases of samples from suspected sites such as the Tokyo subway attack and the other incidents described above being analyzed *post factum*. The dissemination of CWA is highly dependent on atmospheric conditions and it is difficult to achieve effective dispersion. The most probable analytical scenario will require analysis of an agent which is deposited on a surface close to the site of application, and which will degrade rapidly due to atmospheric or soil humidity. The effectiveness of gas phase detectors is questionable under these circumstances. Liquid samples from the suspected site can be transported to the laboratory for GC–MS or HPLC–MS analysis and identification. However, this causes a significant time delay that may be critical in cases that require a rapid response. *In situ* analysis with robust analysis protocols and minimum sample preparation will be highly desirable. The "Guide for the Selection of Chemical Detection Equipment for Emergency First Responders" [6] lists about two hundred instruments for the detection of chemical weapons, most of them handheld or hand portable, which are designed to be used in field. Surprisingly, except for semi-qualitative colorimetric kits, only a few are suitable for liquid or solid samples (such as FPD instruments which scrape and heat the collected soil or Raman spectroscopy-based instruments). Portable field instruments based on CE technology could provide a viable solution in these situations.

In this paper, four main objectives were addressed that could have a significant impact on the acceptance of portable CE instrumentation for the detection and analysis of genuine NA. First, we conducted experiments to support the results obtained from CE analysis of NA degradation products, by sampling and identifying the genuine nerve agents sarin, soman and VX in a real-life situation using a portable CE instrument with C4D. Second, we developed robust, rapid and efficient extraction procedures that could be used by an individual wearing a protective suit. Third, we sought to validate the CE findings with results obtained from GC and HPLC. To the best of our knowledge, no such research has been previously reported in the published literature. Fourth, by using an effective sampling strategy with two internal standards and "smart" data-processing software, the low reproducibility that is frequently considered to be the main disadvantage of CE can be overcome.

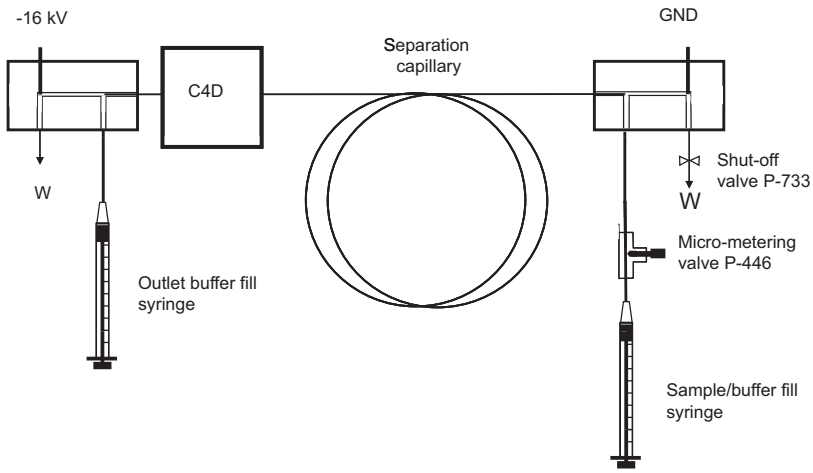

Fig. 1. Schematic of a portable CE instrument with C4D.

2. Experimental

2.1. Materials and methods

2.1.1. Electrophoretic system

A purpose-built portable CE instrument was fitted into a water-tight, crush-proof, dust-proof case made of durable plastic (Peli 1200 Case©, Peli Products, Barcelona, Spain). The instrument size was 30 cm × 30 cm × 15 cm and its weight was approximately 5 kg. The instrument was equipped with an HV safety interlock and included a negative high-voltage power supply (EMCO, Sutter Creek, CA, USA) capable of delivering voltages up to −25 kV, an in-house built C4D detector operating at 200 kHz and a voltage of 60 $V_{p\text{-}p}$, and a in-house built data acquisition system based on LTC2440 high speed differential delta-sigma converter (sampling rate 10 Hz, resolution 24-bit). The instrument is controlled and the signal obtained through a USB connection with in-house written, software using a Netbook computer. The instrument is powered by 10 rechargeable AA-batteries, which provide more than 4 h of operation time. A single electrophoretic run takes approximately 5 min; the number of samples that can be analyzed with the stated power capacity is approximately 50. This is sufficient for the analysis of several NA samples on various matrices, as well as the identification and quantification of the analytes. There is no built-in thermostatic control; however, the instrument case is closed during the analysis, which provides sufficient thermal insulation for a single electrophoretic run. Minor EOF fluctuations are corrected by means of two internal standards. In addition, recently developed software for data normalization [52] was applied for peak identification, baseline drift correction and the improvement of injection precision [53].

Fused-silica (FS) capillaries (75 μm I.D., 375 μm O.D., 35 cm total length, 27 cm effective length, Polymicro Technologies Inc. AZ, USA) were used for the separation. Prior to the first use, the separation capillaries were preconditioned with 0.1 M NaOH for 30 min, deionized water for 10 min, and background electrolyte (BGE) solution for 10 min. Before each analysis sequence, the capillaries were manually washed with approximately 100 column volumes of 0.1 M NaOH, 150 column volumes of DI water and 150 column volumes of the background electrolyte, using a syringe. Each of these steps took approximately 0.5–1 min. The rinsing step was followed by high voltage conditioning of the capillary for 2 min. The total time to prepare the instrument before the first analysis was approximately 5 min. Between two successive injections, the capillary was flushed with 100 column volumes of the BGE solution (1 min). At the end of each day, the capillaries were washed with at least 150 column volumes of DI water and kept in DI water overnight. This procedure allowed for a quick start-up, as described above.

2.1.2. Injection

The experimental set up is shown in Fig. 1. The sample injection apparatus includes a splitter interface machined to 35 mm × 15 mm × 15 mm from a block of polyimide. The splitter interface has a 2-cm-long horizontal flow-through channel of 1 mm I.D. to which two vertical channels of the same diameter are connected. A separation capillary is inserted into the side of the horizontal channel and its tip is positioned exactly at the intersection with the first vertical channel. A grounding Pt electrode is inserted into the second vertical channel. Both the capillary and the Pt electrode are secured with 1/16″ flangeless fittings (Upchurch). The injection syringe is connected to the inlet (the first vertical channel in the interface) via a micro-metering valve (P-446, Upchurch Scientific Oak Harbor, WA, USA). The function of the micro-metering valve is to restrict the manually applicable pressure and thus achieve uniform sample flow rates through the splitter interface. Its function and details on the operation are described in a previous publication [53]. During the injection process, a 500 μL volume of sample is first injected manually into the splitter interface with a 1 mL disposable plastic syringe (Omnifix 100 Duo, Braun, Melsungen, Germany), followed by an injection of 500 μL of the background electrolyte solution to remove any remaining sample from the splitter interface. Only an infinitesimal part of the 500 μL sample and buffer volume is hydrodynamically introduced into the separation capillary, while the majority of the volume is directed to the waste.

The outlet side of the second vertical channel is connected with 10-cm-long, 700 μm I.D. PTFE tubing to a waste reservoir. A shut-off valve (Upchurch, P-733) connected to the waste line of the first splitter interface is used for pressurized capillary flushing using the inlet syringe. The other end of the separation capillary is inserted into the second, identical, interface with the high voltage Pt electrode and a wash syringe is connected to the vertical channels of the interface. The outlet side of the second vertical channel is connected to the second waste reservoir.

2.1.3. GC–MS and LC–MS

An Agilent 6890N GC chromatograph with an Agilent 5975B MS detector was used for comparative data analysis. The column was a 30 m × 0.25 mm × 0.25 μm HP-5MS, with He as the flow gas at a constant velocity of 0.9 mL/min. An Agilent 1200 Series LC chromatograph with a 6410 Triple Quadrupole MS detector was used for HPLC analysis. Agilent, Zorbax Eclipse XDB, 150 × 4.6 mm, 5 μm particle size, with aqueous eluent containing trifluoroacetic acid (TFA) was used at a flow rate of 0.4 mL/min.

2.2. Chemicals

2.2.1. Reagents, standards, electrolytes

All chemicals were of reagent grade and deionized (DI) water was used throughout. Stock solutions of NA degradation products (10 mM) were prepared from acids (butylphosphonic acid, BPA, Alfa Aesar; propylphosphonic acid, PPA, Alfa Aesar; methylphosphonic acid, MPA, Sigma–Aldrich) or their sodium salts (pinacolyl methylphosphonate, PMPA; ethyl methylphosphonate, EMPA; 2-aminoethyldihydrogenphosphonate, AEDHPA, all from Sigma–Aldrich). Isopropylmethyl-phosphonic acid (IMPA) was purchased as a 1000 mg/L methanolic solution (Cerilliant Corp., TX, USA). Salicylic acid was of p.a. quality and purchased from Sigma–Aldrich. All multi-ion standard solutions were freshly prepared from these stock solutions and diluted with DI water. Background electrolyte (BGE) solutions for CE measurements were prepared daily from 100 mM stock solutions of 2-(N-Morpholino)ethanesulfonic acid (MES, Sigma–Aldrich) and L-histidine (HIS, Sigma–Aldrich). Sarin (purity >99%), soman (purity >96.7%) and VX (purity >90.3%) was supplied by the staff of the testing site near Vyškov (Czech Republic) under the licence of the Ministry of Defence and Armed Forces of the Czech Republic.

2.3. Sampling and extraction procedures

2.3.1. Application and sampling of nerve agents

The extraction procedures were developed and the robustness of the sampling procedures was validated at a testing site near Tallinn, Estonia using NA degradation products and the help of staff of the Pioneer Battalion of the Estonian Army. Field experiments with genuine NA were performed in September 2010 at a testing site near Vyškov (Czech Republic). The weather conditions at the testing site were as follows: low pressure and cloudy, with a temperature of about 9 °C. NA application and sample extraction were performed by trained personnel at the test site, and the actual CE analysis of the NA was done by the authors in the vicinity of the sampling site. Five different matrices (Teflon, ceramic tile, concrete, grass and soil) with an equal surface area of 25 cm^2 were contaminated with 100 mg of pure nerve agent (sarin, soman, VX) and kept outdoors (temperature 9 °C), one batch for 30 min and the other for 3 h. After the elapsed exposure time, two procedures were used as described below.

2.3.2. Extraction procedures

Teflon, ceramic tile, concrete matrices: After application of the nerve agent, the surface of the matrix was carefully wiped with a DI water pre-moistened Ghost wipe tissue (Environmental Express, Mt. Pleasant, SC, USA) using tweezers. The tissue was placed into a plastic sample vial containing 10 mL of DI water. The NA hydrolysis products as well as the unhydrolyzed NA were extracted by vigorous shaking for 1 min. The extract was filtered through a 0.45 μm filter (Filtropur S, Sarstedt, Numbrecht, Germany). Internal standards (400 μM AEDHPA, 100 μM salicylic acid) were added to the filtered sample, which was then directly injected into the CE system.

Soil and grass matrices: The matrices consisted of 20 g of sandy soil and 1 g of finely cut grass, respectively. After application of the nerve agent, the samples were placed into a plastic sample vial with 10 mL of DI water and extracted by vigorous shaking for 1 min, followed by filtration through a 0.45 μm filter, the addition of internal standards and direct injection into the CE system.

The total extraction time for each matrix was no longer than 5 min.

3. Results and discussion

3.1. Aqueous extraction of nerve agents

It is well known that nerve agents undergo rapid hydrolysis in aqueous solutions; this is typically a two-step process, as shown in Fig. 2. In the first step, the O-alkyl-phosphonofluoridates (sarin, soman) quickly hydrolyze to isopropyl methylphosphonate (IMPA, the hydrolysis product of sarin) or pinacolyl methylphosphonate (PMPA, the hydrolysis product of soman). O-Alkyl-S-(2-dialkyl-aminoethyl)alkylphosphonothiolates (VX) follow different hydrolysis patterns depending on the pH of the solution. At pH <6.5, as in the case of extraction with deionized water, the predominant reaction is the P-S cleavage [54] that results in the formation of ethyl methylphosphonate (EMPA) and diisopropylaminoethanethiol (DIAET). In the second hydrolysis step, which is typically much slower than the first, all three alkylphosphonates further degrade to methylphosphonate (MPA) and alcohol.

As both sarin and soman are fairly soluble in water, it was expected that aqueous extraction would yield high recoveries of the degradation products for most of the matrices. The solubility of VX in water is rather low; however, below 9.4 °C, VX becomes fairly soluble as well [55]. As the average outside temperature at the sampling site did not exceed 9 °C, high recoveries for VX were also expected. In all matrices, the respective alkylphosphonates from the first hydrolysis step were found in sufficient quantities; however, no MPA peak appeared even in the samples that were exposed to NA for 3 h. These results are indicative of the speed of hydrolysis, as discussed above. The type of nerve agent can thus be identified based on the presence of the hydrolysis product from the first hydrolysis step.

3.2. Separation of the hydrolysis products of nerve agents

The background electrolyte used for the separation of the NA degradation products was comprised of an equimolar mixture of MES and HIS. Separation of all selected alkylphosphonates including internal standards was achieved in less than 5 min in a 7.5 mM MES/HIS electrolyte with a pH of 6 at −16 kV. The separation of the analytes in this research was counter-electroosmotic, e.g. the negative electrode was placed on the detection side. Because phosphonic acids are deprotonated and migrate as anions against the EOF, the slowest migrating analyte, PMPA, will appear first in the electropherogram, while the fastest one, MPA, will appear last. The measured peak areas will also increase accordingly, as the conductivity of the separated acids increases with increasing mobility. The counter-electroosmotic separation mode with negative polarity (on the detection side) has some advantages over the positive polarity mode used by other authors [48–51]. First, there is no need to add EOF modifiers, such as CTAB, into the background electrolyte. Second, there is no interference from small inorganic anions, which are often present in aqueous samples and extracts from environmental matrices. In the negative polarity mode small anions do not reach the detector, because they migrate in the opposite direction to the EOF, at velocities exceeding it. The separation of standard solutions of PMPA, IMPA, EMPA, MPA and two internal standards

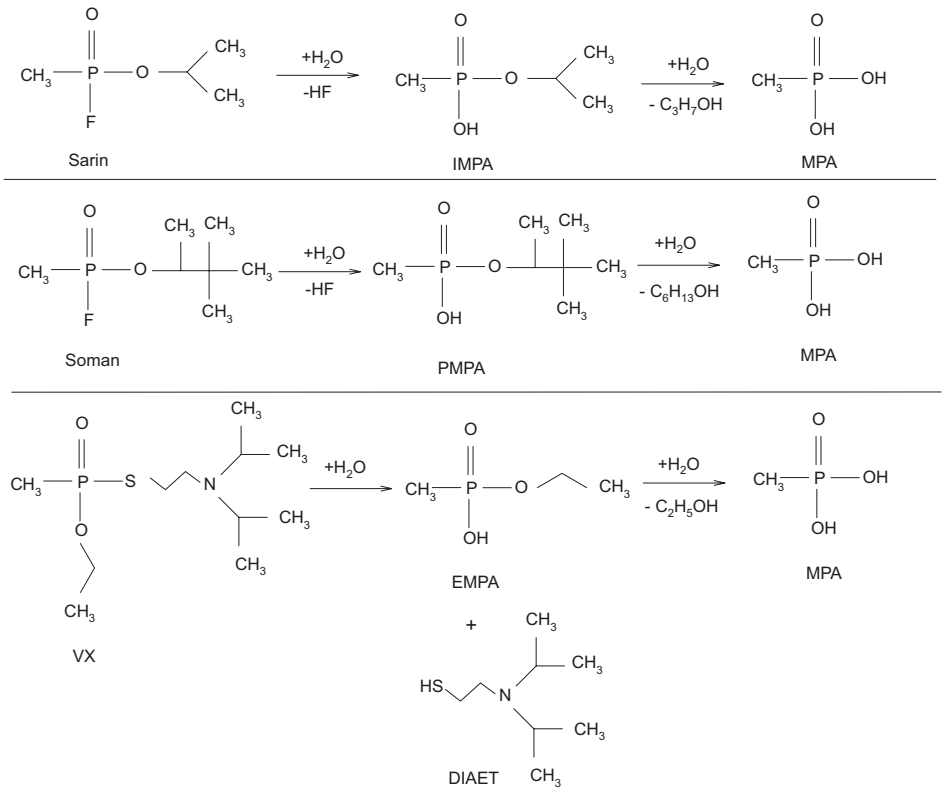

Fig. 2. Aqueous hydrolysis paths of nerve agents sarin, soman and VX.

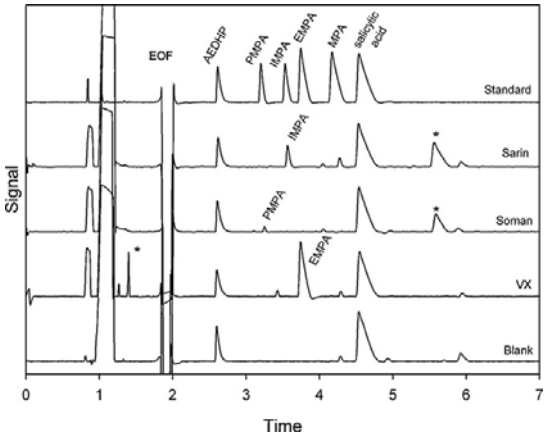

Fig. 3. Separation of hydrolysis products of nerve agents sarin, soman and VX in a concrete matrix. CE conditions: Separation voltage: −16 kV, Background electrolyte: 7.5 mM MES/HIS, pH 6, C4D detection. Injection: 500 μL of standard solution followed by 500 μL of BGE.

(AEDHPA and salicylic acid) is shown in Fig. 3. Two internal standards were selected so that they would effectively bracket the analytes to facilitate their qualitative identification. A previously developed signal processing algorithm [52] was used for baseline correction, signal alignment, peak identification and integration. Unwanted shifts in the time axis caused by variations in electroosmotic flow were corrected based on the premises advanced by Reijenga et al. [56] By linking peaks of two internal standards, these variations can be overcome, and corrected electropherograms were obtained, free from any migration time bias due to minor fluctuations of EOF.

Fig. 3 shows the separation of a standard solution, extracts of sarin, soman and VX obtained from wipe-sampling a concrete matrix, and also a blank solution of the same matrix to which no nerve agent was applied. The figure shows an excellent match between the transformed migration times of the standards and the nerve agent hydrolysis products from aqueous extracts. Note that the electropherograms were recorded on three consecutive days, demonstrating excellent reproducibility of the portable CE system and the effectiveness of the software data processing.

3.3. Calibration linearity, limits of detection

The calibration solutions for quantitative determination of the NA hydrolysis products were prepared in the range of 25–150 μM. AEDHPA at a concentration of 400 μM and salicylic acid at a concentration of 100 μM were added to each standard solution. The calibration curves for raw peak areas were linear throughout the measured range, with coefficients of variation better than 0.94. The linearity was significantly improved by applying a correction with the first internal standard (AEDHPA). By dividing the respective analyte peak areas by the peak area of the AEDHPA, the coefficients of variation improved and were better than 0.98. The second internal standard, salicylic acid, was used for purposes of identification

Table 1
Calibration data for the determination of NA degradation products.

Degradation product	RSD, %	$(a \pm s_a)$[a]	$(b \pm s_b)$[a]	R^2	LOD[b], μM
PMPA	6.2	9.20 ± 0.23	−80.0 ± 2.7	0.9853	25.8
IMPA	6.8	10.02 ± 0.28	−104.2 ± 24.2	0.9815	26.1
EMPA	5.1	18.07 ± 0.38	−117.1 ± 32.7	0.9895	15.2
MPA	8.3	17.24 ± 0.36	−118.6 ± 30.7	0.9898	16.0

[a] Calibration line equation $y = a + bc$ parameters: a – intercept, s_a its standard deviation, b – slope, s_b its standard deviation; y – detector response c – concentration.
[b] Limit of detection calculated as three times the standard deviation of the noise level.

but not for quantitation, because in some samples, a co-migration of unidentified matrix peaks with salicylic acid was observed. The correction procedure was legitimate, because one internal standard is usually sufficient to achieve reasonable precision of the measured data [57] with CE hydrodynamic injection. The calibration data including calibration ranges, linearity and limits of detection are shown in Table 1.

3.4. Analysis of different matrices

Different matrices were analyzed as described in the section on details of the experiments. They included one reference matrix (Teflon) on which the absorption of NA was expected to be negligible. The other matrices included concrete and ceramic tile, which represent typical solid surfaces that are found in locations where there is a greater probability of NA usage, such as urban and public areas with high population concentrations. On the other hand, soil and vegetation represent types of samples that would be found in rural areas, and in which higher adsorption of NA would be expected. The latter matrices cannot be sampled by simple surface wiping techniques, as the NA penetrate deep into the matrix. Aqueous extraction was selected for these samples. Duplicate experiments with different exposure times (30 min and 3 h after contamination, respectively) were performed on each matrix. Fig. 4 shows a separation of an aqueous extract of sarin (A) and VX (B) from all matrices. For each matrix, a typical hydrolysis product peak appears that can be used to identify the nerve agent. The IMPA peak for sarin was observed in all extracts from all matrices and was quantified using the previously described calibration procedure with one internal standard. Soman produced a similar eletropherogram with a PMPA peak appearing for all matrices (data not shown). A large, unknown peak (marked with an asterisk) occurred for all matrices contaminated with sarin and soman. This peak is not fluoride, as was confirmed by spiking the samples with fluoride standard. Additionally, this peak is not visible on the second set of electropherograms, which are for nerve agent VX. On the contrary, a specific, large cationic peak (marked with an asterisk in Fig. 4B) appears at approximately 83 seconds for all matrices contaminated with VX. Heleg-Shabtai et al. [25] have separated VX and its degradation products (EMPA) by CE using a 1 mM carbonate background electrolyte at pH 7.7 with LIF detection. As the pKa of VX is high (the values given in the literature range between 8.6 and 9.4) [58,59], the undegraded VX migrated ahead of the EOF as a cationic peak in their electrolyte system at pH 7.7. The MES/HIS electrolyte used in this work has a pH of 6. Any remaining VX should also be positively charged; we therefore assume that the large positive peak corresponds to unhydrolyzed VX.

Table 2 contains the recovery values for sarin, soman and VX from the different matrices with corresponding concentrations of particular degradation products detected by the portable CE analyser. The results reveal that the lowest recovery (ranging between 0.02 and 0.4%) was obtained from the concrete matrix. This is an obvious consequence of the nature of concrete, which is much more porous than the other solid matrices. In some cases, the recovery rate of the samples obtained from the concrete matrix using the wiping technique is up two orders of magnitude lower than

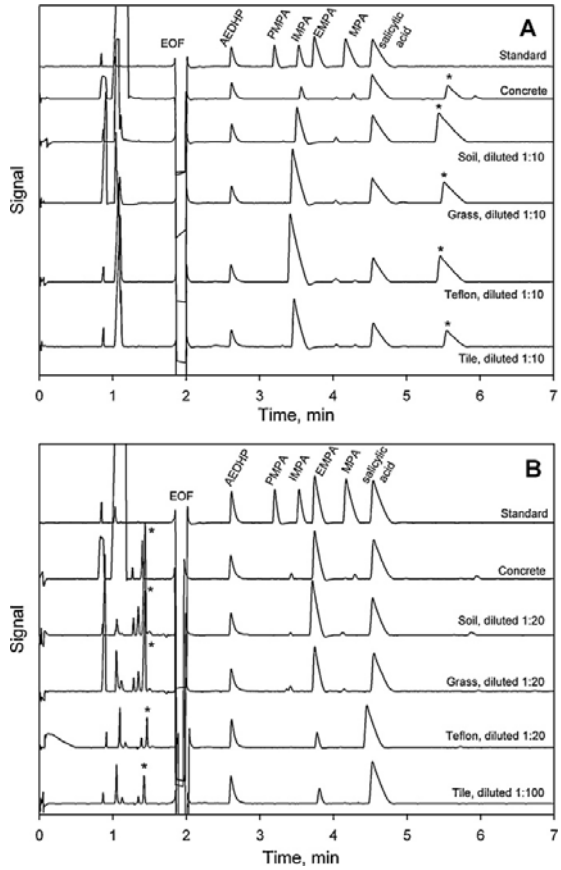

Fig. 4. Separation of hydrolysis products of nerve agents sarin (A) and VX (B) in various matrices. CE conditions: as in Fig. 3.

the recoveries from other matrices. To confirm that the wiping technique is appropriate for concrete samples and that the low recoveries were due to the absorption of the NA into the matrix, control experiments were performed using a different sampling method. The same (previously wiped) concrete samples were put into enclosed containers, covered with 10 mL of deionized water, sonicated for 10 min and the extracts analyzed. Because the recoveries were still much lower than they were from the other matrices even with the sonication approach (by at least one order of magnitude), wipe sampling was deemed to be an appropriate option as it involves less handling and does not require the use of an ultrasound bath. The recoveries for the samples obtained from the other matrices ranged between 4.6–34.5% for Teflon, 2.7–16.7% for tile, 3.2–9.4% for grass and 2.3–8.7% for soil. There was no obvious trend in the behaviour of the various nerve agents on different matrices.

Table 2
Recovery data for sarin, soman and VX on various matrices.

Matrix	sarin				soman				VX			
	Concentration of IMPA, mM		Recovery, %		Concentration of PMPA, mM		Recovery, %		Concentration of EMPA, mM		Recovery, %	
	30 min	3 h	30 min	3 h	30 min	3 h	30 min	3 h	30 min	3 h	30 min	3 h
Soil	1.67	5.43	2.34	7.60	1.25	3.24	2.28	5.91	3.26	1.91	8.72	5.11
Grass	3.73	6.72	5.22	9.42	2.47	2.03	4.51	3.70	2.18	1.19	5.84	3.19
Teflon	5.64	24.62	7.89	34.49	2.55	9.25	4.64	16.84	2.40	2.22	6.43	5.94
Tile	3.16	1.93	4.42	2.71	3.62	9.16	6.60	16.69	2.00	1.39	5.35	3.71
Concrete, wiped	0.04	0.03	0.05	0.04	0.02	0.06	0.03	0.11	0.12	0.15	0.32	0.41
Concrete, sonicated	0.40	0.57	0.56	0.79	0.15	0.42	0.27	0.76	0.85	0.88	2.26	2.35

Table 3
Ratios of NA peak areas after 0.3 and 3 h of application of NA (possible outliers are given in bold italic).

Nerve agent	Matrix				
	Teflon	Tile	Concrete	Soil	Grass
CE: $A_3^{CE}/A_{0.5}^{CE}$					
sarin	4.6	0.6	***0.8***	3.2	1.8
soman	***3.7***	2.5	3.4	3.0	0.8
VX	1.0	0.7	1.3	0.6	0.5
GC–MS: $A_{0.5}^{Chr}/A_3^{Chr}$					
sarin	4.6	0.3	0.1	3.0	1.6
soman	1.8	2.8	3.1	3.7	3.2
VX	0.6	0.3	***3.2***	1.6	1.1
HPLC–MS: $A_{0.5}^{Chr}/A_3^{Chr}$					
sarin	2.3	***97.9***	2.5	2.0	1.6
soman	1.6	1.6	4.0	3.8	1.9
VX	0.9	1.0	1.1	1.1	1.0

In most cases, the recoveries for the soil and vegetation samples were lower than for the solid surface samples, such as tile or Teflon.

3.5. Comparison of CE data with GC–MS and HPLC–MS

To compare the results of the CE analysis with GC–MS and HPLC–MS, the nerve agents were applied to the five matrices, extracted with acetonitrile and immediately analyzed in a laboratory using standard analytical protocols for GC and HPLC determination of the nerve agents and their hydrolysis products. Due to differences in the chemical nature of the extraction solutions applied to the different matrices, direct comparison of CE and chromatographic methods would be difficult. However, the degradation process of NA in different matrices and their extraction should not depend on the analytical method. The NA peak area ratio $A_{0.5}^{Chr}/A_3^{Chr}$ was compared with that of the NA degradation products $A_3^{CE}/A_{0.5}^{CE}$. The indexes *Chr* and *CE* indicate the peak area ratios obtained by the corresponding chromatographic and CE measurements, and 0.5 and 3 denote the duration of exposure to the nerve agents. The data are presented in Table 3. If the nerve agents had decomposed appreciably over time, the numbers in Table 3 (within the margin of experimental error) should be greater than one, which is the case only for the Teflon matrix. Deviations from that premise can be observed for the other matrices, and these may be explained by the nature of a particular matrix and the extent of absorption. Nevertheless, it is still possible to compare the different matrices. With the exception of the obvious outliers (the point was considered an outlier when it was outside the 0.995 confidence band of the corresponding regression line (Student's $t = 3.5$)), the square of correlation coefficients and the regression equation can be calculated from the data represented in Table 3. The results for CE and GC–MS data are as follows:

$$\frac{A_{0.5}^{GC-MS}}{A_3^{GC-MS}} = (0.93 \pm 0.13)\frac{A_3^{CE}}{A_{0.5}^{CE}} + (0.2 \pm 0.3); \quad R^2 = 0.89$$

The square of correlation coefficients between CE and HPLC–MS and GC–MS and HPLC–MS were $R^2 = 0.41$ and $R^2 = 0.30$, respectively.

There is a good correlation between the CE and GC–MS data, with a slope close to unity, whereas the correlation between CE and HPLC–MS and between GC–MS and HPLC–MS is nonexistent. This may be a result of further degradation of the NA during HPLC aqueous elution.

Assuming abundant atmospheric humidity at the test site compared to the amount of NA applied to the various matrices, and an irreversible pseudo-first-order reaction of decomposition, the rate of degradation product formation can be estimated from CE measurements using degradation product peak areas from electropherograms recorded at 0.5 and 3 h after the application of the nerve agent to the matrix. However, due to the occurrence of absorption in many of the matrices, meaningful data for Teflon can only be obtained for sarin and soman. The formation rate of IMPA (the degradation product of sarin) was $0.28 \pm 0.02\ h^{-1}$ and that of PMPA (the degradation product of soman) was $0.5 \pm 0.2\ h^{-1}$. The data reported in the literature vary significantly. Assuming average values for humidity, rainfall, and solar flux, reported approximate lifetimes under equivalent conditions are 5 h for soman and 30 min for sarin [60], which compare roughly with our data. Since soman is more persistent than sarin, our data indicate that the formation rates of primary degradation products might not give an accurate indication of degradation rates of NA. VX is too persistent to measure its decay in 3 h.

4. Conclusions

This research demonstrates for the first time that a portable CE system with contactless conductometric detection can be used for rapid and accurate identification and quantification of genuine nerve agents that have been deposited on various matrices. The extraction procedures that were developed allow for timely and efficient sampling of nerve agents from contaminated areas and analysis of their degradation products. The entire procedure

including instrument start-up, sampling and analysis takes approximately 10 min, which is the fastest screening with a liquid phase separation method available to date. Three nerve agents (sarin, soman and VX) were positively identified in the five matrices studied, based on hydrolysis product peak identification. Nonexistent or very minor interference from the sample background was observed with the selected BGE and CE polarity, as the major interfering compounds migrate ahead of or behind the degradation products of CWA. Recoveries from different matrices were compared and ranged from 2 to 35% with the exception of the sample taken from concrete, for which the recovery was up to two orders of magnitude lower. The hydrolysis rate constants were estimated for the duplicate samples that were taken at 30 min and 3 h after exposure, and they compare favorably with the data in the literature. The CE data correlated well with the results obtained with the GC–MS reference method. The sampling and analysis techniques described above represent the most rapid method of screening for genuine NA using portable CE instruments that has been presented to date.

Acknowledgements

This research project was assisted by the Estonian Ministry of Defense. We acknowledge staff members of the Pioneer Battalion of the Estonian Army for their help during the field tests. P.K. acknowledges the funding from the European Union's Seventh Framework Programme under grant agreement No. 229830 IC-UP2.

References

[1] http://treaties.un.org/Pages/ViewDetails.aspx?src=TREATY&mtdsg_no=XXVI-3&chapter=26&lang=en (accessed 28.01.11).
[2] G. Black, Genocide in Iraq: The Anfal Campaign Against the Kurds, Human Rights Watch, New York, 1993, p. 271.
[3] T. Nakajima, S. Sato, H. Morita, N. Yanagisawa, Occup. Environ. Med. 54 (1997) 697.
[4] H. Murakami, Underground: The Tokyo Gas Attack and the Japanese Psyche, Vintage International, New York, USA, 2000.
[5] A search of the ISI Web of Science for the last ten years yields about 100 publications with titles containing the words "chemical warfare" and "detection" or "determination".
[6] Guide for the Selection of Chemical Detection Equipment for Emergency First Responders, 3rd ed., Department of Homeland Security, Coordinated by NIST-OLES, January 2007, 437 pp. Can be downloaded from https://www.rkb.us/contentdetail.cfm?content_id=97670 (accessed 28.01.11).
[7] M.A. Mäkinen, O.A. Anttalainen, M.E. Sillanpää, Anal. Chem. 82 (2010) 9594.
[8] R. Sferopoulos, A Review of Chemical Warfare Agent (CWA) Detector Technologies and Commercial-Off-The-Shelf Items, Human Protection and Performance Division DSTO Defence Science and Technology Organisation, Victoria 3207, Australia, 2009, 99 pp.
[9] C.E. Kientz, J. Chromatogr. A 814 (1998) 1.
[10] H. John, F. Worek, H. Thiermann, Anal. Bioanal. Chem. 391 (2008) 97.
[11] S. Kendler, S.M. Reidy, G.R. Lambertus, R.D. Sacks, Anal. Chem. 78 (2006) 6765.
[12] C.E. Kientz, A. Verweij, H.L. Boter, A. Poppema, R.W. Frei, G.J. de Jong, U.A.Th. Brinkman, J. Chromatogr. 467 (1989) 385.
[13] G.A. Sega, B.A. Tomkins, W.H. Griest, J. Chromatogr. A 790 (1997) 143.
[14] P.A. D'Agostino, J.R. Hancock, L.R. Provost, J. Chromatogr. A 840 (1999) 289.
[15] A.M. Degenhardt-Langelaan, C.E. Kinetz, J. Chromatogr. A 723 (1996) 210.
[16] P.A. D'Agostino, J.R. Hancock, L.R. Provost, J. Chromatogr. A 912 (2001) 291.
[17] R. Mustachich, Detection of Chemical Warfare Agents by Transportable GC/MS, Application Note, Agilent Technologies, September 2010, 6 pp.
[18] E.W.J. Hoojschuur, C.E. Kientz, U.A.Th. Brinkman, J. Chromatogr. A 982 (2002) 177.
[19] M. Pumera, J. Chromatogr. A 1113 (2006) 5.
[20] J. Wang, Anal. Chim. Acta 507 (2004) 3.
[21] B. Papouskova, P. Bednar, P. Bartak, P. Frycak, J. Sevcik, Z. Stransky, K. Lemr, J. Sep. Sci. 29 (2006) 1531.
[22] J.E. Melanson, C.A. Boulet, C.A. Lucy, Anal. Chem. 73 (2001) 1809.
[23] C.L. Copper, G.E. Collins, Electrophoresis 25 (2004) 897.
[24] J. Jiang, C.A. Lucy, J. Chromatogr. A 966 (2002) 239.
[25] V. Heleg-Shabtai, N. Gratziany, Z. Liron, Electrophoresis 27 (2006) 1996.
[26] R. Kostiainen, A.P. Bruins, W.M.A. Hakkinen, J. Chromatogr. 634 (1993) 113.
[27] M. Lagarrigue, A. Bossee, A. Begos, N. Delaunay, A. Varenne, P. Gareil, B. Bellier, J. Chromatogr. A 1178 (2008) 239.
[28] M. Lagarrigue, A. Bossee, A. Begos, N. Delaunay, A. Varenne, P. Gareil, B. Bellier, Electrophoresis 30 (2009) 1522.
[29] J.-P. Mercier, P. Chaimbault, Ph. Morin, M. Dreux, A. Tambute, J. Chromatogr. A 825 (1998) 71.
[30] C.E. Kientz, E.W.J. Hooijschuur, U.A.Th. Brinkman, J. Microcolumn Sep. 9 (1997) 253.
[31] E.W.J. Hooijschuur, C.E. Kientz, U.A.Th. Brinkman, J. Chromatogr. A 928 (2001) 187.
[32] G.A. Pianetti, M. Taverna, A. Baillet, G. Mahusier, D. Baylocq-Ferrier, J. Chromatogr. 630 (1993) 371.
[33] A.-E.F. Nassar, S.V. Lucas, W.R. Jones, L.D. Hoffland, Anal. Chem. 70 (1998) 1085.
[34] A.-E.F. Nassar, S.V. Lucas, C.A. Myler, W.R. Jones, M. Campisano, L.D. Hoffland, Anal. Chem. 70 (1998) 3598.
[35] J.E. Melanson, B.L.-Y. Wong, C.A. Boulet, C.A. Lucy, J. Chromatogr. A 920 (2001) 359.
[36] J.-P. Mercier, Ph. Morin, M. Dreux, A. Tambute, J. Chromatogr. A 741 (1996) 279.
[37] J.-P. Mercier, Ph. Morin, M. Dreux, A. Tambute, J. Chromatogr. A 779 (1997) 245.
[38] R.L. Cheicante, J.R. Stuff, H.D. Durts, J. Chromatogr. A 711 (1995) 347.
[39] W. Robins, B.W. Wright, J. Chromatogr. A 680 (1994) 667.
[40] S.A. Oehrle, P.C. Bossle, J. Chromatogr. A 692 (1995) 247.
[41] T.E. Rosso, P.C. Bossle, J. Chromatogr. A 824 (1998) 125.
[42] A. Zemann, E. Schnell, D. Volgger, G.K. Bonn, Anal. Chem. 70 (1998) 563.
[43] J.A. Fracassi da Silva, C.L. do Lago, Anal. Chem. 70 (1999) 4339.
[44] Y. Ding, C.D. Garcia, K.R. Rogers, Anal. Lett. 41 (2008) 335.
[45] A. Seiman, M. Jaanus, M. Vaher, M. Kaljurand, Electrophoresis 30 (2009) 507.
[46] N. Makarotseva, A. Seiman, M. Vaher, M. Kaljurand, Proc. Chem. 2 (2010) 20.
[47] A. Seiman, N. Makarotseva, M. Vaher, M. Kaljurand, Chem. Ecol. 26 (2010) 145.
[48] J. Wang, M. Pumera, G.E. Collins, A. Mulchandani, Anal. Chem. 74 (2002) 6121.
[49] L. Xu, X.Y. Gong, H.K. Lee, P.C. Hauser, J. Chromatogr. A 1205 (2008) 158.
[50] L. Xu, P.C. Hauser, H.K. Lee, J. Chromatogr. A 1216 (2009) 5911.
[51] L. Xu, P.C. Hauser, H.K. Lee, J. Chromatogr. A 1214 (2008) 17.
[52] A. Seiman, M. Vaher, M. Kaljurand, Electrophoresis, doi:10.1002/elps.20100057.
[53] P. Kuban, A. Seiman, M. Kaljurand, J. Chromatogr. A 1218 (2011) 1273.
[54] S. Budavari, M.J. O'Niel, A. Smith, P.E. Heckelmanm (Eds.), The Merck Index, 11th ed., Merck & Co., Rahway, 1989, p. 594, compound no. 3716.
[55] http://www.opcw.org/about-chemical-weapons/types-of-chemical-agent/nerve-agents/ (accessed 28.01.11).
[56] J.C. Reijenga, J.H.P.A. Martens, A. Giuliani, M. Chiari, J. Chromatogr. B 770 (2002) 45.
[57] E.V. Dose, G.A. Guiochon, Anal. Chem. 63 (1991) 1154.
[58] Y.-Ch. Yang, J.A. Baker, J.R. Ward, Chem. Rev. 92 (1992) 1729.
[59] M.J. Van der Schaans, B.J. Lander, H. van der Wiel, J.P. Langenberg, H.P. Benschop, Toxicol. Appl. Pharmacol. 191 (2003) 48.
[60] http://www.noblis.org/MissionAreas/nsi/BackgroundonChemicalWarfare/ChemicalWarfareAgentsandChemicalWeapons/Pages/DispersalChemicalWarfareAgents.aspx (accessed 28.01.11).

Publication IV

Seiman, A., Vaher, M., Kaljurand, M., Monitoring of the electroosmotic flow of ionic liquid solution in non-aqueous media using thermal marks. *Journal of Chromatography A* **2008**, *1189*, 266-273.

Available online at www.sciencedirect.com
ScienceDirect
Journal of Chromatography A, 1189 (2008) 266–273
JOURNAL OF CHROMATOGRAPHY A
www.elsevier.com/locate/chroma

Monitoring of the electroosmotic flow of ionic liquid solutions in non-aqueous media using thermal marks

Andrus Seiman*, Merike Vaher, Mihkel Kaljurand

Department of Chemistry, Tallinn University of Technology, Akadeemia tee 15, 12618 Tallinn, Estonia

Available online 11 January 2008

Abstract

The possibility of applying a new method employing thermal marks to measuring the rate of the electroosmotic flow (EOF) in non-aqueous capillary electrophoresis (NACE) was investigated. The thermal marks were monitored by using a contactless conductivity detection. During one experiment and in between the series of experiments the reproducibility of the method was excellent. The EOF rate was measured 4–7 times during one experiment, the precision of measurement being around 0.5%. In this study, the influence of 1-butyl-3-methyl-imidazolium salts in organic solvents on the rate of the EOF was investigated. Various organic solvents were mixed with an ionic liquid of various concentrations and the EOF rate was measured using thermal marks. The accuracy of the method was compared with that of the neutral marker one. Five benzoic acid derivatives were separated while the EOF was monitored. The relative standard deviations of the corrected effective mobilities of the above analytes were in the range of 1.0–6.1%.

Keywords: Alkylimidazolium salts; Elecroosmotic flow; Ionic liquids; Non-aqueous capillary electrophoresis; Thermal marks

1. Introduction

The electroosmotic flow (EOF), an electrokinetic phenomenon present in capillary electrophoresis (CE) and is one of its most important features, allows separation of an extremely wide range of analytes. The EOF carries cations, neutral molecules and anions from the sample inlet towards the detector in the same direction. CE could be compared with the high-performance liquid chromatography (HPLC) as EOF acts like a HPLC pump, except there is no need for complex mechanical pumps, and flow profile is flat. These two aspects have immensely contributed to the popularity CE nowadays enjoys.

In CE, analytes are mostly identified by their peak migration times. Therefore, in CE experiments the reproducibility of the migration time is of crucial importance. The latter is directly affected by the EOF which depends on the ζ-potential of the capillary wall, the electric field, and the temperature. The changes in the pH, temperature, buffer composition, or the chemical composition of the capillary surface can lead to changes of the magnitude of the rate of the EOF. It is important to monitor the EOF during the experiment to fully achieve good separation and an excellent resolution of CE.

The neutral marker method is a straightforward approach to measure the rate of the EOF [1–4]. Neutral species are inserted in the sample plug and the EOF rate is calculated using the migration times of the species. The neutral marker method is limited to providing a single, average EOF value for the time marker migrating through the capillary. This means that the neutral marker method does not represent changes of the EOF after the marker has passed the detector. Besides, the method is not very suitable for measuring weak electroosmosis as it takes a very long time for the neutral marker to reach the detector. Righetti and co-workers have proposed an alternate time-saving method that is based on the injection of the neutral marker by means of electroosmosis [5]. After injection, a low pressure is applied to the capillary and the marker is recorded at the detector. The EOF rate is calculated from the quantified peak area. Weighting the effluent from the capillary is another approach to measuring an average rate of the EOF. Due to the extremely low-volume EOF rates, the method is impractical, though it has demonstrated good precision [6].

A technique that is used to measure the average rate of the EOF and is very similar to the neutral marker method, is called the current monitoring. The solution filling the capillary is elec-

* Corresponding author. Tel.: +372 620 4323.
E-mail address: andrusseiman@gmail.com (A. Seiman).

0021-9673/$ – see front matter © 2008 Elsevier B.V. All rights reserved.
doi:10.1016/j.chroma.2008.01.015

trophoretically replaced by the background electrolyte (BGE) of different concentrations. Consequently, the total conductivity in the capillary changes as the solution at the inlet replaces the solution in the capillary. The average EOF rate is calculated using the time it takes from the beginning of experiment till the current stop changing as the capillary has been filled with the solution from the inlet. The current monitoring has been used to measure the EOF rate in capillaries [2,7], and microfluidic devices [8,9].

Many research groups have made an effort to develop systems for an on-line monitoring of the EOF. Zare and co-workers proposed a method for the real-time measurement of the EOF in CE [10]. The operating mechanism of the method proposed is based on the measurement of the dilution of the fluorescent dye solution introduced into the BGE downstream the detection zone. The fluorescent dye and the exuding buffer are mixed on-line, using a concentric capillary design for the post-column solution mixing. Another on-line method for monitoring the electroosmotic flow in CE separation is based on a periodic photobleaching and the laser-induced fluorescence (LIF) detection of the dilute neutral fluorophore mixed with a BGE [8,11,12]. Before experiment, the dilute neutral fluorophore is simply added to the running buffer, therefore the post-column detection and solution addition are unnecessary.

Recently, do Lago and co-workers proposed a new method for the measurement of the EOF by a contactless conductivity detection based on the use of the so-called thermal marks [13]. Thermal marks are small disturbances in the concentration profile of the BGE which are generated by a punctual heating of the capillary. These disturbances can be easily generated by heating the capillary with short pulses, using a tungsten filament or a surface mount device (SMD) resistor. do Lago and his group have demonstrated the potential use of thermal marks with different BGEs and in real experiment conditions using egg white as sample.

According to literature thermal marks can be generated in different electrolytes dissolved in water. An alternative is to use non-aqueous buffers in CE (NACE). NACE owes its growing popularity to many aspects. To name only a few amongst the many, firstly, most organic solvents exhibit a higher solvation strength than water, which enables the CE analysis of hydrophobic substances to be performed [14]. Secondly, organic solvents have a wide range of physicochemical properties that allow a greater manipulation of selectivity [15]. And, thirdly, the BGEs based on highly volatile solvents like methanol (MeOH) and acetonitrile (ACN) have made it easier to couple CE with mass spectrometry (MS) [16,17].

Ionic liquids (IL) are defined as materials containing only ionic species and having a melting point lower than 298 K. Many properties of IL, which can be made use of in chemical analysis, have been described in literature (see recent reviews [18–25]). In NACE ILs have been used as ionic additives to achieve electrophoretic separation in pure ACN [26,27]. The aim of this paper was to investigate the possibility of using thermal marks in non-aqueous capillary electrophoresis (NACE) in the presence of ionic liquids, and to compare the performance of this method with the neutral marker one. In this work, seven different organic solvents were used. For each solvent, the rate of the EOF was measured at different IL additive concentrations.

2. Experimental

2.1. Reagents and chemicals

In this study, the 1-butyl-3-methyl imidazolium ($[BMIm]^+$) based salt with a trifluoroacetate ($[CF_3COO]^-$) anionic part, which is air- and water-stable and miscible with most CE solvents, was used as an additive to the separation media. All solvents—acetonitrile, methanol, ethanol (EtOH), propylene carbonate (PC), formamide (FA), nitromethane (NM), *N*,*N*-dimethylformamide (DMF), dimethyl sulfoxide (DMSO) were chromatographic grade and were obtained from Sigma–Aldrich (Steinheim, Germany). Five different benzoic acid derivatives (*p*-aminobenzoic acid, benzoic acid, salicylic acid, 3,5-dihydroxybenzoic acid, 3,5-dinitrobenzoic acid) and dodecylbenzene were purchased from Merck (Darmstadt, Germany). Sodium hydroxide was purchased from Chemapol (Prague, Czech Republic).

2.2. Instrumentation

The CE system consisted of a 0–30 kV Spellmann CZE2000 (Haupauge, NY, USA) high voltage power supply and a house-made capacitively coupled contactless conductivity detector (C^4D). This detector was made according to the ideas outlined in Refs. [28–30]. The device consisted of two tubular electrodes placed around the separation capillary at the detection point. One of the electrodes was exited with a 60 V peak-to-peak 180 kHz oscillating frequency. The signal was picked up by the second electrode and further amplified. ADAM modules (Advantech Inc., Taipei, Taiwan) were used for an analog-to-digital (AD) conversion of the detector signal. The fused silica capillary (i.d. 75 μm × o.d. 365 μm) was obtained from Polymicro Technologies (Tucson, AZ, USA). The total and effective length of the capillary was 61.5 and 57.5 cm, respectively. The high voltage power supply had an output voltage of about 18.5 kV, though the exact voltage was measured at the beginning of each day. The applied electric field was around 300 V cm^{-1}.

The thermal marks were generated using tungsten filaments of common light bulbs as proposed by do Lago and co-workers [13]. The glass bulb was carefully removed and the tungsten filament was placed in contact with a fused silica capillary. The 100 W light bulbs were powered with an external power supply, the applied voltage being in the range of 10–40 V. The lowest voltage capable of producing still visible thermal marks was chosen separately for each experiment. The initial tests were carried out with one tungsten filament, the distance to the detection point being 8.3 cm. After adding another tungsten filament to the capillary, distances from the detector were 6.3 and 14.3 cm. An additional second filament reduces errors as the distance between two filaments is easier to measure than that from the filament to the detection point since the exact position of the latter cannot always be precisely identified. 250 ms width heating pulses were controlled by the software written in-house using

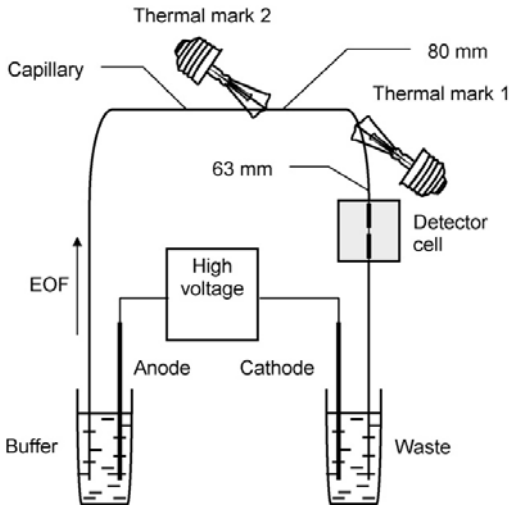

Fig. 1. A schematic of the instrument used for the measurement of EOF using the contactless conductivity detector with the thermal marks generated by tungsten filaments.

the LabVIEW programming language (National Instruments, Austin, TX, USA). An illustrative schematic of the CE system with an additional instrumentation to measure the EOF rate is depicted in Fig. 1.

2.3. Procedures

The BGEs with an IL additive concentration of 20 mM were prepared by dissolving the weighted amount of an ionic liquid in various organic solvents and then diluted to the necessary concentration. The dodecylbenzene peak served as a neutral marker in assessing the velocity of the EOF. For separation, the samples were prepared as solutions in acetonitrile (the solute concentration of 1 mg/L), diluted to need and then mixed.

In the beginning of each day the capillary was rinsed with 1 M NaOH (5 min) and water (1–2 min), dried in vacuum for 1–2 min and then thoroughly flushed with the separation buffer until the current was constant. The neutral marker and the samples were introduced hydrodynamically by lifting the sample reservoir with an anodic end of the capillary approximately 15 cm for 5 s.

After applying the high voltage, it took a few seconds for the current to become stable, therefore the first thermal marks were generated on the 10th second of the experiment. When the thermal marks had passed the detector, the heating pulses were repeated.

3. Results and discussion

3.1. Thermal marks in organic solvents

According to do Lago and co-workers the thermal marks are small concentration disturbances in BGE consisting of high- and low-concentration zones [13]. The marks detectable by the contactless conductivity detection are generated by short heating pulses using the tungsten filament. These marks move with the velocity of the EOF if the difference in concentration between low- and high-concentration zones is negligible. Therefore, heating voltage was chosen separately for each experiment aiming at obtaining the smallest possible, but still visible thermal marks. A 250 ms optimal width of heating pulses was chosen after few experiments. On the one hand, pulses shorter than 150 ms were not able to generate visible marks. On the other hand, pulses longer than 500 ms produced very wide marks. Besides, an AD converter used in the experiments was working at a 4 Hz rate. Therefore, 250 ms heating pulses were optimal which means that the duration of a heating pulse also matched the lowest AD conversion digitalization interval. So the converter and heating controlling relays could work synchronously which simplified the control program of the device.

The first series of experiments was performed using seven different organic solvents. In studying pure organic solvents the generation of visible thermal marks was in most cases impossible, although the EOF was always present as could be measured with a neutral marker. For instance, in a pure acetonitrile it was impossible to generate thermal marks, even when longer pulses and higher voltages were applied. Extreme heating conditions led to an anomalous behavior of the detector signal due to the temperature rise along the capillary. The only two solvents that were able to produce thermal marks in a pure solvent were formamide and *N*,*N*-dimethylformamide. The conductivity of formamide is one or two orders of magnitude superior to that of the other organic solvents used in this work. Formamide consists of a chain structure and ring-dimers chained together by hydrogen bonding, causing relatively high melting and boiling temperatures and high viscosity [31]. The formation of thermal marks in formamide could be explained by an uneven change of the velocity of these large agglomerates caused by the heating.

The use of 1-butyl-3-methylimidazolium trifluoroacetate ($[BMIm]^+[CF_3COO]^-$) as an additive in organic solvents increased the conductivity of BGEs and made the generation of visible thermal marks possible. Fig. 2 shows electropherograms of thermal marks generated in different organic solvents. The intensity of thermal marks is affected by the composition of the running electrolyte as well as the heating time and voltage. It is very difficult to control the amount of the heat generated and transferred from the tungsten filament to the running electrolyte inside the silica capillary. Therefore, the thermal marks generated by different tungsten filaments may have different intensities as the contact between the capillary and the filament is difficult to control. Though it is not an drawback, as both thermal marks are moving with a velocity close to that of the EOF calculated from the migration time of the neutral marker peak.

As can be seen from Fig. 2, thermal marks can be grouped into two classes by shape, though the exact shape of the marks depends on the properties of the running electrolyte. Generating thermal marks with a peak-valley shape, acetonitrile, ethanol, propylene carbonate and nitromethane, belong to one group. The other group of thermal marks consists of methanol, formamide and dimethyformamide with a valley-peak shape.

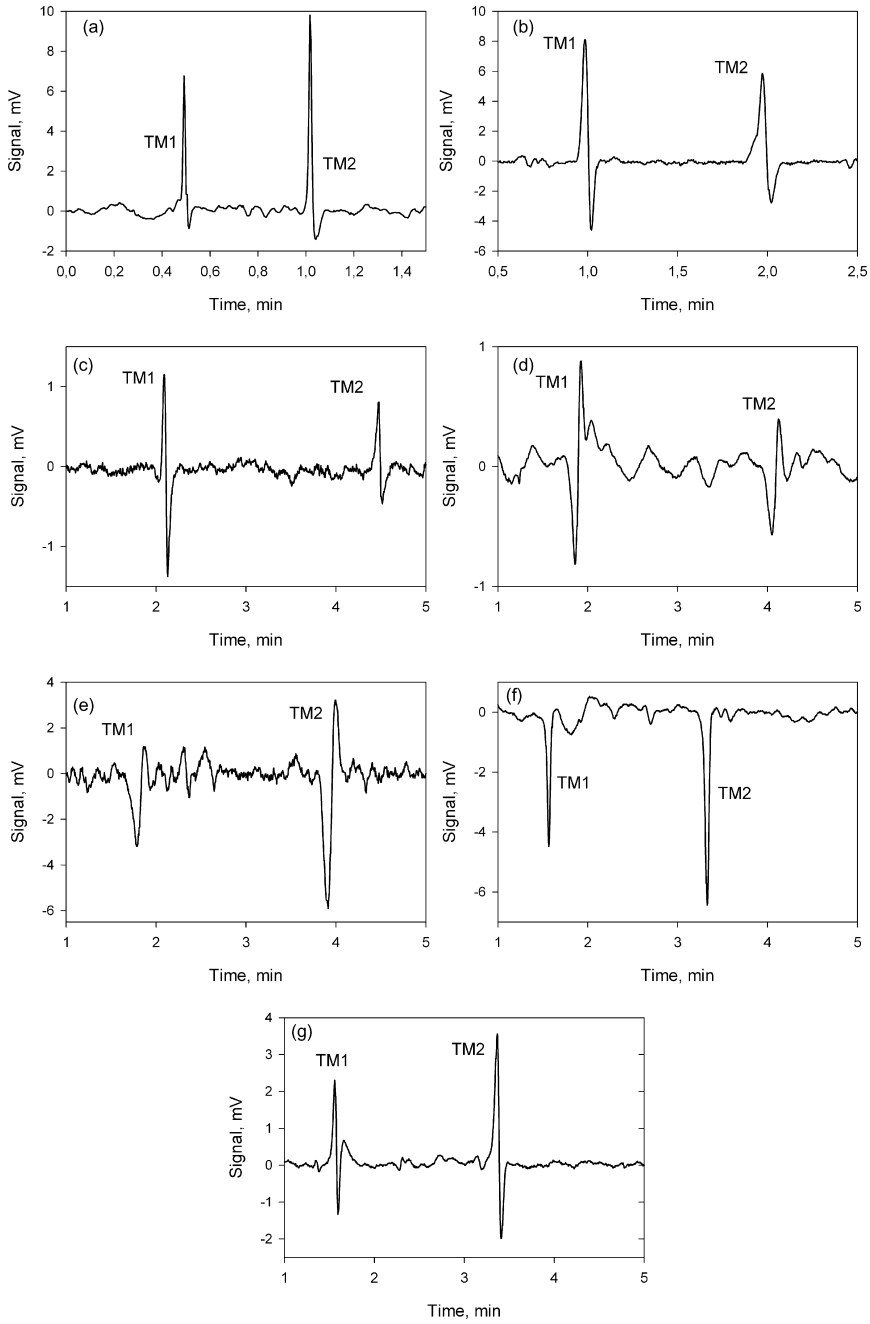

Fig. 2. Electropherograms of thermal marks formed in ionic liquid solutions ($[BMIm]^+[CF_3COO]^-$) in organic solvents. (a) Acetonitrile, (b) nitromethane, (c) ethanol, (d) methanol, (e) formamide, (f) DMF, and (g) propylene carbonate. The concentration of ionic liquid is 1 mM.

An explanation for the formation of the peak shape of thermal marks has been provided in Ref. [13] for aqueous buffers with NaCl and KCl additives. A simple explanation for the peak shape formation could be the following: due to the heating hot Na^+ ions move faster than that hot Cl^- ions, while hot K^+ ions move slower than hot Cl^- ions. The peak-valley shape of NaCl is formed when the hot and quickly migrating Na^+ ions while cooling down form a zone with a higher concentration. The low-

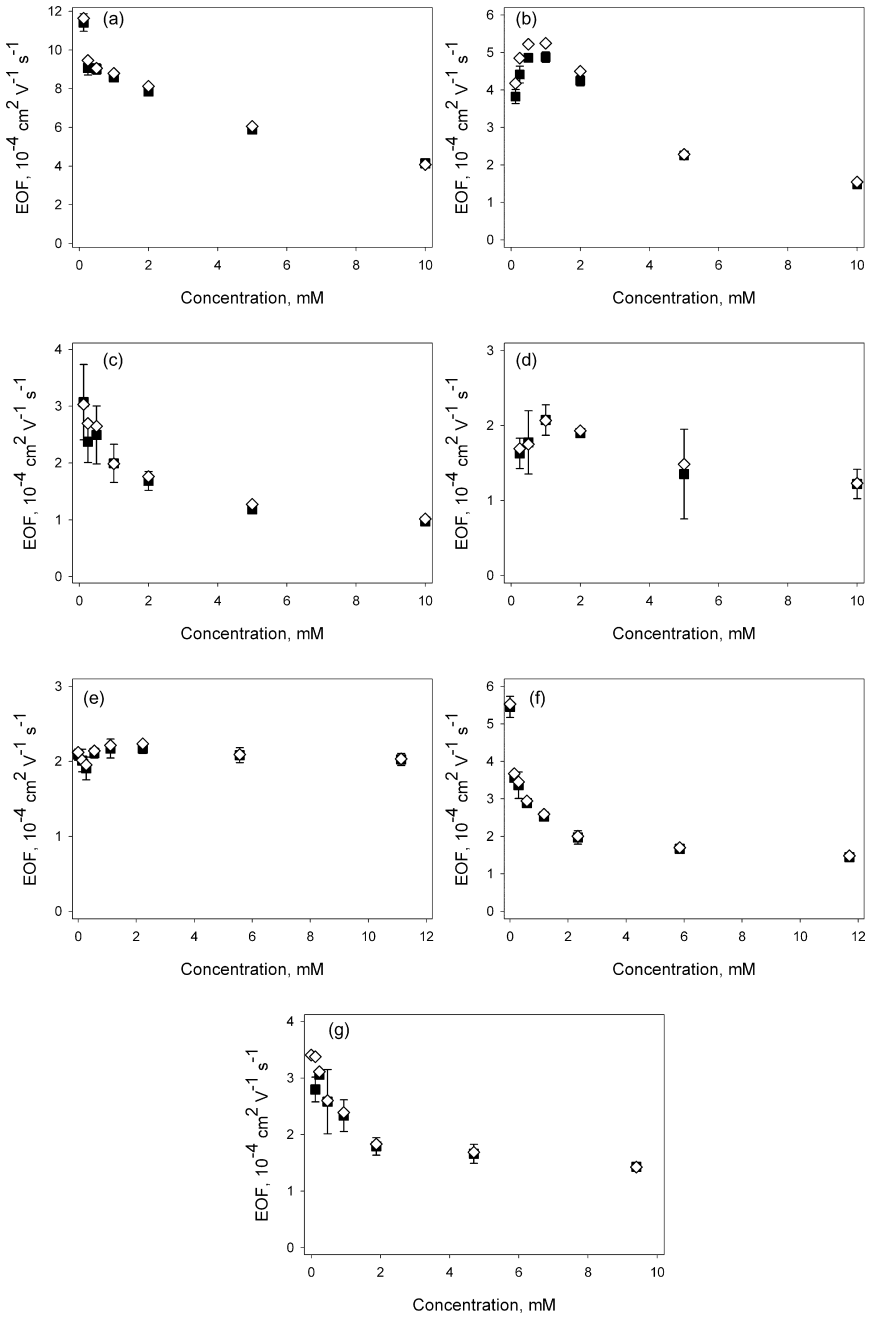

Fig. 3. EOF as a function of the concentration of the IL additive ($[BMIm]^+[CF_3COO]^-$) to the BGE. (a) Acetonitrile, (b) nitromethane, (c) ethanol, (d) methanol, (e) formamide, (f) *N*,*N*-dimethylformamide, (g) propylene carbonate, (◊) neutral marker, dodecylbenzene in BGE, and (■) thermal marks and 95% confidence error bars.

concentration zone of the diluted sodium is formed after the formation of the peak of Na^+. The principles of formation of the peaks of thermal marks in KCl are opposite. The same reasoning is apparently valid for an explanation for the formation of the peak shape of the thermal marks investigated in this work. In case of organic solvents the formation of the peak shape of thermal marks may be obviously influenced by the difference in mobility between the anionic and cationic parts of ILs, i.e. the

mobility of the ions vary with temperature. It is not completely understood yet what specifically influences the peak shape formation of a thermal mark. Moreover, these variations must be solvent dependant to account for the existence of the two types of thermal marks in different organic solvents.

Dimethyl sulfoxide does not fall into either class of solvents measured in this work. Apparently, the generation of visible thermal marks in DMSO was impossible even if the concentration of the IL additive was over 10 mM. Moreover, when a huge amount of KCl or KNO_3 was added to the DMSO thermal marks appeared neither. It has been reported in [13] that thermal marks may be obtained in 10 mM KCl in a DMSO solution only with a dibenzo-18-crown-6-ether additive.

3.2. Effect of an ionic liquid on EOF

The EOF in organic solvents is relatively fast. Its rate depends on the concentration of dialkylimidazolium-based room-temperature liquid organic salts used as electrolyte additives in CE. ILs are used as additives to the BGE to enhance the separation efficiency [26]. As reported in Ref. [32], the addition of ILs to organic solvents increases the conductivity and viscosity of the latter. Besides, using the contactless conductivity detection the conductivity of BGE influences the direction of the peaks on the electropherogram and the detection limit [33]. Therefore, the choice of an optimal concentration of the IL additive in the BGE is extremely important.

The dependence of the concentration of the IL additive on the rate of the EOF in seven different organic solvents was investigated. The EOF rate was measured using thermal marks. The results were compared to those obtained when the neutral marker dodecylbenzene was used. The results are presented in Fig. 3. During a single experiment the thermal marks were fired 4–5 times to gather information on the EOF rate before and after the detection of the neutral marker. No systematic differences in velocity between thermal marks fired before and after the detection of the neutral marker were observed.

Fig. 3 illustrates the influence of the concentration of IL on the velocity of EOF. Also, a comparison of the results obtained with the use of thermal marks with those obtained when using the neutral marker was made. Although it seems that the velocity of thermal marks is always slightly smaller than the velocity of neutral markers, this difference is not statistically significant as judged by 95% confidence error bars. Moreover, in most cases the plot of the average EOF rate measured using thermal marks versus that measured using the neutral marker method was linear ($R^2 > 0.995$). In case of formamide ($R^2 = 0.9555$), methanol ($R^2 = 0.9726$) and ethanol ($R^2 = 0.9752$) the linearity was less perfect. This result confirms a conclusion that the thermal mark is a reliable tool for estimating the rate of the EOF.

Except for formamide, the organic solvents under study can be classified into two groups according to the results illustrated in Fig. 3. The EOF rate of the first group increases with decreasing concentration of the IL additive. In case of a pure solvent, the rate of the EOF was the highest, when the neutral marker was used for its measurement. This is true for acetonitrile, ethanol, propylene carbonate and DMF. An increase in ionic strength caused by an IL additive reduces the ζ-potential of the capillary wall and, consequently, causes a reduction of the rate of the EOF. VanOrman et al. [34] have shown a linear relationship to exist between the EOF rate and the logarithm of the concentration of ideal electrolytes. The results obtained by the authors (Fig. 4) demonstrate a near linear relationship to exist between the two.

The graphs of the second group are almost the same. However, there is a maximum near the zero concentration of IL. The second group consists of methanol and nitromethane. In a certain way, these two types of graphs resemble the relationship between viscosity and conductivity on the one hand and the concentration of the IL additive reported in on the other [32].

Unexpectedly, the IL additive seems not to have any influence on the rate of the EOF in formamide. The EOF rate seems to be even slightly lower at a low concentration of IL, though all the values of the EOF rate are close to 2×10^{-4} cm^2 V^{-1} s^{-1}. The irregular behavior of formamide could have also been witnessed by observing the electric current in the capillary. Except for this solvent, we were not able to measure the electric current in pure organic solvents as it was below the smallest unit (1 μA) of the ammeter used. At the same time, the increasing concentration of the IL additive could raise the electric current up to 15–20 μA. Compared to the near zero electric current of other solvents, the electric current of pure formamide was about 20 μA and it was not affected by the concentration of IL. The lack of the influence of the IL additive could be explained by that in formamide IL exists as an ion pair. Formamide is not capable of destroying the ion-pairing between the cationic and anionic parts of IL and therefore, the IL concentration affects the rate of neither the EOF nor the electric current.

3.3. Application of thermal marks in separation experiment

The feasibility of using thermal marks to measure the rate of the EOF was demonstrated in the separation of benzoic acid

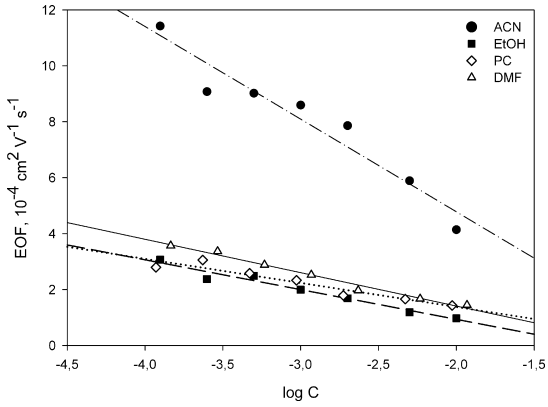

Fig. 4. An average EOF rate measured using thermal marks versus the logarithm of the concentration of the IL additive ($[BMIm]^+[CF_3COO]^-$). (●) Acetonitrile ($R^2 = 0.9228$), (■) ethanol ($R^2 = 0.9645$), (◇) propylene carbonate ($R^2 = 0.9174$), and (△) DMF ($R^2 = 0.9838$).

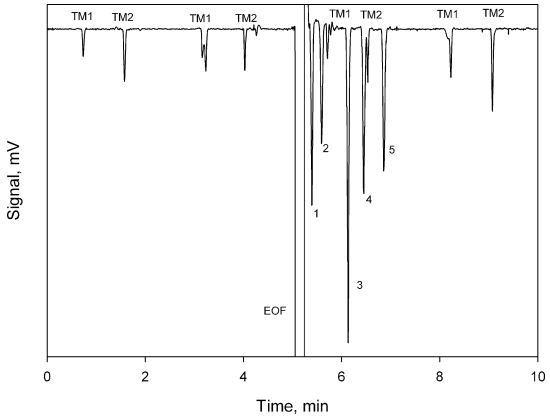

Fig. 5. Electropherograms of separation of the derivatives of benzoic acid coupled with EOF rate monitoring using thermal marks. Peak 1: *p*-aminobenzoic acid; 2: benzoic acid; 3: salicylic acid; 4: 3,5-dihydroxybenzoic acid; 5: 3,5-dinitrobenzoic acid; TM1 and TM2: thermal marks of the first and second filament. BGE is 5 mM $[BMIm]^+[CF_3COO]^-$ in acetonitrile, 60 μg/mL samples were prepared in pure acetonitrile. Applied voltage, 18.53 kV; hydrodynamic injection $h = 20$ cm for 5 s.

derivatives. A mixture of five substances was injected, while the EOF was monitored using thermal marks. Tungsten filaments were fired constantly at intervals of 150 s. Taking into account the width of thermal marks and their migration time, it is possible to fire filaments and measure the EOF rate more often than in traditional CE measurements. In our experiments a certain fixed interval was chosen to assure that there are thermal marks of only one heating pulse in the capillary at a time. The interval chosen allowed 4–7 EOF rate measurements to be made during one experiment.

Fig. 5 demonstrates the application of thermal marks in the separation of benzoic acid derivatives. For the BGE, the solution of a 5 mM $[BMIm]^+[CF_3COO]^-$ solution in ACN was chosen. During the experiment thermal marks were generated 4 times, but only 3 EOF rate values were used to calculate its average value $(5.82 \pm 0.18) \times 10^{-4}$ cm^2 V^{-1} s^{-1} as the second thermal mark of the third pair is partially overlapped by the analyte peak. Though, the EOF rate could be calculated from only one thermal mark as the distance from the filament to the detection point is also known. The reproducibility of thermal marks of one experiment is excellent as the relative standard deviation (RSD) of the calculated EOF rate value is less than 1.3%. The separation shown in Fig. 5 was repeated 6 times. The repeatability of the rate of the EOF calculated using the neutral marker and thermal marks during the series of experiments was nearly the same (RSD = 1.3%). The repeatability of peak migration times was in the range of 1.0–2.2% and slightly higher for the effective mobility (1.0–6.1%).

The huge EOF peak of a pure ACN has almost overlapped the first analyte peak of *p*-aminobenzoic acid. This demonstrates one important advantage of thermal marks over the neutral marker. When a real sample of the neutral marker is injected into the capillary, it is difficult to predict the size of the peak. The peak of the neutral marker very likely overlaps the analyte peaks that migrate at the velocity close to that of the EOF. Besides, the neutral marker may be injected only once at the beginning of the experiment, while thermal marks could be used at any moment of the experiment.

4. Conclusions

Thermal marks are disturbances in the concentration profile of the BGE generated as two components of the latter to obtain different velocities during heating. After having been cooled down these disturbances travel with the EOF to the detector and may be registered by a contactless conductivity detector. This work demonstrates the potential use of a new and practical method for monitoring the rate of the EOF in non-aqueous media using thermal marks. A rather simple device makes it easy to apply the thermal marks method to various kinds of CE systems using the contactless conductivity detection. Although the size of thermal marks is difficult to control, the EOF rates calculated were indicative of an excellent reproducibility and fair repeatability of the method. Moreover, it was demonstrated that the rate of the EOF measured traditionally, i.e. by using a neutral marker, is similar to that measured by using thermal marks. Therefore, the thermal marks may be used to index electropherograms and identify the analyte peaks. The thermal marks may be generated in a pure organic solvent in a small number of cases only. Fortunately this is not a significant drawback as in NACE pure organic solvents are rarely used without electrolytic additives since the latter modify the ionic strength and afford a proper separation efficiency. In the present case, the IL additive makes the use of thermal marks in most organic solvents possible as the marks are formed at different velocities of the hot cationic and anionic components of IL.

Acknowledgement

This work was supported by the Estonian Science Foundation, Grant nos. 6166.

References

[1] K.D. Lukacs, J.W. Jorgensen, J. High Resolut. Chromatogr. Chromatogr. Commun. 8 (1985) 407.
[2] X. Huang, M.J. Gordon, R.N. Zare, Anal. Chem. 60 (1988) 1837.
[3] K. Kenndler-Blachkolm, I. Popelka, B. Gaš, E. Kenndler, J. Chromatogr. A 734 (1996) 351.
[4] P. Azelova, V. Kašička, D. Koval, Z. Prusik, S. Fanali, Z. Aturki, Electrophoresis 28 (2007) 756.
[5] S.V. Ermakov, L. Capelli, P.G. Righetti, J. Chromatogr. A 744 (1996) 55.
[6] A.A.A.M. Van der Goor, F.M. Everaerts, J. Chromatogr. 470 (1989) 95.
[7] S. Arulanandam, D. Li, J. Colloid Interface Sci. 225 (2000) 421.
[8] J.L. Pittman, C.S. Henry, S.D. Gilman, Anal. Chem. 75 (2003) 361.
[9] J. Gaudioso, G.H. Craighead, J. Chromatogr. A 971 (2002) 249.
[10] T.T. Lee, R. Dadoo, R.N. Zare, Anal. Chem. 66 (1994) 2694.
[11] K.F. Schrum, J.M. Lancaster III, S.E. Johnston, S.D. Gilman, Anal. Chem. 72 (2000) 4317.
[12] J.L. Pittman, K.F. Schrum, S.D. Gilman, Analyst 126 (2001) 1240.
[13] R.M. Saito, C.A. Neves, F.S. Lopes, L. Blanes, J.G.A. Brito-Neto, C.L. do Lago, Anal. Chem. 79 (2007) 215.
[14] F. Steiner, M. Hassel, Electrophoresis 21 (2000) 3994.
[15] H. Salimi-Moosavi, R.M. Cassidy, Anal. Chem. 68 (1996) 293.

[16] Q. Yang, L.M. Benson, K.L. Johnson, S. Naylor, J. Biochem. Biophys. Methods 38 (1999) 103.
[17] G.K.E. Scriba, J. Chromatogr. A 1159 (2007) 28.
[18] A.M. Stalcup, B. Cabovska, J. Liq, Chromatogr. Relat. Technol. 27 (2004) 1443.
[19] M.J. Markuszewski, P. Stepnowski, M.P. Marszall, Electrophoresis 25 (2004) 3450.
[20] J.F. Liu, J.A. Jonsson, G.B. Jiang, TrAC 24 (2005) 20.
[21] G.A. Baker, S.N. Baker, S. Pandey, F.V. Bright, Analyst 130 (2005) 800.
[22] M. Koel, Crit. Rev. Anal. Chem. 35 (2005) 177.
[23] S. Pandey, Anal. Chim. Acta 556 (2006) 38.
[24] J.L. Anderson, D.W. Armstrong, G.T. Wei, Anal. Chem. 78 (2006) 2892.
[25] M.P. Marszall, R. Kaliszan, Crit. Rev. Anal. Chem. 37 (2007) 127.
[26] M. Vaher, M. Koel, M. Kaljurand, J. Chromatogr. A 979 (2002) 27.
[27] M. Vaher, M. Koel, M. Kaljurand, Chromatographia 53 (2001) S302.
[28] J.A.F. da Silva, C.L. do Lago, Anal. Chem. 70 (1998) 4339.
[29] A.J. Zemann, E. Schnell, D. Volgger, G.K. Bonn, Anal. Chem. 70 (1998) 563.
[30] K. Mayrhofer, A.J. Zemann, E. Schnell, G.K. Bonn, Anal. Chem. 71 (1999) 3828.
[31] K. Izutsu, Electrochemistry in Nonaqueous Solutions, Wiley–VCH, Weinheim, 2002, p. 17.
[32] Y. François, K. Zhang, A. Varenne, P. Gareil, Anal. Chim. Acta 562 (2006) 164.
[33] M. Borissova, J. Gorbatšova, A. Ebber, M. Kaljurand, M. Koel, M. Vaher, Electrophoresis 28 (2007) 3600.
[34] B.B. VanOrman, G.G. Liversidge, G.L. McIntire, T.M. Olefirowicz, A.G. Ewing, J. Microcolumn Sep. 2 (1990) 176.

Publication V

Seiman, A., Vaher, M., Kaljurand, M, Thermal marks as signal processing aid for portable capillary electropherograph, *Electrophoresis* **2011**, *DOI:10.1002/elps.20100057*

Andrus Seiman
Merike Vaher
Mihkel Kaljurand

Department of Chemistry, Tallinn University of Technology, Tallinn, Estonia

Received October 29, 2010
Revised December 2, 2010
Accepted December 13, 2010

Research Article

Thermal marks as a signal processing aid for a portable capillary electropherograph

The interpretation of raw signals in capillary CE can be challenging if there are unknown peaks, or the signal is corrupt due to baseline fluctuations, EOF velocity drift, etc. Signal processing could be required before results can be interpreted. A suite of signal processing algorithms has been developed for CE data analysis, specifically for use in field experiments for the detection of nerve agents using portable CE instruments. Everything from baseline correction and electropherogram alignment to peak matching and identification is included in these programs. Baseline correction is achieved by interpolating a new baseline according to points found using all local extremes, by applying an appropriate outliers test. Irreproducible migration times are corrected by compensating for EOF drift, measured with the aid of thermal marks. Thermal marks are small disturbances in the capillary created by punctual heating that move with the velocity of EOF. Peaks in the sample electropherogram are identified using a fuzzy matching algorithm, by comparing peaks from the sample electropherogram to peaks from a reference electropherogram.

Keywords:
Baseline correction / Fuzzy matching / Peak matching / Signal alignment / Thermal marks
DOI 10.1002/elps.201000572

1 Introduction

Capillary CE has been considered a powerful separation technique since it was first introduced nearly three decades ago. Despite extremely small sample consumption, high separation efficiency, short analysis times, and other advantages in comparison with liquid chromatography, CE as a technique has not lived up to initial expectations. The two main reasons for this are low sensitivity, due to the small sample volumes required, and low reproducibility, both in terms of migration times and peak areas. Although a significant amount of research has been dedicated to these technical problems, overcoming the inherent low sensitivity of CE has been difficult. Sample stacking [1] and other sample pre-concentration techniques, as well as the use of more sensitive detectors (e.g. LIF detectors) are common ways to improve sensitivity. In addition, numerous ''unconventional'' attempts to improve sensitivity have been reported, such as increasing the optical path length (e.g. with the aid of bubble- [2] or Z-shaped [3] detector cells) and incorporating multiplex signal processing (e.g. cross-correlation CE [4–6] or Hadamard transform CE [7, 8], both of which measure several signals simultaneously, yielding an electropherogram with improved signal-to-noise).

For analyses conducted under laboratory conditions, where there is ample time for testing and optimization, reproducibility problems might not be an issue. However, to use CE in point-of-care testing and in field analysis, where fast and accurate decisions are required, CE's reproducibility problems must be corrected. Upgraded instruments, with enhanced robustness, could possibly solve these reproducibility problems, improving the reliability of results. However, such new instrumentation would require significant technological innovations that, currently, could be extremely costly. Alternatively, increased reliability of the results could be achieved with proper signal processing.

Problems with reproducibility are due mainly to irreproducible peak areas and migration times. This affects both quantitative and qualitative analysis, as concentrations are usually calculated using peak areas and analyte species are often identified according to their migration times or electrophoretic mobilities. Although poor integration algorithms can also contribute to quantification errors [9], the low reproducibility of peak areas is mainly caused by imprecise sampling. While the reproducibility of quantitative analysis can be controlled by the use of very precise injection procedures, in practice it is often more convenient to use internal standards for correction purposes [10].

Correspondence: Andrus Seiman, Department of Chemistry, Tallinn University of Technology, Akadeemia tee 15, 12618 Tallinn, Estonia
E-mail: andrusseiman@gmail.com
Fax: +372-620-2828

Abbreviations: COW, correlation optimized warping; **C^4D,** capacitively coupled contactless conductivity detector; **EMPA,** ethyl methylphosphonic acid; **HV,** high voltage; **MPA,** methylphosphonic acid

The need for improved signal processing has long been recognized by separation scientists. Various signal processing algorithms have been developed since the early days of chromatography [11]. Although commercial instruments are provided with algorithm packages for signal processing and peak integration, the software provided by CE instrument manufacturers is not adequate for fixing electroosmotic flow (EOF) drift or proper baseline correction. In this work, a suite of signal processing algorithms has been developed with the overall aim of improving the reliability of CE results and simplifying the interpretation of electropherograms. Although these algorithms were developed specifically for use with a portable CE analyzer for the analysis of nerve agents, in principle they are universal and could be easily applied to any type of CE analysis. The algorithms presented in this work cover every step of basic data acquisition from baseline correction, which is needed for precise peak area integration, to peak detection and integration. Additionally, algorithms for the comparison of two electropherograms have been added to allow comparison of sample signals with reference electropherograms for the identification of matching peaks. The idea behind the whole suite of algorithms is to give quick answers to the question of what kind of nerve agent (if any) is contained in a sample. The use of such algorithms should enable non-qualified personnel to run the analysis, even if they do not have enough experience to make crucial decisions. Although various commercial signal processing software packages have many very powerful options, they were found not to be suitable for portable CE instruments developed especially for field experiments, where signal processing should be as automated as possible.

Noise and baseline drift are two common problems in analytical chemistry, as both can lead to reduced precision and accuracy. Noise, a high-frequency signal usually associated with the electronic components of the instrumental set up, in most cases can be removed by applying moving average filtering, exponential smoothing, Savitzky-Golay filtering, Fourier or wavelet transforms. Baseline drift, on the other hand, is low frequency noise usually resulting from temperature variations during a separation, or the presence of impurities in the composition of the background electrolyte (BGE). Baseline drift is a common problem not only in separation science but also in spectroscopy. Approximation of the correct baseline is the most common method for overcoming baseline drift problems. To calculate peak areas or peak heights, most integration algorithms simply use a straight baseline, drawn from the start of the peak to the end. As such, calculations will lead to errors when the real baseline does not coincide with this straight line. Thus, for more reliable results, the baseline needs to be corrected before peak integration can be conducted. To date, reports in the literature have proposed several methods of baseline correction including the following: multi-pass moving averages [12], cubic smoothing splines with multi-variate data analysis [13], improved iterative polynomial fitting [14], and wavelet analysis [15–17]. Wätzig [18] has developed an algorithm that considers all local maxima as potential baseline points. Of course, some of these maxima are actually located at peak maxima, and these points are subsequently removed using a secondary outlier elimination test.

Reliable peak identification and precise integration are as important as baseline correction for accurate quantification. A simple option for automated peak detection is selecting the part of a signal that exceeds a certain threshold. Although this approach is very sensitive to baseline fluctuations, it can be very effective and extremely fast if the baseline is properly removed. However, the separation capabilities of CE are limited, and baseline separation between peaks is often not achievable. Thus, threshold-based peak detection does not appear to be capable of deconvoluting how many components are present in a particular peak. Therefore, more advanced peak detection techniques are preferred. Algorithms that use a second or sometimes even a third derivative are capable of evaluating properly the actual number of peaks [19]. In addition, for the determination of exact peak boundaries, there is an algorithm that expands the initial boundaries by one data point at a time to the left or the right [20], resulting in an increase in peak area. The process stops when the resulting increase is smaller than a threshold, which is set as the standard deviation of the baseline noise. When used together with a smoothing spline function baseline correction algorithm, RSD was reduced by roughly 50%.

For historical reasons, comparison of electrophoretic mobilities calculated according to migration times has been the most widely used approach for qualitative analysis. Only lately, with the development of fast scanning diode array detectors, has it become possible to use spectral data for identification purposes. When using electrophoretic mobilities for identification, it is essential to ensure the reproducibility of migration times. Shifts in migration times are a commonly observed problem in CE. For a good reproducibility, a number of parameters must be precisely controlled including temperature [21] and pre-treatment of the inner capillary surface [8]. Nevertheless, adsorption of analytes on the inner surface of the separation capillary may heavily affect migration times and could lead to faulty identification of unknown species.

Dynamic time warping (DTW) [22, 23] and correlation optimized warping (COW) [22, 24] are two algorithms that have shown great potential for alignment correction of various signals in spectroscopy and chromatographic techniques. Therefore, these algorithms should also be suitable for improving the alignment of different electropherograms. Although dynamic time warping is sensitive to differences in peak intensities, COW is considered to be better because it is assumed to preserve peak areas and shapes. However, in situations with significant changes in peak shape (e.g. severe peak tailing), COW algorithms face problems [25]. Alternatively, CE-specific alignment techniques could be used for standardization, for example, by replacing the

time axis with an electrophoretic mobility axis [26], or by normalization of migration times with the aid of two identified peaks [27].

In this study, we demonstrate the use of thermal marks to determine changes in EOF during an experiment, and we show how this data can be used for normalization of electropherograms. Thermal marks are small disturbances in the detector signal produced by punctual heating of the separation capillary, which move with nearly the same velocity as EOF, and therefore can be used for monitoring EOF [28, 29]. Heating causes changes in the electrophoretic mobility of BGE components. As these changes are not equal for different BGE components, a concentration-dependent disturbance is formed. Inhomogeneity zones created by thermal marks move through the capillary. Ideally, they would have effective mobility equal to EOF. However, the problem of moving concentration boundaries is slightly more complicated. Behavior of concentration boundaries created by thermal marks could be explained by the system zones theory [30]. As it is possible to observe difference between the migration of a neutral marker and migration of actual EOF [31], therefore, the difference between the mobilities of thermal marks and EOF is also possible.

However, it has been demonstrated that thermal marks is moving with the velocity of EOF if the concentration difference between thermal mark and BGE is low [27].

Thermal marks can be monitored by conductivity detection or indirectly using UV or LIF. Thermal marks are usually produced somewhere in between the sample inlet and the detector. Therefore, thermal marks have relatively smaller migration times than most sample components. Moreover, thermal marks can be produced several times during a single run, as there is no need for high-voltage interruptions like in the case of conventional sample injections. Thus, it is feasible to monitor EOF during a run with the aid of thermal marks.

2 Materials and methods

2.1 Apparatus

CE experiments were carried out using a portable CE instrument equipped with a capacitively coupled contactless conductivity detector (C^4D). This particular CE instrument was built in our laboratory as previously described [32]. Briefly, the CE instrument has dimensions of $330 \times 180 \times 130$ mm and consists of a C^4D detector, a high-voltage power (HV) supply, and a data acquisition part with a 16-bit analog-to-digital converter. The system runs on batteries and is capable of performing CE experiments for at least 4 h. A limiting factor appears to be the HV power supply (EMCO DX250NR, EMCO High Voltage Corporation, Sutter Creek, CA, USA) because the detector could be easily operated for a minimum of 8 h during data acquisition without HV.

The detector cell design is similar to that of commercially available C^4D detectors. Two tubular electrodes 8 mm in length are located in a rectangular detector cell made of aluminium. One electrode is excited by a sine wave 60 V in amplitude, peak-to-peak, and a controlled frequency ranging from 50 to 300 kHz. The second electrode picks up and amplifies the signal after it has passed the capillary walls and the liquid in the capillary. All detector parameters are controlled by a computer. In this work, all experiments were carried out with the detector oscillation frequency set to 200 kHz.

Thermal marks were generated using a heating coil constructed of stainless steel wire (od 100 μm), wrapped five times around the separation capillary. A general DC power supply was used for heating purposes. Computer controlled relays (ADAM 4060 module, Advantech, Taipei, Taiwan) were used for switching the heating on and off. Relays were controlled using custom software written in the Matlab environment (The Math Works, Natick, MA, USA). Precise parameters used for generating thermal marks were 20 V and 0.5 s. Parameters were chosen so that the resulting thermal marks would have the maximum possible amplitude. There appears to be a limit to the amount of thermal energy that can be transferred from the heating coil to the capillary without damaging the solution inside of the capillary, and even slightly higher heating voltages or heating periods longer than 1 s will ruin the experiment. Attempts to produce more intensive thermal marks resulted in a drop in electric current and detector signal, and indicate a failed experiment.

CE experiments were carried out in a fused-silica capillary (internal diameter 75 μm and outer diameter 360 μm) (Polymicro Technologies, Phoenix, AZ, USA) with a full length of 55 cm and an effective length of 32 cm. The heating coil for generating the thermal marks was located 8.2 cm from the detector. Because the distance that the thermal marks have to cover is much smaller than the effective length of the separation capillary covered by each sample component, it is possible to produce several thermal marks both before and after the analyte peaks reach the detector.

2.2 Materials and reagents

For separation experiments, a mixture of some harmless degradation products of organophosphorus nerve agents were chosen, as the portable CE instrument used in this experiment was developed for the analysis of nerve agents. Three phosphonic acids – methylphosphonic acid (MPA), ethyl MPA (EMPA), and 1-butylphosphonic acid (1-BPA) were purchased from Alfa Aesar, Lancaster Synthesis (Windham, NH, USA). Two other components of the sample mixture – propylphosphonic acid (PPA) and pinacolyl MPA (PMPA) – were purchased from Sigma-Aldrich (Steinheim, Germany).

L-Histidine (His) and 2-(*N*-morpholino)ethanesulfonic acid hydrate (MES) were purchased from Merck (Darmstadt, Germany). For the separation, a 15-mM mixture of MES and His was used. This mixture is a very common BGE for C^4D-CE experiments due to its low conductivity and adequate ionic strength. The BGE for CE analysis was prepared by dissolving an exact amount of His and MES in MilliQ purity water.

3 Results and discussion

3.1 Baseline correction

In addition to common problems such as constant drift, problematic baselines might be due to other baseline disturbances described by various amplitude directions or speeds. Proper baseline correction algorithms should be able to deal equally efficiently with these various baseline disturbances. Because the velocity and direction of baseline drift can also vary during a CE experiment, the baseline algorithm developed in this study considers only a small part of the baseline at a time. In general, the baseline correction algorithm we propose here is developed from the algorithm that tries to mimic human judgment [17]. Specifically, the algorithm considers all local maximums as potential points of the baseline. Subsequently, a series of outlier test algorithms discards points corresponding to peak maxima.

Several small but significant improvements have been added to this baseline correction algorithm. Most importantly, the outliers test algorithm considers only one point at a time and compares it only to neighboring local extremes. Because of this small improvement, our proposed baseline correction algorithm is not sensitive to changes in baseline drift speed or direction. A demonstration of this baseline correction algorithm is shown in Fig. 1.

The following is a step-by-step description of how the baseline correction algorithm works. First, the algorithm locates all local minima and maxima. Due to detector noise, most of these minima and maxima are actually located on the baseline, in addition to the tops of positive and negative peaks.

Second, the algorithm uses a simple outlier test to figure out which of the points are actually located on the baseline. The algorithm is developed to check one point at a time by comparing it with a certain number of potential baseline points located before and after the particular point. Basically, the baseline correction algorithm fits a straight line to these points and calculates confidence intervals according to the coordinates of the test point and a certain number of points located around the test point. Probability levels can be set by the operator to suit particular experimental data. If the point under evaluation is located between the confidence intervals, it is considered to be a point located on the baseline. When a point is located outside of the confidence intervals, the point is discarded and not used for testing other potential baseline points. Specific outlier tests have been described in Fig. 1B and C. In experiments, this very simple outlier test has proven to be a very fast and efficient way to determine true baseline points from points located at the tops of peaks. Although the algorithm is not capable of testing the few points in the beginning and at the end of the detector signal, this is not a major drawback as

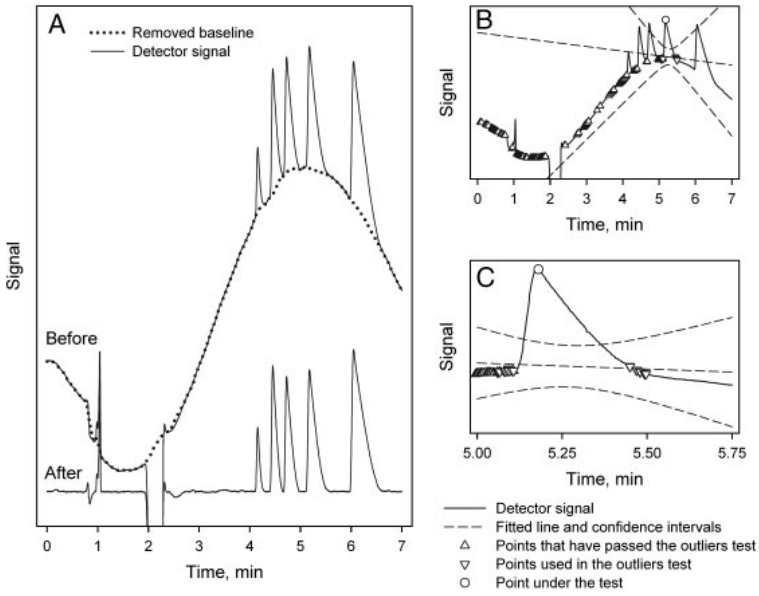

Figure 1. Baseline correction algorithm. (A) Electropherogram before and after baseline correction, along with the removed baseline. (B and C) Outliers test in the baseline correction algorithm. ○ – tested point; ∇ – points used in the outliers test; Δ – points that have passed the outliers test and are considered to be points located in the baseline; dashed lines belong to the straight line fitted through the points and to the confidence intervals used in the outliers test.

there are no peaks in the beginning of the experiment, and at the end it is possible to record additional data after the migration of the last peak.

Finally, after discarding all unsuitable points, a new baseline is calculated by interpolation of the remaining points that have passed the outliers test over the whole length of the time axis. Various interpolation algorithms can be chosen to better suite the particular data. In the experiments reported in this study, cubic spline interpolation was used.

A good baseline correction algorithm must satisfy certain requirements. Basically, such algorithms must remove all baseline drift without affecting the size and shape of the peaks, and do so in a period of time as short as possible. The baseline algorithm developed here requires two input parameters: a probability level and the number of points used in the outliers test. Optimization of the input parameters was done experimentally. For this purpose, several electropherograms were constructed with various artificial baseline disturbances. Functions used for baseline drift generation were linear, cubic, sinus, and sinus with increased frequency. In addition to these functions, a signal with no baseline drift and a signal with baseline drift modeled after real experimental data were used.

The algorithm was applied to the generated electropherograms while the input parameters were varied. The performance of the algorithm was evaluated by comparing two values. First, the difference between the original baseline drift and the new baseline calculated by the algorithm describes the efficiency of baseline drift removal. Second, peak areas after baseline correction were compared with original peak areas. Varying the number of the points used in the outliers test revealed that if this parameter value is too small, the algorithm will consider peaks to be part of the baseline and will remove them, resulting in the loss of analytical information. On the other hand, if the value is too high, the algorithm is no longer capable of removing baseline noise. For the experimental data tested here, an optimal parameter value 17 points before and after the particular evaluated point for a total of 35 points in each outliers test (Fig. 2). Optimal probability level for outliers test was found to be 95%.

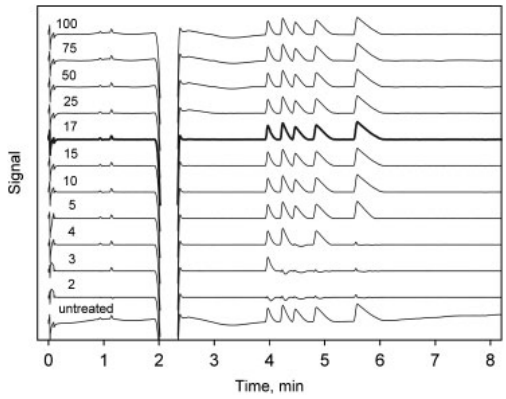

Figure 2. Performance of the baseline correction algorithm. The baseline correction algorithm depends on the number of points used in the outliers test before and after a particular test point. Baseline drift is modeled according to the experimental data. Bold line – baseline correction using an optimal number of points; 17 points before and after the test point, i.e. 35 points in total were found to be the most effective in the tests. Experimental conditions: BGE 15 mM MES/His; separation voltage 18 kV; sample peaks from left to right to PMPA, BPA, PPA, EMPA, and MPA. Sample concentration is 100 μM.

3.2 Alignment of electropherograms

In addition to baseline drift, the irreproducibility of migration times is a very common problem in CE analysis. Various factors such as temperature control, pre-treatment of the inner capillary surface before and during the analysis, ionic strength dependent variable stacking of the sample matrix, etc. could affect migration times. Common approaches for dealing with signal alignment in general are not really suitable for CE analysis because these algorithms simply shift data points to minimize the difference between the two signals and do not take into consideration CE-specific facts. For example, in CE, peaks that migrate longer are more affected by drift of EOF velocity. Other approaches, developed specifically for CE, usually treat signals as if the EOF velocity is constant during an experiment and try to fix differences between the two signals by some specific method. Although in general EOF velocity can be considered to be constant during one experimental run, in some rare occasions EOF velocity can shift during a run, for example, due to the adsorption of some analyte to the inner surface of the capillary wall.

Here, we present a method for aligning several electropherograms, which also takes into account EOF velocity drift during a run. EOF velocity was monitored with the aid of thermal marks [27, 28] generated using a heating coil. As the generation of thermal marks takes place very close to the detection point compared to the sample inlet, it is possible to produce and monitor several thermal marks during one run as their migration time is much shorter compared to the migration times of sample analytes. Thus, it is possible to collect sufficient data points with precise data on the EOF velocity to construct an approximation of the exact changes in EOF mobility during an experimental run.

In experiments performed in this study, a spline function was used to fit a curve to the collected data. A spline function was preferred to linear interpolation because its smoother results may correspond slightly better to real-life situations. After an estimate of the EOF mobility drift has been calculated (dash dot line, Fig. 3), it is relatively easy to use an electrophoretic mobility equation to calculate a new time axis for the electropherogram where EOF velocity is held constant (dotted line, Fig. 3). To calculate a new time axis, first the electrophoretic mobilities corresponding to

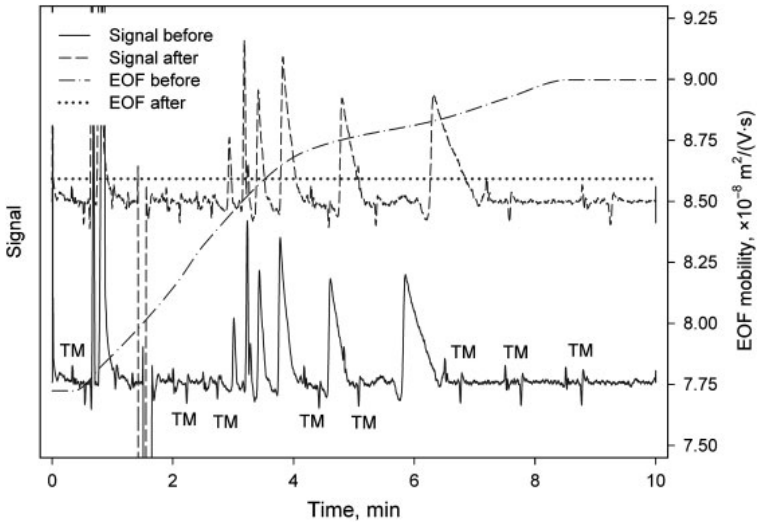

Figure 3. Electropherogram before and after EOF mobility drift has been corrected, using data obtained with the aid of thermal marks. TM – location of the thermal marks. The dash dotted line is an estimate of EOF mobility changes during the experiment, calculated using thermal mark migration times. EOF mobility after the corrections is constant (dotted line). The solid line and dashed line correspond to the detector signal before and after EOF mobility correction. Corrections have been performed using the electrophoretic mobility equation. Corrections were conducted by calculating a new time axis, while the electrophoretic mobility corresponding to a particular point is kept constant.

every single point in the electropherogram are determined using the estimated EOF mobilities. While keeping the electrophoretic mobilities of each point constant, it is then straightforward to calculate new values for the time axis using a constant value for EOF mobility. In the example provided in Fig. 3, an average EOF mobility value was used as a new constant value for EOF mobility. If the experimentally recorded detector signal (solid line, Fig. 3) is compared to the resulting corrected detector signal (dashed line, Fig. 3), it is apparent that the first peaks are shifted forward because the corrected EOF value (as monitored with the aid of thermal marks) is higher than the original EOF value. On the contrary, last peaks are shifted backwards as here the corrected EOF values are lower than the original values, and therefore anionic compounds migrate slower.

After EOF drift is corrected, several electropherograms can be aligned, simply by recalculating the time axis according to the new EOF value, using the same electrophoretic mobility equation. Figure 4 demonstrates the efficiency of the signal alignment, using data obtained by monitoring EOF with the aid of thermal marks. Extreme differences in migration times can easily cause major misinterpretations in electropherograms. Figure 4A and C demonstrates the efficiency of electropherogram alignment with the aid of thermal marks. These two figures correspond to the same pair of electropherograms before and after signal alignment. Migration times before alignment are shifted, although it is still possible to tell it is the same sample by the number and size of the peaks.

In situations where there is no independent technique available for acquiring additional information, migration times provide the only information that can be used for the identification of unknown species. Nerve agent analysis using C^4D-CE relies on the detection of degradation products that are specific for every nerve agent. For the nerve agent VX, the specific degradation product is EMPA. By simply comparing the untreated signal of EMPA (Fig. 4B, solid line) to standard mixture of various nerve agent degradation products (dashed line), it is impossible to identify EMPA without any additional information. In extreme cases, precise identification cannot be confirmed without proper signal alignment. After alignment (Fig. 4D), it is not difficult to identify the peak corresponding to EMPA.

3.3 Peak matching

Comparison of unknown peaks from a sample electropherogram with reference peaks from standard substances is still the most widely used method for peak identification. Although the comparison of two electropherograms is simple for an experienced researcher, and is usually performed manually, this process could also be automated by applying the proper computer algorithm. However, in situations where the number of electropherograms to be compared is very high, when CE is to be used for monitoring purposes, or when personnel operating the instruments are not experienced, peak matching algorithms would be beneficial.

All of the algorithms described in this work have been developed for use with portable CE instruments for the determination of specific compounds of interest, such as nerve agents, environmental pollutants, etc. Peak identification is achieved by matching peaks in a sample with reference electropherograms. Peak identification is based on the same principles of the fuzzy matching algorithm developed for chromatogram warping by Walczak and Wu [33].

According to fuzzy sets theory, membership of a given element to a set of interest is described by a continuous

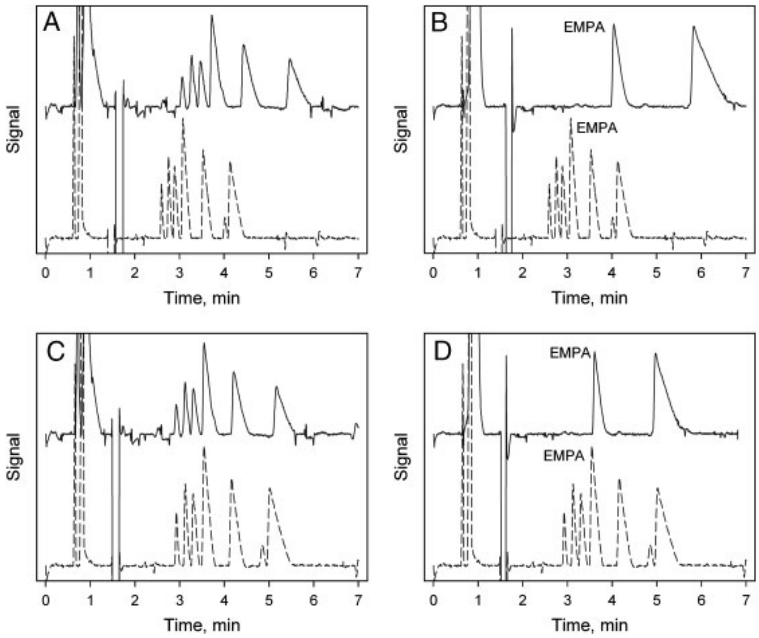

Figure 4. Two examples of the signal alignment with the aid of thermal marks. (A and B) Uncorrected electropherograms; (C and D) the same pairs of electropherograms after alignment using thermal marks. Solid line – sample electropherogram; dashed line – reference electropherogram. Peaks from left to right: PMPA, BPA, PPA, EMPA, MPA, and salicylic acid. In example B, notice how the migration times of EMPA differ before and after alignment. This could potentially lead to identification errors. After signal alignment has been performed (example D), peaks of EMPA in both electropherograms have similar migration times and should be identified without any problems.

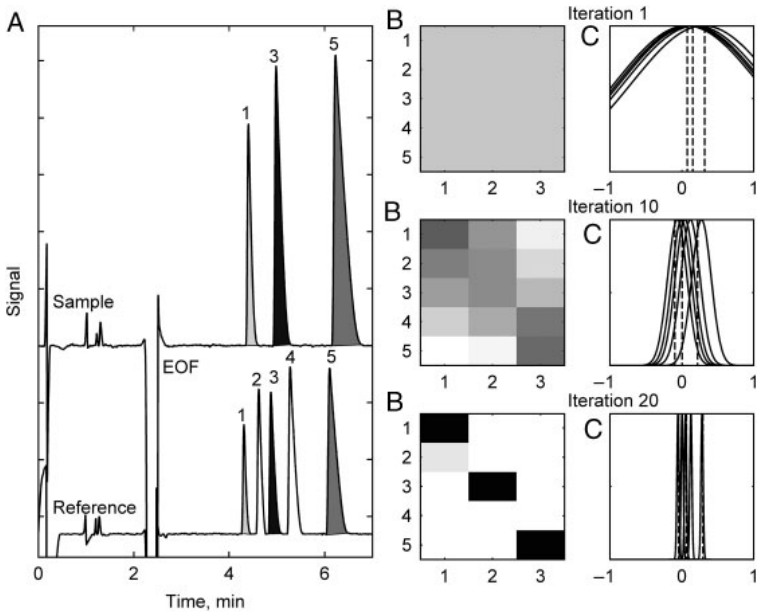

Figure 5. Automatic peak matching between sample and reference electropherograms, using migration times and a fuzzy matching algorithm. (A) Matched peaks in the sample and reference electropherograms. Peaks 1–5 correspond to PMPA, BPA, PPA, EMPA, and MPA. Separation conditions are as follows: sample concentration 100 μM; BGE 15 mM MES/His; separation voltage 18 kV. (B) Similarity matrix, rows correspond to 5 peaks from the reference electropherogram; 3 columns correspond to 3 peaks from the sample electropherogram. Darker colors correspond to higher similarity. (C) Fuzzy peak matching, 5 Gaussian functions corresponding to peaks in the reference sample; 3 dashed lines correspond to peaks in the sample solution.

membership function varying from 0 to 1. Each peak of a reference electropherogram is considered as the centre of a Gaussian membership function. Thus, because there are five standards in our reference sample, there are five Gaussian functions (Fig. 5C). There are three peaks in the sample electropherogram that intersect with the Gaussian functions defined from our reference electropherogram. Values of the resulting intersections are defined as a measure of similarity and can be collected into a similarity matrix (Fig. 5B).

As several peaks from the sample electropherogram could simply by chance be highly similar to a peak from the reference electropherogram, a normalization process is needed. Sinkhorn standardization [34] is used to obtain a matrix with the sum of elements in each row and column equal to 1. After centering and scaling of the results, the whole process is repeated. Due to the Sinkhorn normalization and scaling used, time axis in Fig. 5C has been replaced with arbitrary units, where −1 and +1 mark the start and the end of electropherograms.

The width of the Gaussian functions is reduced following each iteration. This process is repeated until convergence is achieved, or a certain number of iterations have been performed. Peaks from two electropherograms (Fig. 5A) are considered belonging to the same substance if the measure of similarity is higher than a certain set value.

Successful peak identification relies on proper alignment of electropherograms because identification is based on fuzzy matching of migration times. To test the reliability of the algorithms developed in this work, a random group of electropherograms measured over a 1-month period were selected. Various combinations of sample and reference electropherograms were then created and analyzed. The results of this test were satisfying; only one electropherogram could not be correctly aligned using the automatic alignment algorithm and therefore subsequent peak matching failed. This kind of improper alignment could, however, be easily recognized by the operator. After manual alignment of this particular electropherogram, fuzzy matching was able to identify the peaks correctly.

Out of 500 tests, only nine pairs of electropherograms were discovered where peaks from one or two nerve agent degradation products were not recognized. No problems with matching the wrong peaks were discovered. For these tests, alignment was achieved without using thermal marks. A new time axis was calculated according to the migration time of a neutral marker, i.e. the EOF peak. This type of alignment was chosen because a data set already existed and there was no need for additional experiments. More importantly, the purpose of conducting these tests was to study the performance of the fuzzy matching algorithm, and not the alignment.

Analysis of such a high number of electropherograms is possible because the algorithm does not require more than 3 s for analyzing a pair of electropherograms. It should be noted that during analysis of one pair of electropherograms, the baseline correction and peak detection algorithms were run twice for both the sample and the reference electropherograms. The fuzzy matching algorithm was also tested without alignment on the same data set, but the tests were stopped after 50 experiments because 60% of the calculated results had mismatching peaks due to irreproducible migration times, further indicating that precise peak matching is not possible without proper electropherogram alignment. These results are contrary to those reported by Walczak and Wu [33], who used fuzzy matching to locate pairs of peaks belonging to the same substance from two electropherograms with the intention of aligning these signals.

3.4 Discussion

Production of thermal marks can be done using various heating sources, as long as the region of the capillary that is heated is very small. Thermal marks in this paper have been produced using a simple heating coil made out of stainless steel wire wrapped a couple of times around the separation capillary. Other previously reported possibilities for the generation of thermal marks are a surface-mounted device (SMD) resistor [27] or the tungsten filament from a light bulb [27, 28]. No matter what technique is used for thermal mark generation, precise control of certain parameters is necessary. Precise generation time for the thermal marks is necessary for calculating the estimated EOF mobility used for precise electropherogram alignment. The length of the heating impulse and the temperature of the source must be precisely controlled to yield reproducible thermal mark shapes and sizes.

Since no complex instrumentation is needed for the generation of thermal marks, the possibility to generate thermal marks can be easily implemented in future CE instruments. Thermal marks could also be easily applied to CE experiments to monitor changes in EOF velocity, so that changes in EOF mobility can be later reproduced. Information about EOF mobility changes during an experiment enables correction of these changes, allowing one to then treat the EOF mobility as a constant. Moreover, electropherograms with constant EOF mobilities can be easily aligned. The biggest challenge using this approach is producing thermal marks that will not co-migrate with analyte peaks. With an unknown sample, this cannot be prevented before the first run. Beginning with the second experiment, sample peak migration times can be predicted, and it is thus possible to produce thermal marks that will not co-migrate with the sample peaks.

CE as a separation technique has always been promoted for its very efficient separation, low sample consumption, and simple instrument design (e.g. CE does not require high-pressure pumps like those used in HPLC). However, in practice, CE has never been accepted for routine analyses. This is mostly because of the low level of reproducibility that accompanies CE, as has been reported many times in the literature. Signal processing could be a key solution to solve the reproducibility problems of CE. What cannot be solved before the experiment on the instrumental side can possibly be corrected after the experiment by applying proper signal processing. Qualitative analysis results can be improved by applying electropherogram alignment algorithms that can correct irreproducible migration times, whereas quantitative analyses can benefit from precise baseline correction and proper peak integration.

4 Concluding remarks

Together with peak detection, integration, signal alignment, and peak identification algorithms, signal processing programs are capable of identifying and quantifying target compounds in the field, such as nerve agent degradation products, in as little as a few seconds. With proper electropherogram alignment, satisfactory results have been obtained.

An automatic baseline correction algorithm was developed based on testing local extremes. Points that pass this test are then used to interpolate a new baseline that is subtracted from the original signal. Because the algorithm works only on small parts of the baseline at a time, this approach is very flexible and is capable of dealing with baseline disturbances of various speeds, amplitudes, and directions.

Electropherogram alignment based on information gathered with the aid of thermal marks is very efficient because it not only takes into account the EOF differences between runs considered by most current approaches but also considers changes in EOF during a run.

Signal processing as a field of research should earn more attention because with the aid of appropriate computer algorithms it is possible to improve the reliability of CE experiments both in quantitative and qualitative analysis. With improved reproducibility, it may finally be possible to really take advantage of the very efficient separation and low sample consumption always associated with CE.

This work has been supported by the graduate school "Functional materials and processes," and funding from The European Social Fund munder project 1.2.0401.09-0079 in Estonia. This work has also been supported by Estonian Science Foundation, grant no. 7818.

The authors have declared no conflict of interest.

5 References

[1] Chien, R.-L., Helmer, J. C., *Anal. Chem.* 1991, *63*, 1354–1361.

[2] Chevret, J. P., Van Soest, R. E. J., Urzem, M., *J. Chromatogr.* 1991, *541*, 439–449.

[3] Xue, Y., Yeung, E. S., *Anal. Chem.* 1994, *66*, 3575–3580.

[4] van der Moolen, H., Louwerse, D. J., Poppe, H., Smit, H. C., *Chromatographia* 1995, *40*, 368–374.

[5] Kuldvee, R., Kaljurand, M., Smit, H. C., *J. High Resolut. Chromatogr.* 1998, *21*, 169–174.

[6] Seiman, A., Reijenga, J., *Procedia Chem.* 2010, *2*, 59–66.

[7] Kaneta, T., Yamaguchi, Y., Imasaka, T., *Anal. Chem.* 1999, *71*, 5444–5446.

[8] Seiman, A., Kaljurand, M., Ebber, A., *Anal. Chim. Acta* 2007, *589*, 71.

[9] Faller, T., Engelhardt, H., *J. Chromatogr. A* 1999, *853*, 83–94.

[10] Dose, E. V., Guiochon, G. A., *Anal. Chem.* 1991, *63*, 1154–1158.

[11] Kullik, E., Kaljurand, M., Koel, M., *Use of Electronic Computing Machine in Gas Chromatography*. Science, Moscow 1978.

[12] Solis, A., Rex, M., Campiglia, A. D., Sojo, P., *Electrophoresis* 2007, *28*, 1181–1188.

[13] Bernabe-Zafon, V., Torres-Lapasio, J. R., Ortega-Gadea, S., Simo-Alfonso, E. F., Ramis-Ramos, G., *J. Chromatogr. A* 2005, *1065*, 301–313.

[14] Gan, F., Ruan, G., Mo, J., *Chemometr. Intell. Lab.* 2006, *82*, 59–65.

[15] Shao, X. G., Cai, W. S., Pan, Z. X., *Chemom. Intell. Lab. Syst.* 1999, *45*, 249–256.

[16] Perrin, C., Walczak, B., Massart, D. L., *Anal. Chem.* 2001, *73*, 4903–4917.

[17] Ma, X. G., Zhang, Z. X., *Anal. Chim. Acta* 2003, *485*, 233–239.

[18] Wätzig, H., *Chromatographia* 1992, *33*, 218–224.

[19] Vivo-Truyols, G., Torres-Lapasio, J. R., van Nederkassel, A. M., Vander Heyden, Y., Massart, D. L., *J. Chromatogr. A* 2005, *1096*, 133–145.

[20] Schirm, B., Wäitzig, H., *Chromatographia* 1998, *48*, 331–346.

[21] Altria, K. D., Fabre, H., *Chromatographia* 1995, *40*, 313–320.

[22] Kassidas, A., MacGregor, J. F., Taylor, P. A., *AIChE J.* 1998, *44*, 864–875.

[23] Pravdova, V., Walczak1, B., Massart, D. L., *Anal. Chim. Acta* 2002, *456*, 77–92.

[24] Vest Nielsen, N.-P., Carstensen, J. M., Smedsgaard, J., *J. Chromatogr. A* 1998, *805*, 17–35.

[25] Skov, T., van den Berg, F., Tomasi, G., Bro, R., *J. Chemometrics* 2006, *20*, 484–497.

[26] Ikuta, N., Yamada, Y., Yoshiyama, T., Hirokawa, T., *J. Chromatogr. A* 2000, *894*, 11–17.

[27] Reijenga, J. C., Martens, J. H. P. A., Giuliani, A., Chiari, M., *J. Chromatogr. B* 2002, *770*, 45–51.

[28] Saito, R. M., Neves, C. A., Lopes, F. S., Blanes, L., Brito-Neto, J. G. A., do Lago, C. L., *Anal. Chem.* 2007, *79*, 215–223.

[29] Seiman, A., Vaher, M., Kaljurand, M., *J. Chromatogr. A*, 2008, *1189*, 266–273.

[30] Gas, B., Kenndler, E., *Electrophoresis* 2004, *25*, 3901–3912.

[31] Kenndler-Blachkolm, K., Popelka, S., Gas, B., Kenndler, E., *J. Chromatogr. A*, 1996, *734*, 351–356.

[32] Seiman, A., Jaanus, M., Vaher, M., Kaljurand, M., *Electrophoresis* 2009, *30*, 507–514.

[33] Walczak, B., Wu, W., *Chemom. Intell. Lab. Syst.* 2005, *77*, 173–180.

[34] Sinkhorn, R. A., *Ann. Math. Stat.* 1964, *35*, 876–879.

Publication VI

Makarõtševa, N., Seiman, A., Vaher, M., Kaljurand, M. Analysis of the degradation products of chemical warfare agents using a portable capillary electrophoresis instrument with various sample injection devices. *Procedia Chemistry* **2010**, *2(S1)*, 20-25.

Available online at www.sciencedirect.com

ScienceDirect

Procedia Chemistry 2 (2010) 20–25

Procedia Chemistry

www.elsevier.com/locate/procedia

5th Conference by Nordic Separation Science Society (NoSSS2009)

Analysis of the degradation products of chemical warfare agents using a portable capillary electrophoresis instrument with various sample injection devices

Natalja Makarõtševa*, Andrus Seiman, Merike Vaher, Mihkel Kaljurand

Institute of Chemistry, Tallinn University of Technology, Akadeemia tee 15, 21618 Tallinn, Estonia

Abstract

In the present research, the performance of three sample injection devices in a portable capillary electrophoresis (CE) instrument was examined. These were the so-called cross-sampler, horizontal injection channel and vertical injection channel. All the three showed a good reproducibility of migration times (the relative standard deviation (RSD) was 4.3% in the case of the cross-sampler, 6.0% in the case of the horizontal injection channel and 1.7% in the case of the vertical channel). However, the reproducibility of peak areas was not sufficient. Hence, this study was mainly focused on qualitative analysis. The cross-sampler injection device was used in the portable CE instrument to analyse the composition of degradation products of chemical warfare agents (CWA). For the analysis of CWA degradation products simple procedures for the extraction of phosphonic acids from different surfaces, such as soil, concrete and granite blocks, tile floor, were developed.

Keywords: chemical warfare agents; phosphonic acids; portable CE instrument; sample injection

1. Introduction

The development and miniaturization of portable instrumentation is becoming more and more important in analytical chemistry research. In field analysis its total time or cost may greatly benefit from the use of portable instruments. This way it is possible to skip sample storage and transportation from the sampling site to the lab and obtain results for fast decisions. Portable instruments find mostly use in environmental applications, forensic and clinical analyses as well as detection of chemical warfare agents (CWA). At present the portable instruments are usually made only for some specific task. The detection techniques employed are often based on electrochemical sensors [1], photometry [2] and voltammetry [3,4]. The portable instruments based on separation methods enable a wider range of analyses to be carried out. Nowadays there exist portable versions of almost all separation methods,

* Corresponding author:N. Makarõtševa. Tel.: +372-620-4322; fax: +372-620-2828.
E-mail address: natalja.makarotseva@ttu.ee.

1876-6196/09/$– See front matter © 2010 Published by Elsevier B.V.
doi:10.1016/j.proche.2009.12.006

like gas chromatography (GC) [5,6], high-performance liquid chromatography (HPLC) [7], ion chromatography (IC) [8] or capillary electrophoresis (CE) [9-15].

In terms of a potential use in portable instruments CE has one main advantage over the other separation methods. CE does not require high pressure pumps for operating as liquid chromatography does. Separation is done by high voltage (HV). The simplicity of generating HV in portable devices is beyond comparison while the pressure needed for chromatographic techniques can only be achieved using complicated mechanical high-pressure pumps.

Today most portative CE instruments are based on contactless conductivity detection (CCD) [16-18]. CCD has sufficient sensitivity and can easily be coupled to portative instruments as its power consumption is very low. Also, because of its very simple detection cell construction, CCD is much more convenient than the other electrochemical detection techniques like amperometry, potentiometry and conductometry This is especially important in the case of CE considering the small dimensions of the separation capillary. The CCD detectors are basically constructed of two axially placed tubular electrodes which encompass the separation capillary. This means that the signal of CCD is gathered longitudinally along the capillary, instead of a transversal mode of conventional absorbance detection schemes. One of the two electrodes is excited with AC signal and the other electrode is used to register the same signal after passing through the cell.

So far portable CE instruments have mostly been used in traditional electrokinetic or hydrodynamic injection techniques that involve a lot of repeated operations with a background electrolyte (BGE) and sample vials. In commercial bench-top instruments these operations are automated by an auto-sampler, but in portable field instruments they must be carried out manually. In portable instruments the use of sampling techniques with as low a number of manual operations as possible should be considered. Therefore, the development of new sample injection approaches is highly welcome. The present contribution tests several different types of injection devices that could be operated using conventional plastic syringes.

2. Materials and methods

2.1. Chemicals

For the analysis of the degradation products of chemical warfare agents the following phosphonic acids were used: methylphosphonic acid (MPA), ethylphosphonic acid (EPA), 1-butylphosphonic acid (1-BPA), propylphosphonic acid (PPA), and pinacolyl metylphosphonic acid (PMPA). MPA, EPA and 1-BPA were purchased from Alfa Aesar, Lancaster Synthesis (Windham, NH, USA) and PPA and PMPA from Sigma-Aldrich (Steinheim, Germany). L-Histidine (His) and 2-(*N*-morpholino)ethanesulfonic acid hydrate (MES hydrate) were also purchased from Sigma-Aldrich. Sodium hydroxide was purchased from Chemapol (Prague, Czech Republic).

Stock solutions were prepared by dissolving an exact amount of each phosphonic acid in MilliQ water to a concentration of 10 mM. This was followed by a further mixing of all five analytes into a standard solution of different concentrations.

BGE was prepared by dissolving an exact amount of His and MES in MilliQ water.

2.2. Instrumentation

The in-house made portable CE instrument was equipped with a CCD detector and various injection devices. The dimensions of the instrument were 330×180×130 mm. The system ran on 10 common AA-type rechargeable batteries with an overall ouput of 15 V. Its operating time running on batteries was up to 4 hours. The system high-voltage output was up to 25 kV. The cell of the CCD detector was made of a rectangular piece of aluminium. There were milled three holes for two tubular electrodes and an operational amplifier. 8 mm electodes made of syringe needles were placed in separate chambers with a gap of 0.8 mm between them. One of the electodes was excited with a peak-to-peak sine wave at 60 V which can oscillate in a frequency range of 50-300 kHz. The second electrode picked up and amplified the signal after it had passed the capillary walls and the liquid in the capillary. The detection process was controlled by a computer with in-house written software. In the present work, all expreriments were carried out at a detector oscillation frequency of 200 kHz.

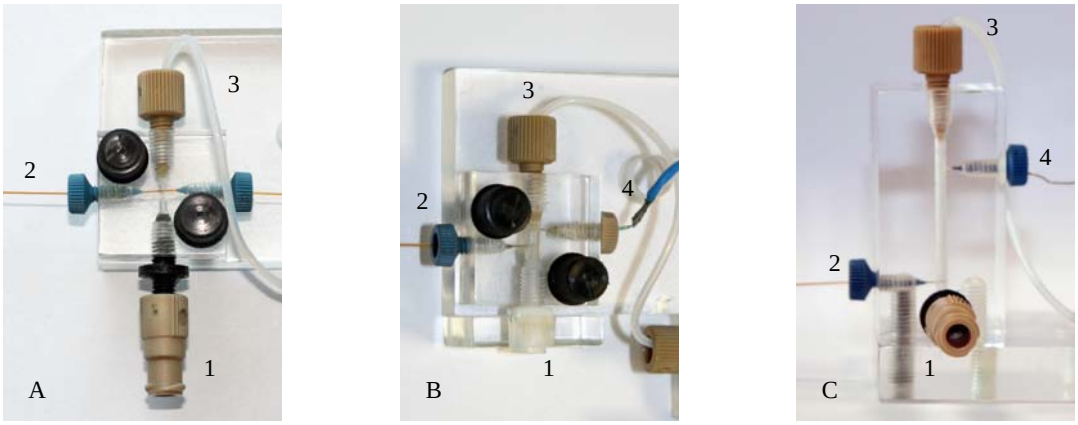

Fig. 1. The construction of various injection devices for a portable CE instrument: (a) cross-sampler; (b) horizontal injection channel; (c) vertical injection channel. 1 – sample injection socket for syringe, 2 – separation capillary, 3 – waste channel, 4 – grounding electrode.

The use in the portable CE system of three different injection devices was examined. The aim was to replace plastic vials commonly used in CE with a more convenient system and to minimize the number of manual operations in the injection procedure. For this purpose the cross-sampler, so-called horizontal channel and vertical channel were tested. The construction of the cross-sampler (Fig. 1a) was similar to that of the devices used in the microchip electrophoresis. It consisted of two perpendicular channels, one was for injection and the other, for separation. At the crossing point of both channels the ends of two capillaries were inserted. The analytes were separated in the longer capillary (a total length 44 cm, an effective length 36 cm), the shorter capillary (6 cm) was connected to the vial containing BGE. A small amount of the sample was introduced into the cross-sampler and then the voltage was applied to carry out the experiment. A detailed description of the cross-sampler and the whole portable CE equipment used in this work has been presented by Seiman *et al.* [15]. The amount of the sample introduced into the cross-sampler was 0.02 ml.

The second injection device was the horizontral channel (Fig. 1b) made of the polymethylmethacrylate (PMMA) block with dimensions of 10×25×25 mm. The length of the injection channel was 10 mm. The channel served as an inlet vial. The inlet end of the separation capillary was connected with the injection channel, while the electrode was placed on the opposite side. For the analysis 0.1 ml of the sample solution was introduced with the syringe into the injection channel. After the sample injection the inlet channel was filled with 0.25 ml of BGE. Capillary electrophoresis injection device with this type of construction was reported first by Kuban *et al.* [19]. It was used for flow injection analysis combined with CE. Injection device was operated by two peristaltic pumps. In our case simplier approach is used and injections are made manually using plastic syringes.

The operation of the vertical channel device with the dimensions of 25×25×47 mm (the length of the injection channel 33 mm) was based on the same principle as that of the horizontal channel (Fig. 1c). The difference between the two injection devices was in sample inlet channel direction. In both injection devices the separation capillaries with a total length of 55 cm and effective length of 45 cm were used. For the injection 0.25 ml of the sample solution was injected into the sample inlet channel which was later filled with 0.5 ml of BGE.

The fused silica capillary (i.d. 75 μm and o.d. 360 μm) was purchased from Agilent Technologies (Santa Clara, CA, US). In all experiments the BGE used was a 15 mM MES/His solution, the separation voltage was 16 kV.

2.3. Extraction procedure for CWA degradation products

To analyse CWA degradation products a simple procedure for their extraction from different surfaces was developed. First, for sample preparation 5 ml of the stock solution of five phosphonic acids with a concentration of 2 mM was sprayed on a small ground area and exposed for approximately 1.5 h. 2 g of sample was taken from the upper layer of soil and placed into 50 ml plastic vials. For the extraction 10 ml of MilliQ water was added to the soil sample. The sample was sonicated for 30 minutes, and filtered through a medium fast paper filter (Whatman, Maidstone, UK) and 0.45 μm Millipore filter (Sarstetd, Germany).

For the extraction of CWA degradation products from varoius surfaces (granite blocks, concrete blocks, asphalt, tile floor, etc) 5 ml of a 2 mM 5 phosphonic acid solution was sprayed. After complete drying the surface was wiped with a filter paper (medium fast paper filter, Aldrich, USA) moistened in 2 ml of MilliQ water. The filter was then introduced into a 50 ml vial and 8 ml MilliQ water was added. The sample was sonicated for 30 minutes and after that filtered through a 0.45 μm Millipore filter.

3. Results and Discussion

3.1. Repeatability of the injection devices tested

The convenience of the sample injection procedure is crucial in portable CE instruments. Replacing plastic vials with sample and BGE in the field may be unhandy. The injection devices requiring no operations with sample and BGE vials should be preferred.

As a detailed description of the work dedicated to the cross-sampler has been presented in [15], this study compared advantages and disadvantages of the sampler over the other injection devices. Sample injection in all three samplers is performed by pushing a certain amount of the sample into the channel with a syringe. In horizontal and vertical channels the sample is then washed out with a certain amount of BGE. Theoretically, the injected volume should be dependent only on the sample volume introduced into the channel and configuration of the injection device. However, as all these manipulations are made by hand, it is difficult to control the pushing force and make always reproducible injections. By pushing harder, more sample is introduced into the capillary. In the case of horizontal and vertical channels, the pushing force also plays a certain role when washing with BGE as then the sample zone is pushed further into the separation capillary. By pushing the syringe with BGE too hard or using too much liquid for washing, it is possible to push the sample so far into the separation capillary that it will affect migration times.

The performance of the samplers was estimated on a standard mixture of five phosphonic acids with a concentration of 100 μM. The results are given in Table 1.

Table 1. The migration time reproducibility for five phosphonic acids

Injection device	Relative standard deviation (RSD, %)
Cross-sampler	4.3*
Horizontal injection channel	6.0*
Vertical injection channel	1.7**

*at least three-day reproducibility

** one-day reproducibility

The vertical sampler had a better reproducibility of migration times than the other two injection devices. Though, the RSD data for the vertical channel was calculated only during one day, as it was found to suit less for routine analysis than the horizontal channel. At the same time, the cross-sampler was found to be more convenient to be used in the portable CE instrument as it required a minimum number of operations and so was used for the analysis of CWA degradation products in the portable CE instrument.

3.2. Analysis of the phosphonic acids extracted from different surfaces

As the reproducibility of peak areas was not sufficient for all the injection devices investigated, we focused only on the qualitative analysis of CWA samples. A simple and fast procedure for the exraction of CWA degradation products from different surfaces was worked out. A 2 mM phosphonic acid mixture was sprayed on the ground (and other surfaces, like asphalt or concrete blocks) outside, but CE experiments with the portable CE instrument were carried out in the laboratory, not on-site. These were preliminary experiments for the newly-built portable instrument which was first tested in laboratory conditions.

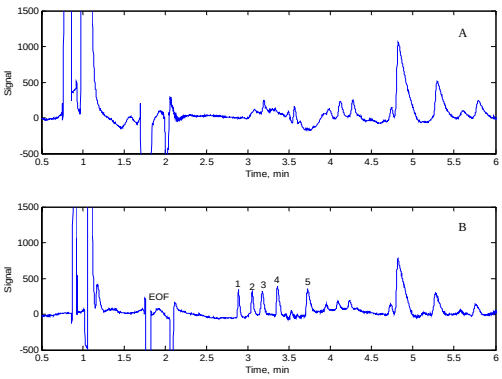

Fig. 2. The electropherograms of soil extracts (sample injected with the cross-sampler). The BGE solution is 15 mM MES/His. Separation voltage: 16 kV. A – blank sample, pure soil exctract without any standards, B – phosphonic acids extracted from soil. 1 – PMPA, 2 – 1-BPA, 3 – PPA, 4 – EPA, 5 – MPA, EOF – electroosmotic flow.

Soil extracts were prepared as described in section 2.3. The extraction experiments were carried out using soil samples collected from different places. In all cases it was possible to extract all five phosphonic acids (Fig. 2). During the extraction, some components of the soil were also extracted, but their peaks did not overlap with those of phosphonic acids. Thus, the procedure for extraction of CWA degradation products from soil might be suitable for the qualitative analysis. During this stage of the study the recovery of phosphonic acid standards was not measured.

A universal procedure of extraction of CWA degradation components from different hard surfaces such as granite, concrete blocks and tile floor was also successfully worked out. The results are presented in Figs. 3 and 4. Using this procedure all five phosphonic acids were extracted from the surfaces investigated. Some unknown compounds were also extracted and separated from phosphonic acids peaks. Again, their peaks did not overlap with those of phoshonic acids.

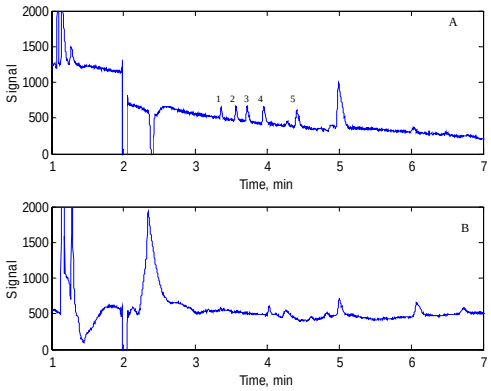

Figure 3. The electropherograms of extracts from concrete blocks (sample injected with the cross-sampler). The BGE solution is 15 mM MES/His. Separation voltage: 16 kV. A – phosphonic acids extracted from concrete blocks. 1 – PMPA, 2 – 1-BPA, 3 – PPA, 4 – EPA, 5 – MPA, EOF – electroosmotic flow; B – blank sample, pure exctract from concrete blocks without any standards.

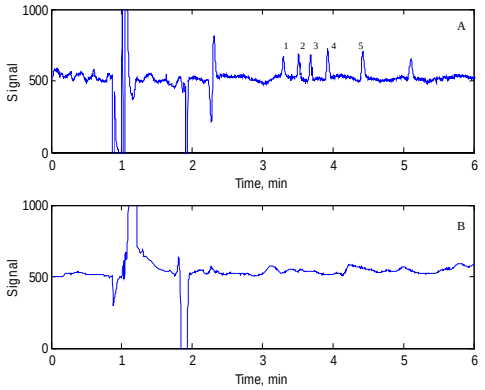

Figure 4. The electropherograms of extracts from tile floor (sample injected with the cross-sampler). The BGE solution is 15 mM MES/His. Separation voltage: 16 kV. A – phosphonic acids extracted from soil. 1 – PMPA, 2 – 1-BPA, 3 – PPA, 4 – EPA, 5 – MPA, EOF – electroosmotic flow; B – blank sample, pure exctract from tile floor without any standards.

4. Conclusions

The present study demonstrated that all three injection devices investigated were suitable for the qualitative analysis of compounds using a portable CE instrument. However, as the cross-sampler required fewer manual operations, it was more convenient to be used in field experiments. In laboratory analysis horizontal and vertical injection channels might also be used as an alternative to plastic vials. Unfortunately, it was not possible to obtain good reproducibility for peak areas with these injection devices and only qualitative analysis was done in the present study. To achieve better peak area reproducibility, further improvements and investigations are needed.

The developed procedures were suitable for the extraction of all five phosphonic acids from soil and various hard surfaces. Though, during the extraction several unknown components were revealed. Their peaks did not overlap with those of phosphonic acids. So, it would be possible to identify CWA degradation products from different surfaces using a simple water extraction procedure.

References

1. J. Wang, TrAC. 21 (2002) 226.
2. K. B. Thurbide, T. C. Hayward, Anal. Chim. Acta 519 (2004) 121.
3. K. Ashley, Electroanalysis 7 (2005) 1189.
4. S. Knight, N. Morley, D. Leech, R. Cave, Enivornmental Chemistry. 3 (2006) 450.
5. J. Ji, C. Deng, W. Shen, X. Zhang, Talanta 69 (2006) 894.
6. F. J. Santos, TrAC. 21 (2002) 672.
7. G. I. Baram, J. Chromatogr. A. 728 (1996) 387.
8. O. P. Kalyakina, A. M. Dolgonosov, J. Anal. Chem. 58 (2003) 951.
9. T. Kappes, P. Schnierle, P. C. Hauser, Anal. Chim. Acta 393 (1999) 77.
10. D.-C. Chen, S. S. Chang, C.-H. Chen, Anal. Chem.71 (1999) 3200.
11. B. L. De Backer, L. J. Nagels, Anal. Chem. 68 (1996) 4441.
12. T. Kappes, P. C. Hauser, Anal. Comm. 35 (1998) 325.
13. P. Kubáň, H. T. A. Nguyen, M. Macka, P. R. Haddad, P. C. Hauser, Electroanalysis 19 (2007) 2059.
14. Y. Xu, W. Wang, S. F. Y. Li, Electrophoresis 28 (2007) 1530.
15. A. Seiman, M. Jaanus, M. Vaher, M. Kaljurand, Electrophoresis 30 (2009) 507.
16. J. A. F. da Silva, C. L. do Lago, Anal. Chem. 70 (1998) 4339.
17. A. J. Zemann, E. Schnell, D. Volgger, G. K. Bonn, Anal. Chem. 70 (1998) 4339.
18. K. J. M. Francisco, C. L. do Lago, Electrophoresis. 30 (2009) 1.
19. P. Kuban, R. Pirmohammadi, B. Karlberg, Anal. Chim. Acta 378 (1999) 55.

Publication VII

Seiman, A.; Vaher, M.; Kaljurand, M.; Kapillaarelektroforeesi ristsisendseade kapillaarelektroforeesi analüsaatorisse proovi sisestamiseks (Capillary electrophoresis cross-injection device for sample introduction into a capillary electrophoresis instrument). EE 2008000037, May 27, 2008

EE 200800037 A

(19) EESTI VABARIIK
PATENDIAMET

(11) **EE 200800037 A**

(51) Int.Cl.
G01N 27/447 (2010.01)
B01L 3/00 (2010.01)

(12) PATENDITAOTLUS

(21) Patenditaotluse number: **P200800037**

(22) Patenditaotluse esitamise kuupäev: **27.05.2008**

(43) Patenditaotluse avaldamise kuupäev: **15.02.2010**

(71) Patenditaotleja.

Tallinna Tehnikaülikool
Ehitajate tee 5, 19086 Tallinn, EE

(72) Leiutise autorid:

Andrus Seiman
Mustamäe tee 159-54, 12913 Tallinn, EE

Merike Vaher
E. Vilde tee 92-29, 12914 Tallinn, EE

Mihkel Kaljurand
Mustamäe tee 177-93, 12913 Tallinn, EE

(54) Kapillaarelektroforeesi ristsisendseade kapillaarelektroforeesi analüsaatorisse proovi sisestamiseks

(57) Leiutise objektiks on kapillaarelektroforeesi ristsisendseade (1) kapillaarelektroforeesi analüsaatorisse proovi sisestamiseks, mis on moodustatud monoliitse ploki sisse, milles on kaks ristuvat kanalit: proovi sisendkanal (10) ja lahutuskanal (5) Monoliitse ploki külge on kinnitatud lahutuskanalisse kaks kapilaari, milles toimub ainete lahutumine. Lahutuskanaliga ristuva proovi sisendkanali (10) külge on ühendatud süstal, pump või süstalpump, millega on võimalik lihtsalt ja mugavalt viia proovi lahutuskapillaari.

(57) A capillary electrophoresis cross-injection device (1) is a device for sample introduction for capillary electrophoresis instruments. The sample injection device (1) is built into monolithic block There are two crossing channels inside monolithic block - one is a separation channel (5) and another sample injection channel (10) Two capillaries (35) are connected to the separation channel (5) into the monolithic block. The separation of sample species takes place in these capillaries (35) For simple sample introduction syringe, pump, or syringe-pump have been connected to the sample injection channel (10)

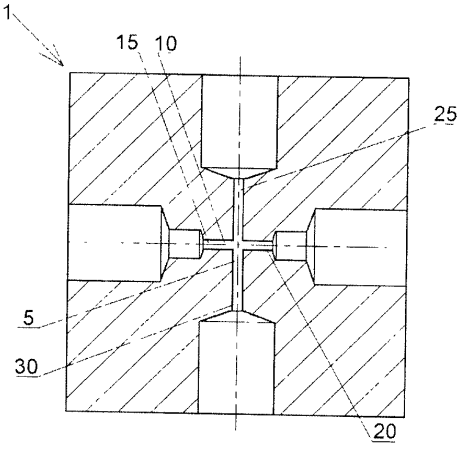

CURRICULUM VITAE

Personal data

Name: Andrus Seiman
Date of birth: 30.10.1982

Contact

Address: Akadeemia tee 15, 12618 Tallinn, Estonia
Phone: +372 55 545 160
e-mail: andrusseiman@gmail.com

Education

2007 - ...	Tallinn University of Technology – *Doctoral* – speciality: chemistry and gene technology
2005 – 2007	Tallinn University of Technology – *Master* – speciality: Applied chemistry and biotechnology – MSc degree
2005	Tallinn University of Technology – *Bachelor* – speciality: applied chemistry and biotechnology – BSc degree
2001 – 2005	Tallinn University of Technology – *Bachelor* – speciality: technology of materials

Degree

Master's degree (MSc) in Applied Chemistry and Biotechnology, 2007, (sup) prof Mihkel Kaljurand, Influence of a stacking phenomenon on the results of Hadamard transform capillary electrophoresis (Proovi kuhjamise mõju Hadamardi transformatsioon kapillaarelektroforeesile), Tallinn University of Technology

Courses

2011	*Data analysis for chemistry*, Department of Chemistry, Tallinn University of Technology
2004	*Estimation of measurement uncertainties in chemistry laboratory*. Testing Centre , University of Tartu

Professional experience

2007 - ...	*Department of Chemistry*, *Tallinn University of Technology*, research within a project on portable CE
2005	*AS Sadolin ES*, developing faster and more reliable quality control methods for new coating products
2004	*Saku Õlletehas AS*, uncertainty estimation in quality control laboratory

Research interests

Capillary electrophoresis, computerized sampling, contactless-conductivity detection, chemometrics, multivariate data analysis, signal processing

List of publications

1. Seiman, A., Vaher, M., Kaljurand, M, Thermal marks as signal processing aid for portable capillary electropherograph, *Electrophoresis*, **2011**, *32*, 1006-1014.
2. Kuban, P., Seiman, A., Makarõtševa, N., Vaher, M., Kaljurand, M. In situ determination of sarin, soman and VX nerve agents in various matrices by portable capillary electropherograph with contactless conductivity detection, *Journal of Chromatography A*, **2011**, *1218*, 2618-2625.
3. Kuban, P., Seiman, A., Kaljurand, M., Improving precision of manual hydrodynamic injection in capillary electrophoresis with contactless conductivity detection. *Journal of Chromatography A*, **2011**, *1218*, 1273-1280.
4. Seiman, A., Makarõtševa, N., Vaher, M., Kaljurand, M., Detection of nerve agent degradation products in different soil fractions using capillary electrophoresis with contactless conductivity detection. *Chemistry and Ecology*, **2010**, *26*, 145-155.
5. Makarõtševa, N., Seiman, A., Vaher, M., Kaljurand, M. Analysis of the degradation products of chemical warfare agents using a portable capillary electrophoresis instrument with various sample injection devices. *Procedia Chemistry*, **2010**, *2(S1)*, 20-25.
6. Reijenga, J., Seiman, A., Cleaning-up dirty isotachopherograms in time and frequency domain. *Procedia Chemistry*, **2010**, *2(S1)*, 67-75.
7. Seiman, A., Reijenga, J., Cross-correlation capillary electrophoresis in unmodified commercial equipment. *Procedia Chemistry*, **2010**, *2(S1),* 59-66.
8. Seiman, A., Jaanus, M., Vaher, M., Kaljurand, M., A portable capillary electropherograph equipped with a cross-sampler and a contactless-conductivity detector for the detection of the degradation products of chemical warfare agents in soil extracts. *Electrophoresis*, **2009**, *30*, 507-514.
9. Seiman, A., Vaher, M., Kaljurand, M., Monitoring of the electroosmotic flow of ionic liquid solution in non-aqueous media using thermal marks. *Journal of Chromatography A*, **2008**, *1189*, 266-273.
10. Seiman, A., Kaljurand, M., Ebber, A., Influence of a stacking phenomenon on the results of Hadamard transform capillary electrophoresis. *Analytica Chimica Acta*, **2007**, *589*, 71-75.
11. Seiman, A., Vaher, M., Kaljurand, M., Kapillaarelektroforeesi ristsisendseade kapillaarelektroforeesi analüsaatorisse proovi sisestamiseks (Capillary electrophoresis cross-injection device for sample introduction into a capillary electrophoresis instrument). *Estonian patent EE 2008000037*, **2008**.

ELULOOKIRJELDUS

Isikuandmed

Nimi: Andrus Seiman
Sünniaeg: 30.10.1982

Contact

Aadress: Akadeemia tee 15, 12618 Tallinn, Estonia
Telefon: +372 55 545 160
e-post: andrusseiman@gmail.com

Haridus

2007 - ...	Tallinna Tehnikaülikool – *Doktorantuur* – eriala: Keemia ja geenitehnoloogia
2005 – 2007	Tallinna Tehnikaülikool – *Magistrantuur* – eriala: Rakenduskeemia ja biotehnoloogia – magistrikraad
2005	Tallinna Tehnikaülikool – *Bakalaureuseõpe* – eriala: Rakenduskeemia ja biotehnoloogia – bakalaureusekraad
2001 – 2005	Tallinna Tehnikaülikool – *Bakalaureuseõpe* – eriala: Materjalitehnoloogia

Kraad

Magistrikraad (MSc) Rakenduskeemias ja biotehnoloogias, 2007, juhendaja prof. Mihkel Kaljurand, Proovi kuhjamise mõju Hadamardi transformatsioon kapillaarelektroforeesile (Influence of a stacking phenomenon on the results of Hadamard transform capillary electrophoresis), TTÜ

Täiendõpe

2011	*Andmetöötlus keemias* (*Data analysis for chemistry*), Tallinna Tehnikaülikool, Keemiainstituut
2004	*Mõõtemääramatuse hindamine keemialaboris: baaskursus*. Tartu Ülikool, Katsekoda

Töökogemus

2007 - ...	*TTU Keemiainstituut*, kaasaskantava KE analüsaatori projekt
2005	*AS Sadolin ES*, uute kvaliteedikontrolli meetodite väljatöötamisega seotud projekt
2004	*Saku Õlletehas AS*, mõõtemääramtuse hindamisega kvaliteedikontrolli laboris seotud projekt

Teadustöö põhisuunad

Kapillaarelektroforees, automatiseeritud proovisisestus, kontaktita juhtivusdetektor, kemomeetria, signaalitöötlus

DISSERTATIONS DEFENDED AT TALLINN UNIVERSITY OF TECHNOLOGY ON *NATURAL AND EXACT SCIENCES*

1. **Olav Kongas**. Nonlinear dynamics in modeling cardiac arrhytmias. 1998.
2. **Kalju Vanatalu**. Optimization of processes of microbial biosynthesis of isotopically labeled biomolecules and their complexes. 1999.
3. **Ahto Buldas**. An algebraic approach to the structure of graphs. 1999.
4. **Monika Drews**. A metabolic study of insect cells in batch and continuous culture: application of chemostat and turbidostat to the production of recombinant proteins. 1999.
5. **Eola Valdre**. Endothelial-specific regulation of vessel formation: role of receptor tyrosine kinases. 2000.
6. **Kalju Lott**. Doping and defect thermodynamic equilibrium in ZnS. 2000.
7. **Reet Koljak**. Novel fatty acid dioxygenases from the corals *Plexaura homomalla* and *Gersemia fruticosa.* 2001.
8. **Anne Paju**. Asymmetric oxidation of prochiral and racemic ketones by using sharpless catalyst. 2001.
9. **Marko Vendelin**. Cardiac mechanoenergetics *in silico*. 2001.
10. **Pearu Peterson**. Multi-soliton interactions and the inverse problem of wave crest. 2001.
11. **Anne Menert**. Microcalorimetry of anaerobic digestion. 2001.
12. **Toomas Tiivel**. The role of the mitochondrial outer membrane in *in vivo* regulation of respiration in normal heart and skeletal muscle cell. 2002.
13. **Olle Hints**. Ordovician scolecodonts of Estonia and neighbouring areas: taxonomy, distribution, palaeoecology, and application. 2002.
14. **Jaak Nõlvak**. Chitinozoan biostratigrapy in the Ordovician of Baltoscandia. 2002.
15. **Liivi Kluge**. On algebraic structure of pre-operad. 2002.
16. **Jaanus Lass**. Biosignal interpretation: Study of cardiac arrhytmias and electromagnetic field effects on human nervous system. 2002.
17. **Janek Peterson**. Synthesis, structural characterization and modification of PAMAM dendrimers. 2002.
18. **Merike Vaher**. Room temperature ionic liquids as background electrolyte additives in capillary electrophoresis. 2002.
19. **Valdek Mikli**. Electron microscopy and image analysis study of powdered hardmetal materials and optoelectronic thin films. 2003.
20. **Mart Viljus**. The microstructure and properties of fine-grained cermets. 2003.
21. **Signe Kask**. Identification and characterization of dairy-related *Lactobacillus.* 2003.
22. **Tiiu-Mai Laht**. Influence of microstructure of the curd on enzymatic and microbiological processes in Swiss-type cheese. 2003.
23. **Anne Kuusksalu**. 2–5A synthetase in the marine sponge *Geodia cydonium*. 2003.

24. **Sergei Bereznev**. Solar cells based on polycristalline copper-indium chalcogenides and conductive polymers. 2003.
25. **Kadri Kriis**. Asymmetric synthesis of C_2-symmetric bimorpholines and their application as chiral ligands in the transfer hydrogenation of aromatic ketones. 2004.
26. **Jekaterina Reut**. Polypyrrole coatings on conducting and insulating substracts. 2004.
27. **Sven Nõmm**. Realization and identification of discrete-time nonlinear systems. 2004.
28. **Olga Kijatkina**. Deposition of copper indium disulphide films by chemical spray pyrolysis. 2004.
29. **Gert Tamberg**. On sampling operators defined by Rogosinski, Hann and Blackman windows. 2004.
30. **Monika Übner**. Interaction of humic substances with metal cations. 2004.
31. **Kaarel Adamberg**. Growth characteristics of non-starter lactic acid bacteria from cheese. 2004.
32. **Imre Vallikivi**. Lipase-catalysed reactions of prostaglandins. 2004.
33. **Merike Peld**. Substituted apatites as sorbents for heavy metals. 2005.
34. **Vitali Syritski**. Study of synthesis and redox switching of polypyrrole and poly(3,4-ethylenedioxythiophene) by using *in-situ* techniques. 2004.
35. **Lee Põllumaa**. Evaluation of ecotoxicological effects related to oil shale industry. 2004.
36. **Riina Aav**. Synthesis of 9,11-secosterols intermediates. 2005.
37. **Andres Braunbrück**. Wave interaction in weakly inhomogeneous materials. 2005.
38. **Robert Kitt**. Generalised scale-invariance in financial time series. 2005.
39. **Juss Pavelson**. Mesoscale physical processes and the related impact on the summer nutrient fields and phytoplankton blooms in the western Gulf of Finland. 2005.
40. **Olari Ilison**. Solitons and solitary waves in media with higher order dispersive and nonlinear effects. 2005.
41. **Maksim Säkki**. Intermittency and long-range structurization of heart rate. 2005.
42. **Enli Kiipli**. Modelling seawater chemistry of the East Baltic Basin in the late Ordovician–Early Silurian. 2005.
43. **Igor Golovtsov**. Modification of conductive properties and processability of polyparaphenylene, polypyrrole and polyaniline. 2005.
44. **Katrin Laos**. Interaction between furcellaran and the globular proteins (bovine serum albumin β-lactoglobulin). 2005.
45. **Arvo Mere**. Structural and electrical properties of spray deposited copper indium disulphide films for solar cells. 2006.
46. **Sille Ehala**. Development and application of various on- and off-line analytical methods for the analysis of bioactive compounds. 2006.
47. **Maria Kulp**. Capillary electrophoretic monitoring of biochemical reaction kinetics. 2006.
48. **Anu Aaspõllu.** Proteinases from *Vipera lebetina* snake venom affecting hemostasis. 2006.
49. **Lyudmila Chekulayeva**. Photosensitized inactivation of tumor cells by porphyrins and chlorins. 2006.

50. **Merle Uudsemaa**. Quantum-chemical modeling of solvated first row transition metal ions. 2006.
51. **Tagli Pitsi**. Nutrition situation of pre-school children in Estonia from 1995 to 2004. 2006.
52. **Angela Ivask**. Luminescent recombinant sensor bacteria for the analysis of bioavailable heavy metals. 2006.
53. **Tiina Lõugas**. Study on physico-chemical properties and some bioactive compounds of sea buckthorn (*Hippophae rhamnoides* L.). 2006.
54. **Kaja Kasemets**. Effect of changing environmental conditions on the fermentative growth of Saccharomyces cerevisae S288C: auxo-accelerostat study. 2006.
55. **Ildar Nisamedtinov**. Application of ^{13}C and fluorescence labeling in metabolic studies of Saccharomyces spp. 2006.
56. **Alar Leibak**. On additive generalisation of Voronoï's theory of perfect forms over algebraic number fields. 2006.
57. **Andri Jagomägi**. Photoluminescence of chalcopyrite tellurides. 2006.
58. **Tõnu Martma**. Application of carbon isotopes to the study of the Ordovician and Silurian of the Baltic. 2006.
59. **Marit Kauk**. Chemical composition of $CuInSe_2$ monograin powders for solar cell application. 2006.
60. **Julia Kois**. Electrochemical deposition of $CuInSe_2$ thin films for photovoltaic applications. 2006.
61. **Ilona Oja Açik**. Sol-gel deposition of titanium dioxide films. 2007.
62. **Tiia Anmann**. Integrated and organized cellular bioenergetic systems in heart and brain. 2007.
63. **Katrin Trummal**. Purification, characterization and specificity studies of metalloproteinases from *Vipera lebetina* snake venom. 2007.
64. **Gennadi Lessin**. Biochemical definition of coastal zone using numerical modeling and measurement data. 2007.
65. **Enno Pais**. Inverse problems to determine non-homogeneous degenerate memory kernels in heat flow. 2007.
66. **Maria Borissova**. Capillary electrophoresis on alkylimidazolium salts. 2007.
67. **Karin Valmsen**. Prostaglandin synthesis in the coral *Plexaura homomalla*: control of prostaglandin stereochemistry at carbon 15 by cyclooxygenases. 2007.
68. **Kristjan Piirimäe**. Long-term changes of nutrient fluxes in the drainage basin of the gulf of Finland – application of the PolFlow model. 2007.
69. **Tatjana Dedova**. Chemical spray pyrolysis deposition of zinc sulfide thin films and zinc oxide nanostructured layers. 2007.
70. **Katrin Tomson**. Production of labelled recombinant proteins in fed-batch systems in *Escherichia coli*. 2007.
71. **Cecilia Sarmiento**. Suppressors of RNA silencing in plants. 2008.
72. **Vilja Mardla**. Inhibition of platelet aggregation with combination of antiplatelet agents. 2008.
73. **Maie Bachmann**. Effect of Modulated microwave radiation on human resting electroencephalographic signal. 2008.
74. **Dan Hüvonen**. Terahertz spectroscopy of low-dimensional spin systems. 2008.

75. **Ly Villo**. Stereoselective chemoenzymatic synthesis of deoxy sugar esters involving *Candida antarctica* lipase B. 2008.
76. **Johan Anton**. Technology of integrated photoelasticity for residual stress measurement in glass articles of axisymmetric shape. 2008.
77. **Olga Volobujeva**. SEM study of selenization of different thin metallic films. 2008.
78. **Artur Jõgi**. Synthesis of 4'-substituted 2,3'-dideoxynucleoside analogues. 2008.
79. **Mario Kadastik**. Doubly charged Higgs boson decays and implications on neutrino physics. 2008.
80. **Fernando Pérez-Caballero**. Carbon aerogels from 5-methylresorcinol-formaldehyde gels. 2008.
81. **Sirje Vaask**. The comparability, reproducibility and validity of Estonian food consumption surveys. 2008.
82. **Anna Menaker**. Electrosynthesized conducting polymers, polypyrrole and poly(3,4-ethylenedioxythiophene), for molecular imprinting. 2009.
83. **Lauri Ilison**. Solitons and solitary waves in hierarchical Korteweg-de Vries type systems. 2009.
84. **Kaia Ernits**. Study of In2S3 and ZnS thin films deposited by ultrasonic spray pyrolysis and chemical deposition. 2009.
85. **Veljo Sinivee**. Portable spectrometer for ionizing radiation "Gammamapper". 2009.
86. **Jüri Virkepu**. On Lagrange formalism for Lie theory and operadic harmonic oscillator in low dimensions. 2009.
87. **Marko Piirsoo**. Deciphering molecular basis of Schwann cell development. 2009.
88. **Kati Helmja**. Determination of phenolic compounds and their antioxidative capability in plant extracts. 2010.
89. **Merike Sõmera**. Sobemoviruses: genomic organization, potential for recombination and necessity of P1 in systemic infection. 2010.
90. **Kristjan Laes**. Preparation and impedance spectroscopy of hybrid structures based on CuIn3Se5 photoabsorber. 2010.
91. **Kristin Lippur**. Asymmetric synthesis of 2,2'-bimorpholine and its 5,5'-substituted derivatives. 2010.
92. **Merike Luman**. Dialysis dose and nutrition assessment by an optical method. 2010.
93. **Mihhail Berezovski**. Numerical simulation of wave propagation in heterogeneous and microstructured materials. 2010.
94. **Tamara Aid-Pavlidis**. Structure and regulation of BDNF gene. 2010.
95. **Olga Bragina**. The role of Sonic Hedgehog pathway in neuro- and tumorigenesis. 2010.
96. **Merle Randrüüt**. Wave propagation in microstructured solids: solitary and periodic waves. 2010.
97. **Marju Laars**. Asymmetric organocatalytic Michael and aldol reactions mediated by cyclic amines. 2010.
98. **Maarja Grossberg**. Optical properties of multinary semiconductor compounds for photovoltaic applications. 2010.

99. **Alla Maloverjan**. Vertebrate homologues of Drosophila fused kinase and their role in Sonic Hedgehog signalling pathway. 2010.
100. **Priit Pruunsild**. Neuronal Activity-Dependent Transcription Factors and Regulation of Human BDNF Gene. 2010.
101. **Tatjana Knazeva**. New Approaches in Capillary Electrophoresis for Separation and Study of Proteins. 2011.
102. **Atanas Katerski**. Chemical Composition of Sprayed Copper Indium Disulfide Films for Nanostructured Solar Cells. 2011.
103. **Kristi Timmo**. Formation of Properties of CuInSe2 and Cu2ZnSn(S,Se)4 Monograin Powders Synthesized in Molten KI. 2011.
104. **Kert Tamm**. Wave Propagation and Interaction in Mindlin-Type Microstructured Solids: Numerical Simulation. 2011.
105. **Adrian Popp**. Ordovician Proetid Trilobites in Baltoscandia and Germany. 2011.
106. **Ove Pärn**. Sea Ice Deformation Events in the Gulf of Finland and This Impact on Shipping. 2011.
107. **Germo Väli**. Numerical Experiments on Matter Transport in the Baltic Sea. 2011.